SCHOOL OF
CIVIL ENGINEERING

INDIANA
DEPARTMENT OF HIGHWAYS

JOINT HIGHWAY RESEARCH PROJECT

FHWA/IN/JHRP-87/7 -/

Final Report

EFFECTS OF ASPHALT COMPOSITION AND COMPACTION ON THE PERFORMANCE OF ASPHALT PAVEMENT MIXTURES

L. E. Wood
A. G. Altschaeffl

PURDUE UNIVERSITY

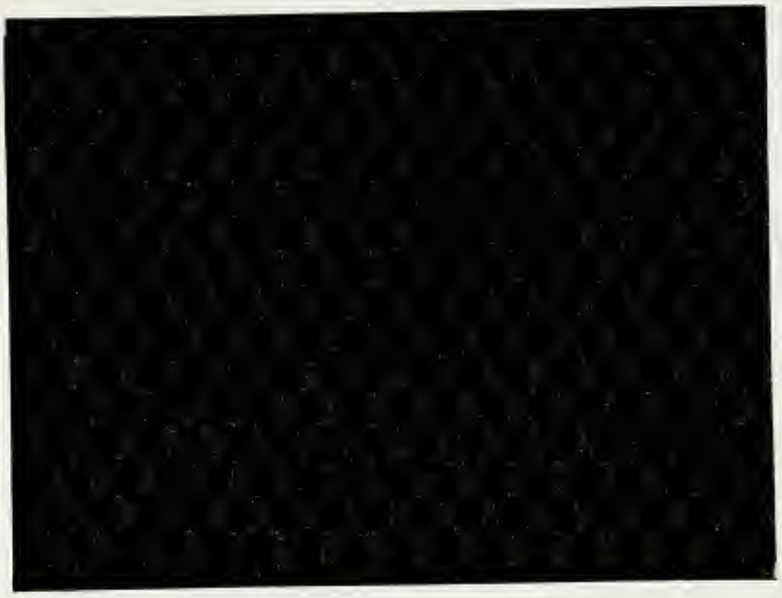

JOINT HIGHWAY RESEARCH PROJECT

FHWA/IN/JHRP-87/7

Final Report

EFFECTS OF ASPHALT COMPOSITION AND COMPACTION ON THE PERFORMANCE OF ASPHALT PAVEMENT MIXTURES

L. E. Wood
A. G. Altschaeffl

Final Report

"Effects of Asphalt Composition and Compaction on the Performance of Asphalt Pavement Mixtures"

To: Harold L. Michael, Director
Joint Highway Research Project

September 9, 1987
Revised May 23, 1988
Project: C-36-66G

From: L. E. Wood
Research Engineer

File: 2-4-33

Please find attached the Final Report entitled "Effects of Asphalt Composition and Compaction on the Performance of Asphalt Pavement Mixtures". It was prepared by L. E. Wood and A. G. Altschaeffl, and represents the work of R. Aunan, R. Luna, and N. Garrick of our staff.

This report is presented in two parts. The first part presents the work done to characterize the fabric of this asphalt sand mix surface and to reproduce this fabric in the laboratory. In addition, it examines the field compaction time requirements for these materials. The second part evaluates the use of blended asphalts, as well as the use of high pressure-gel permeation chromatography to characterize the chemical composition of asphalts.

Based upon the comparison of the pore-size distribution of the fabric of both laboratory and field compacted mixtures, the gyratory and kneading compactors created satisfactorily equivalent laboratory fabrics to those of field cores. Very limited performance data suggested that good performance is associated with fabric that has a wide-spread of void sizes, with no major portion being concentrated at any one size.

No major differences in behavior were found for the artificially blended asphalts, in general, although rich asphaltene asphalts show a higher hardening rate at high temperatures. Blended ROSE asphalts do not create differences in performance than straight-run produced asphalts. The asphalt chemical composition does appear associated with individual performance characteristics; this suggests promise for the use of HP-GPC in the continuing effort to produce quality performance of asphalt pavement mixtures.

This report is presented for review and approval as evidence of fulfillment of the objectives of this project.

Respectfully,

L E Wood fmlc

L. E. Wood
Research Engineer

TECHNICAL REPORT STANDARD TITLE PAGE

1. Report No.	2. Government Accession No.	3. Recipient's Catalog No.
FHWA/IN/JHRP-87/7		

4. Title and Subtitle	5. Report Date
Effects of Asphalt Composition and Compaction on the Performance of Asphalt Pavement Mixtures	September 9, 1987 Revised May 23, 1988
	6. Performing Organization Code
7. Author(s)	8. Performing Organization Report No.
L. E. Wood and A. G. Altschaeffl	JHRP-87/7
9. Performing Organization Name and Address	10. Work Unit No.
Joint Highway Research Project Civil Engineering Building Purdue University West Lafayette, IN 47907	11. Contract or Grant No. HPR-1(24), Part II
	13. Type of Report and Period Covered
12. Sponsoring Agency Name and Address Indiana Department of Highways State Office Building 100 N. Senate Avenue Indianapolis, IN 46204	Final Report
	14. Sponsoring Agency Code NCP (4C2A3022)

15. Supplementary Notes

Prepared in cooperation with the U.S. Department of Transportation, Federal Highway Administration. Study title is "Effects of Asphalt Composition and Compaction on the Performance of Asphalt Pavement Mixtures."

16. Abstract

This report is presented in two parts. The first part presents the work done to characterize the fabric of this asphalt sand mix surface and to reproduce this fabric in the laboratory. In addition, it examines the field compaction time requirements for these materials. The second part evaluates the use of blended asphalts, as well as the use of high pressure-gel permeation chromatography to characterize the chemical composition of asphalts.

Based upon the comparison of the pore-size distribution of the fabric of both laboratory and field compacted mixtures, the gyratory and kneading compactors created satisfactorily equivalent laboratory fabrics to those of field cores. Very limited performance data suggested that good performance is associated with fabric that has a wide-spread of void sizes, with no major portion being concentrated at any one size.

No major differences in behavior were found for the artificially blended asphalts, in general, although rich asphaltene asphalts show a higher hardening rate at high temperatures. Blended ROSE asphalts do not create differences in performance than straight-run produced asphalts. The asphalt chemical composition does appear associated with individual performance characteristics; this suggests promise for the use of HP-GPC in the continuing effort to produce quality performance of asphalt pavement mixtures.

17. Key Words	18. Distribution Statement
pore size distribution; field mix fabric; field compaction time; surface wearing courses; laboratory compaction fabric; asphalt composition; high pressure-gel permeation chromatography; blended asphalts	No restrictions. This document is available to the public through the National Technical Information Service, Springfield, VA 22161.

19. Security Classif. (of this report)	20. Security Classif. (of this page)	21. No. of Pages	22. Price
Unclassified	Unclassified	125	

Form DOT F 1700.7 (8-69)

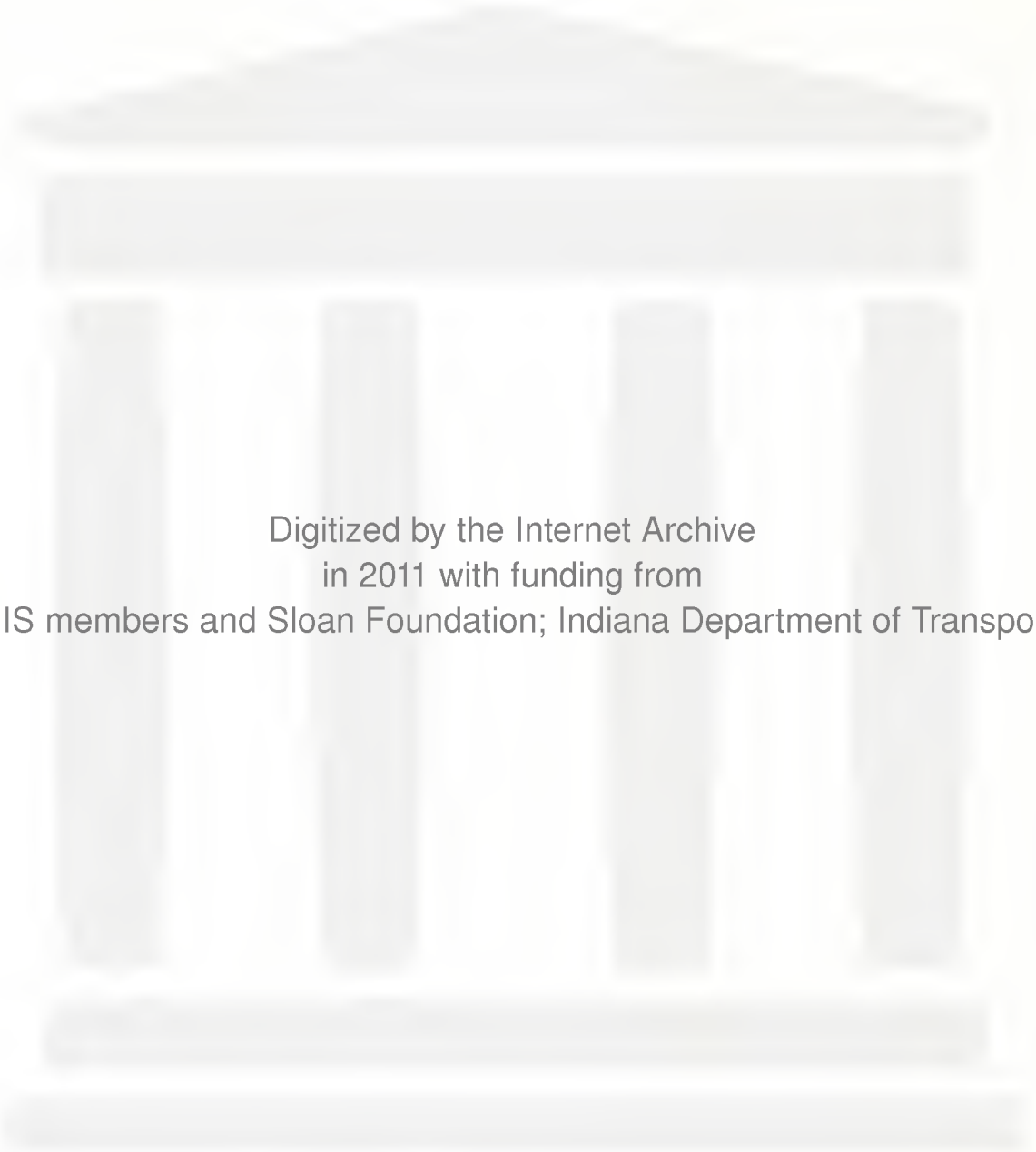

TABLE OF CONTENTS

LIST OF TABLES

LIST OF FIGURES

PART I

EFFECTS OF ASPHALT COMPOSITION AND COMPACTION ON THE PERFORMANCE OF ASPHALT PAVEMENT MIXTURES

Contribution from the
work of R. L. Aunan (1987)
and R. Luna (1985)

CHAPTER 1

INTRODUCTION

In recent years surface courses have suffered distress due to heavy traffic loads mostly on Interstate highways. These thin surface courses have high voids content to obtain good skid resistance and at the same time provide a smooth riding surface. The most common type of distress was delamination due to very high air voids in the "post-construction" stage. A difference of densities in the top and the bottom layer caused by further compaction from in-service traffic loads produced a horizontal plane of failure at approximately mid-depth of the overlay. These observations suggested a focus upon composition and compaction of those materials in the search for a solution to the problem.

The asphalt pavement industry makes use of several standard procedures to study the physical properties and characteristics of most bituminous mixtures. Several compaction methods and testing procedures (destructive and non-destructive) were chosen to study the materials being used in the surface courses noted above.

In the earthwork field the details of how the material is compacted determines the arrangement of components of the mix, i.e., the material fabric. It is the fabric, or the aggregate framework, that controls subsequent performance. It was thought that field procedures produce different fabrics than do laboratory procedures. In the asphalt pavement industry, it is not known which of the laboratory procedures best simulates the fabric development of field procedures. The answer to this question is one of the major objectives of this study.

Measures of the fabric of field cores and laboratory specimens were compared for comparable bulk specific gravity. Correlations were then attempted, and the search was made for which laboratory procedure created analogous fabric descriptors. If the fabric could be correlated to in-service performance it would allow feedback into the mix design process. Thus, a major portion of this study is an examination of fabric of the sand mixes as it affects our understanding of the mix design procedures.

Four compaction methods were used: Gyratory, Kneading, Marshall, and Vibratory. Two kinds of binders were used: an asphalt cement (AC-20) and medium setting high float asphalt emulsion (AE-60). Three aggregates were used in the two mixes: pit-run gravel-sand, crushed gravel-sand, and 70% sand and 30% crushed limestone. A small study was made to determine, for each compaction method, which combination of procedure would replicate

the densities produced in the field. Then the effects of gradation, binder, and aggregate were examined. Pore size distribution studies were performed on the laboratory samples as well as field cores obtained from field installations of those materials. Comparison of the pore size data would then allow the determination of the procedure which best replicated the field fabric.

Compaction of a bituminous mixture must be completed within a certain time frame which depends upon the cooling characteristics of the paving overlay. Compaction occurring within this time frame will help densify and stabilize the pavement for future taffic loads. The temperature-time relationship for a bituminous overlay strongly depends on the mat thickness and prevailing environmental conditions. The thermal properties of the bituminous mixture affect cooling rates to a lesser degree. To determine the allowable time of compaction, the "Compaction Time Window", the thermal conductivity of the compacted mix was determined and use was made of previous thorough investigations into the effects of initial mix temperature and prevailing environmental conditions. This portion of the study created cooling curves for the sand mix overlays for various air and base temperatures and wind velocities. In addition, the minimum compaction temperatures at which mixtures containing AC-20 and AE-60 could be compacted were determined. Visual observation of the cooling curves and knowledge of the

minimum effective compaction temperatures will permit the allowable compaction time to be determined.

It is hoped that the development of the foregoing goals will assist in creating better performing sand mix overlays. These developments as well as suggestions for implementing them in present practice, are described in the sections of this report which follow.

CHAPTER 2

MATERIALS AND EQUIPMENT

2.1 Materials.

The same materials were used for both the fabric characterization study and the compaction duplication study. These materials are described in the sections that follow.

2.1.1 Aggregates.

Three materials were used as aggregates for the bituminous mixture: local material, crushed agricultural limestone (agg lime), and a crushed gravel-sand. The first material was a local pit-run gravel-sand obtained from the Western Material Company in West Lafayette, Indiana. The second material, crushed agg lime, was quarried in Indiana, and the crushed gravel-sand was obtained from Triple G. Perrysville, Terre Haute, Indiana.

2.1.2 Asphalt Binders.

Two asphaltic binders are used in sand mix overlays in Indiana: AC-20 and AE-60. The AC-20 was obtained from the Amoco Oil Company for testing purposes. The AE-60 (IDOH designation) is a high-float medium setting emulsified asphalt formulated and

provided by the laboratory of McConnaughay Emulsions in Lafayette, Indiana. The basic properties of these binders are shown in Table 2.1.

Table 2.1 Properties of Asphaltic Binders.

AC-20	
Kinematic Viscosity	
135 C (275 F), Cs	236.0
Penetration	
25 C (77 F), 100g, 5 sec.	60
AE-60	
Residue by distillation, %	70.7
Penetration of residue after distillation	
25 C (77 F), 100g, 5 sec-min.	60

2.1.3 Job Mix Formula.

2.1.3.1 Gradations.

After some discussion, two gradations, representing those commonly used by the Indiana Department of Highways on Sand Mix Projects, were examined. The first gradation, G2, was based on pavement sections showing good performance characteristics. The second gradation, FM, was based on a Fineness Modulus concept and has only recently been used. The FM and G2 gradation curves, as well as the Indiana State Highway Commission (ISHC) Standard Specifications are shown in Figure 2.1.

2.1.3.2 Combinations of Aggregate.

Initially, three aggregate blends were investigated; one consisted of 100% local gravel-sand, another combined 70% local material and 30% crushed agg lime, while 100% manufactured (crushed) aggregate was the third constituent. The crushed gravel-sand was not studied to obtain field core comparisons, but to determine the effect of aggregate angularity on pore size distribution. Subsequent changes in Indiana specifications concerning the aggregate constituent placed a limit of 20% agg lime in a mix. Therefore, the 70-30 blend was replaced by a 90-10 combination in the latter part of the study. Table 2.2 shows properties of three aggregate proportions used..

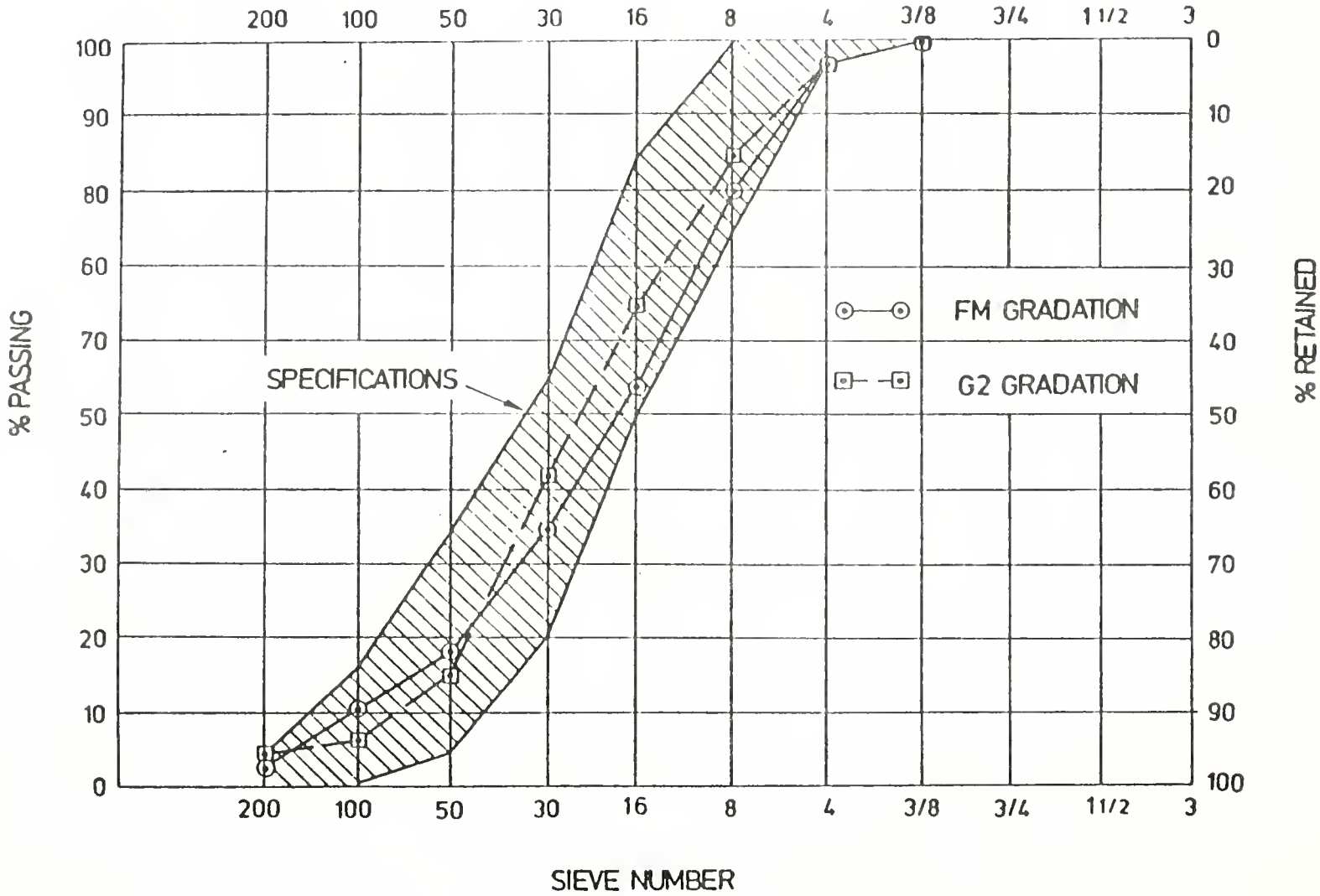

Figure 2.1 FM and G2 Gradation Specifications.

Table 2.2 Properties of Mineral Aggregate.

Local Gravel-Sand		
Apparent Specific Gravity		2.661
Bulk Specific Gravity (SSD)		2.615
Absorption, %		1.08
Florida Bearing Values,	G2	64.0
	FM	67.0
70% Local and 30% Agg Lime		
Apparent Specific Gravity		2.771
Bulk Specific Gravity		2.643
Absorption, %		0.94
Florida Bearing Value,	G2	66.0
	FM	69.0
100% Crushed Aggregated		
Apparent Specific Gravity		2.695
Bulk Specific Gravity		2.669
Absorption, %		0.36
Florida Bearing Value,	G2	86.0
	FM	88.0

2.1.3.3 Asphalt Contents.

Asphalt content (A.C.) of 7.5%, based on total weight of mix, was found to be optimum. This A.C. is the mid-point of the range allowed by ISHC Standard Specifications.

2.2 Equipment.

Four laboratory compaction procedures were used for both studies: the Gyratory, Kneading, Marshall, and Vibratory. These are significantly different procedures for imparting energy to densify the mix, and they offer the possibility of producing different fabrics.

2.2.1 Laboratory Compactors and Compaction Parameters

Compaction of the bituminous mixture to the proper density could be achieved by a number of combinations of compaction variables for each compactor. In addition to varying the independent compactor variables, the amount of material to be compacted at one time, commonly called the compacted lift, can influence the efficiency of a compactor to arrange and compact particles. Thus, the amount of material compacted to form a sample was varied between 500 grams and 1050 grams. Three compaction temperatures, 230, 180, and 150 degrees Farenheit were investigated as well. A target density for the laboratory samples of 135 pcf was the criterion controlling the compactive effort imparted by each compactor and the combinations of variables. Previously, it

had been determined that the Gyratory and Kneading Compactors offered the most potential for reproducing the field fabric (30), and for this reason these two compactors were most extensively studied.

2.2.1.1 Gyratory Testing Machine, GTM.

The Gyratory Testing Machine (Compactor) can simulate the effects of roller compaction and traffic because of its rolling, undulating motion that kneads the test material. Three states of stress are applied to the sample to cause this simulation: vertical, lateral, and shear induced by the combinations of a vertical ram, lateral confinement, and a rotating arm on top of a circular platform which rotates in an inclined plane. When using the GTM, the contact pressure can be controlled by the vertical ram pressure to correspond to the in-service or the rolling pressures. The GTM has three variable parameters: vertical ram pressure, number of revolutions, and gyratory inclination angle. A logical design procedure would be to utilize a ram pressure and angle of gyration similar to actual contact pressures and strains imparted during field rolling. As a guide, a minimum of twenty revolutions is required to account for the initial roller compaction (34). This study varied the vertical ram pressure from 20 to 70 psi with the corresponding number of revolutions varying from 35 to 15. Each of the procedures applied an additional 5 revolutions of leveling pressure (no applied gyratory angle) at the end of the compaction procedure. Analysis of results as testing

progressed showed that lower vertical pressures combined with a longer compaction time between reproduced field fabrics. The physical limitations of the compactor, however, limited the minimum vertical pressure to 20 psi; lower pressures would not compact the sample. The gyratory angle was held constant at 1 degree as suggested (1) and because the gyratory action was ineffective with less applied angle.

2.2.1.2 California Kneading Compactor.

The Kneading Compactor applies pressure to the mixture in an open-end mold through a tamping foot with a contact area of 3.2 square inches, the total sample area being 12.6 square inches. The pressure is applied hydraulically with the magnitude of pressure being regulated by air pressure. After kneading the mixture, a leveling load is applied to the entire sample area through the use of a static loading machine. The variable parameters for this procedure are: maximum contact pressure, number of tamps, and leveling load.

Operation of the Kneading Compactor had to be modified for this study but basically followed the procedure stated in ASTM D-1561. The maximum contact pressure allowable was 90 psi, well below the 250 psi standard pressure required by the Hveem method, because higher pressures resulted in the tamping foot punching through the mixture and pulling it out of the mold on the upstroke. A maximum leveling load of 5000 pounds applied after

kneading the mix was necessary to produce samples which met the density criterion. As with the GTM, it was determined that lower pressures and more compaction time better produced the desired fabric characteristics. Thus, initial contact pressures were near the lower end of the physical capabilities of the compactor. The contact pressure was varied between 90 and 60 psi with the corresponding compaction time varying from 3 to 5 minutes, where one application of pressure occurs every second and a half. Again, due to physical limitations of the Kneading Compactor, 60 psi was the minimum contact pressure capable of compacting the material.

2.2.1.3 Marshall (Impact) Compactor.

Compaction by the Marshall Compactor results from an impact of a weight upon the surface of the mix. This compaction procedure does not try to imitate any field procedures, but it has become a major component of bituminous mix design procedures. The variable parameters are: weight of hammer, free-fall distance, and number of impacts per sample side.

Samples compacted in the Marshall Compactor followed ASTM D-1559. Previous work (1) established the gyratory compaction criteria that are essentially equivalent to 50 and 75 blow Marshall compaction, i.e. 100 psi and 200 psi ram pressure, respectively, with a 1 degree angle of gyration and 30 revolution plus 3 for leveling. Previous studies (30) determined that a 10

pound hammer dropped 18 inches limited the number of trials performed. The difference in densities between 25 and 30 blows per side was indistinguishable so both were tested.

2.2.1.4 Double-End Vibratory Compactor.

The Vibratory Compactor was designed to simulate the action of vibratory rollers. The vibratory action is obtained by compressed air causing a piston to vibrate vertically resulting in the acceleration of the compactor head. Compaction of the samples is obtained by the advance of the vibrating unit through the use of the Riehle Machine, Static Compactor. The variable parameters for this procedure are: maximum applied load, rate of vibrating unit advancement, and air pressure causing vibration.

Vibratory compaction was performed by placing the mold containing the loose mixture in the Riehle Machine. Vibration of the piston was begun then the compacting pressure exerted. The vibratory action was most effective at low vertical pressures and uniquely arrange the particles during this time; as the vertical load was increased, the vibrating action decreased. The air pressure causing the piston vibration was held constant at 50 psi and the maximum load was limited to 15,000 pounds due to the compressibility of the neoprene cushion. This compressibility resulted in densities slightly lower than 135 pcf. The rate of load application was varied between 0.25 and 0.5 inches per minute.

A summary of the combinations of compaction parameters used is shown in Table 2.3. It should be noted that the parameters required to create samples of the correct densities in this study were much less than those used in typical mix design procedures. Compaction with the Kneading Compactor specifies 20 tamping blows at 250 psi and 12,600 pound leveling load and Gyratory Compaction requires 200 psi vertical ram pressure with 60 revolutions.

2.2.2. Testing Equipment.

The low pressure mercury porosimetry intrusion device was used to characterize the fabric. Additionally, the pulse velocity sonic wave device, resilient modulus equipment, Hveem stabilometer, and Marshall testing equipment were used to evaluate the mix behavior.

2.2.2.1. Pulse Velocity Sonic Wave Apparatus.

This simple device is composed of a transmitter and a receiver which are both hooked to an electronic counter (See Figure 2.2). Essentially, this counter measures the time that a wave takes to travel from the transmitter to the receiver. This equipment was specially mounted on a frame designed to apply pressure evenly on both sides of the specimen. A thin coat of petroleum gel was used to improve the contact on the specimen.

2.2.2.2. Diametral Resilient Modulus Apparatus.

Table 2.3 Compaction Parameters Investigated.

Gyratory Compactor (all at 1° gyratory angle)

20 psi vertical pressure, 35 revolutions

50 psi vertical pressure, 20 revolutions

70 psi vertical pressure, 15 revolutions

Kneading Compactor (all with 5000 lb leveling load)

60 psi contact pressure, 150 tamps

80 psi contact pressure, 120 tamps

90 psi contact pressure, 90 tamps

Marshall Compactor

30 blows per side, 10 lb hammer, 18 inch freefall

25 blows per side, 10 lb hammer, 18 inch freefall

Vibratory Compactor (all 50 psi air pressure)

1/4 inch per minute advance rate, 15000 lb max load

1/2 inch per minute advance rate, 15000 lb max load

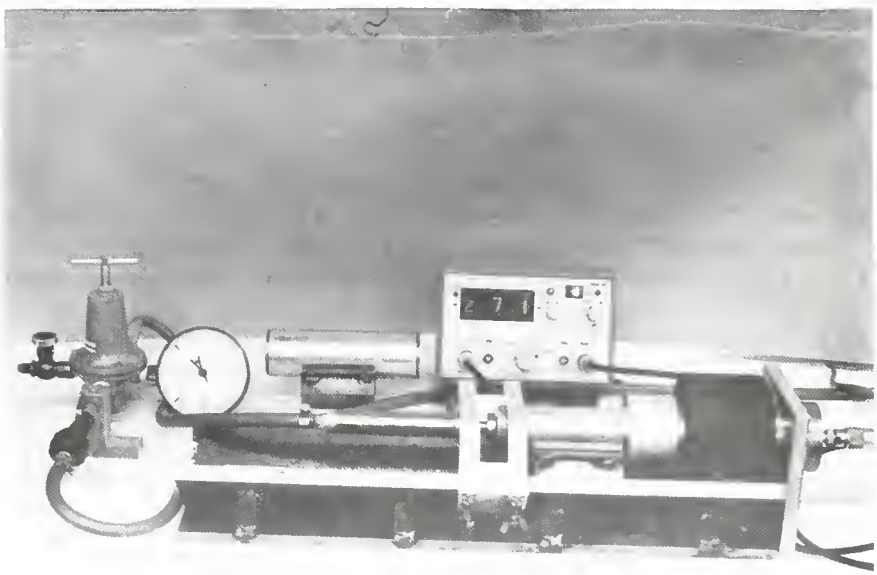

Figure 2.2 Pulse Velocity Sonic Wave Machine.

The Resilient Modulus equipment consisted of a compressed air resource, solenoid valve, piston, load frame, measuring devices, and a two-channel chart recorder. A solenoid valve activated by an electronic circuit was used to provide pulses of compressed air. The pulses transmitted a light pulsating load to the specimen by means of a piston fixed on top of the loading frame.

The load pulses were applied every 3 seconds with a dwell time of 0.1 seconds. The magnitude of the load was controlled by adjusting the activating air pressure. The pulse load used throughout all the testing was 50 lbs. The load was applied across the vertical diameter of the specimen using two curved stainless steel loading strips of 1/2 inch width.

2.2.2.3. Hveem Stabilometer.

The Hveem Stabilometer is a steel triaxial cell that measures the lateral deformation of a compacted mix. This triaxial cell has in its chamber a mixture of oil and air which requires calibration for its proper use. A dial gage that measures the pressure in the chamber is attached on one side and connected to a cylinder with a piston that will measure the displacement of the oil in the chamber by means of a manual handle.

2.2.2.4. Marshall Testing Equipment.

The Marshall Testing Machine is a loading frame that loads

the specimen on its diametral side at a deformation rate of 2 inches per minute. This strength testing machine records simultaneously the deformation (flow) and the load (stability) by means of a servo x-y plotter.

2.2.2.5. Low Pressure Mercury Porosimetry Intrusion Device.

The porosimeter is a high vacuum system that consists of a high-vacuum pump, vacuum-to-atmospheric differential manometer, connecting manifold, McCleod gage, immersing device and penetrometer. The connecting manifold connects the equipment by means of minimum vacuum tubing. The manometer shows the actual pressure in the system to the nearest millimeter of mercury. The McCleod gage is used for readings of high vacuum in the system to the nearest 0.01 mm of Hg. The immersing device holds the penetrometer and sufficient quantities of mercury to allow fill the device by tilting it into its filling position. The penetrometer is an accurately manufactured calibrated stem with a small chamber at the end to hold the sample (See Figure 2.3). This equipment must be tightly sealed.

Mercury intrusion is done in increments by increasing the pressure and recording the volume of mercury entering the sample. A computer program was created to reduce the data to a pore size distribution graph.

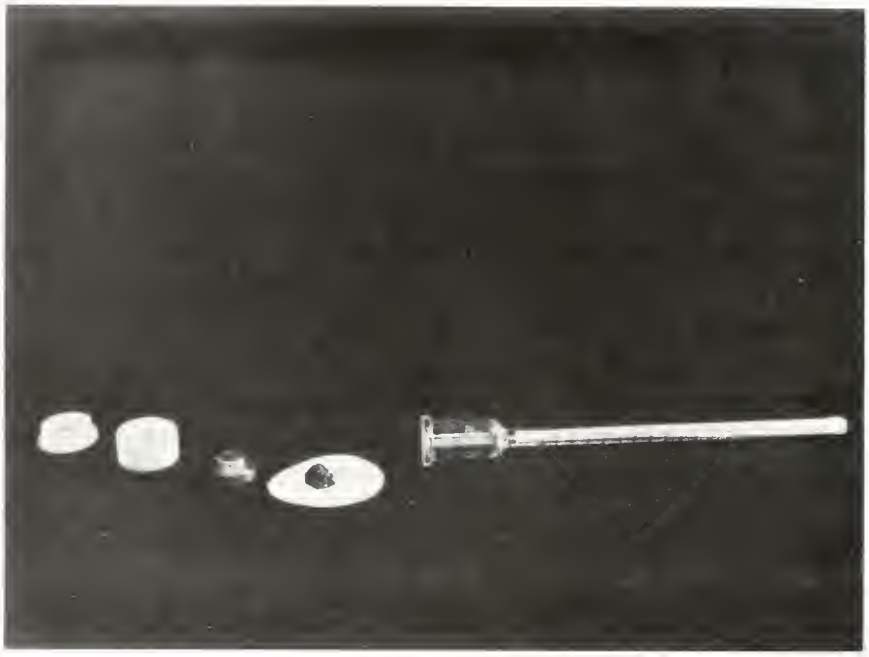

Figure 2.3 Unassembled Penetrometer, Sample, Metal Cap and Teflon Cap.

CHAPTER 3

TESTING PROCEDURE

3.1. Bulk Specific Gravity and Percent Air Voids.

The saturated surface-dry bulk specific gravity was determined for all field cores and laboratory specimens by means of ASTM D 2726-79. The theoretical maximum specific gravity (ASTM D 2041-78) of each mixture was also determined. The results of these two tests make it possible to determine the percent air voids by relating the actual density of the specimen and its maximum density with zero air voids condition.

3.2. Pulse Velocity Sonic Wave Test.

This non-destructive test (ASTM D2845-83) was performed several times for each specimen perpendicular to its diameter. A calibration before using the apparatus was accomplished by using an aluminum rod with known pulse velocity. This test proved to be very sensitive to the placement of the transducers on the specimen and operator technique. A special frame was designed to apply the same pressure (22 psi.) in each test by means of an air activated piston. To obtain a good contact between the transducers and the specimen a thin coat of petroleum gel was placed at

each contact area. The apparatus records the time (micro secs.) it takes for the sonic wave to reach the receiver. The pulse velocity was obtained by dividing the thickness of the specimen by the time average. If enough data are obtained, a correlation between density and pulse velocity can be generated.

3.3. Resilient Modulus Test.

This was the second non-destructive test performed on the specimens (ASTM D4123). Here the specimen was placed on the loading plates on its side and a pulse of 50 psi. was applied through the apparatus, and the resulting deformations while loading were recorded in a linear chart recorder. A typical trace of the vertical deformation pattern is shown in Figure 3.1. It is most important to properly place the specimen on the loading plates, exactly on the center of the loading plates. The pulsating load was applied several times to the specimen before the results were recorded. The specimen was rotated 90 degrees and the load was applied several times in the new position; then rotated 45 degrees, and tested again. If large differences were found between deformation values for these positions, additional testing was performed and the unreasonable results were discarded. Deformations were recorded for each side of the specimen, averaged with the other results; and then the deformation at the point of loading was calculated by linear interpolation. With the value of vertical deformation the Resilient Modulus (MR) can be obtained by using the following equations:

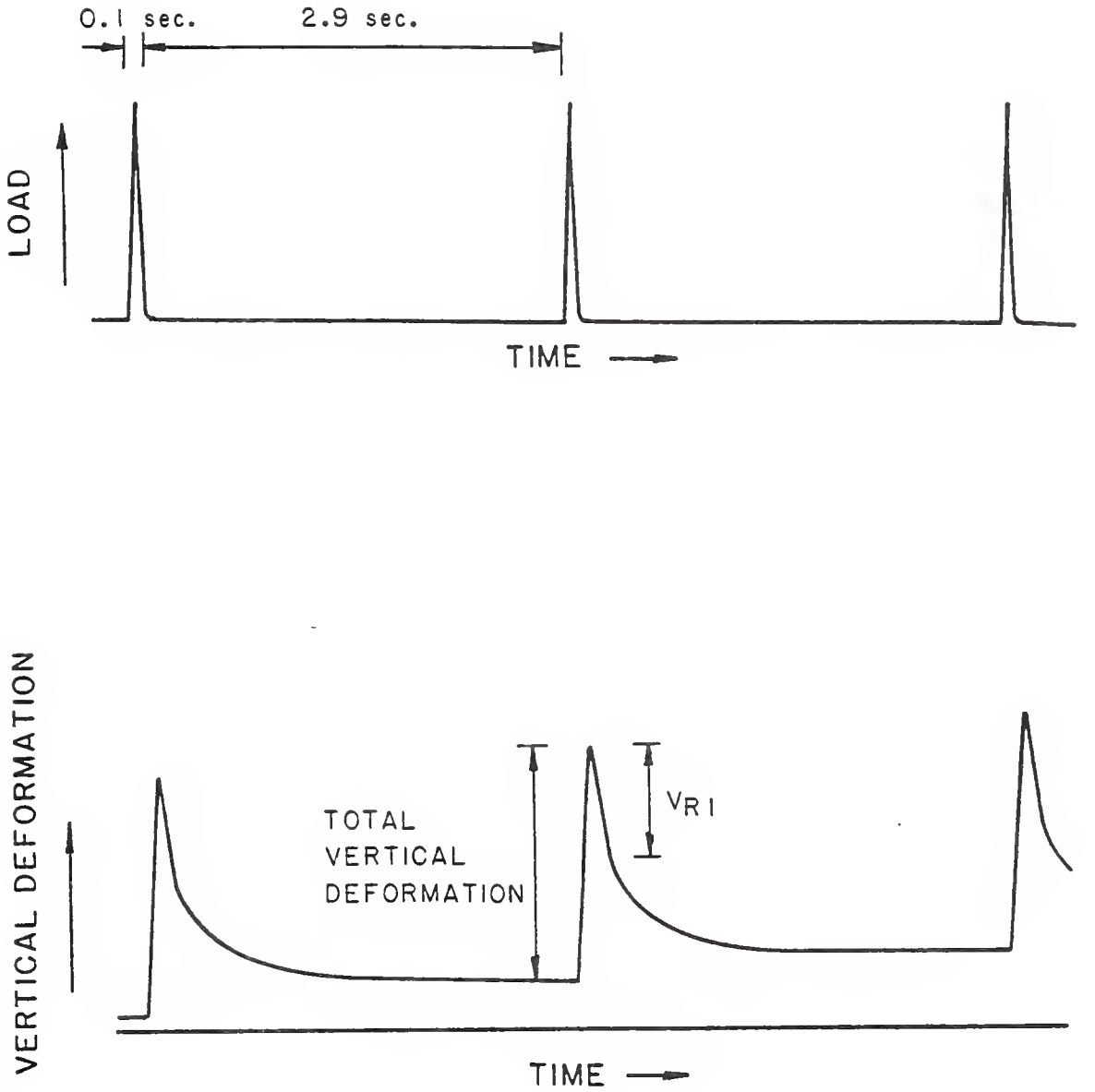

Figure 3.1 Typical Load and Deformation versus time trace in the Resilient Modulus Test.

$$v = 3.59\frac{H_{ri}}{V_{ri}} - 0.27$$

$$M_R = \frac{P(v + 0.27)}{h(H_{ri})}$$

$$M_R = \frac{3.59(P)}{h(V_{ri})}$$

where,

v = instantaneous resilient Poisson's ratio.
M_R = instantaneous resilient modulus, psi.
H_{ri} = instantaneous resilient horizontal deformation, in.
V_{ri} = instantaneous resilient vertical deformation, in.
P_{ri} = repeated load, lbs.
h = specimen height, in.

3.4. Hveem Stabilometer Test Procedure.

Since the State of Indiana makes use of the Hveem test in the design of bituminous mixtures, it was decided that the sand mix should be characterized by the Hveem procedure. This procedure follows ASTM D 1560-76, except the specimens were prepared by different compaction methods. Only the S-value was obtained from the test for the purposes of studying the plastic character of the mix. The following is the equation used to calculate the S-value.

$$S = \frac{22.2}{\frac{P_h(D)}{P_v - P_h} + 0.222}$$

where,

S = stabilometer value
P_h = horizontal pressure, psi
D = displacement on specimen, turns
P_v = vertical pressure, (typical 400 psi)

3.5. Marshall Testing Procedure.

The Marshall procedure was only nominally used because the sand mix has a low Marshall Stability due to its plastic character; secondarily, this test is a destructive test. This test procedure follows the standard ASTM D-1559-76 except that specimens were prepared by different compaction methods.

3.6. Pore Size Distribution by Mercury Porosimetry Intrusion.

This procedure was performed on specimens produced in the laboratory as well as on specimens of field cores. Samples were cured for not less than seven days to assure removal of most of the volatiles. Samples were first frozen to produce a brittle condition. This enabled one to crack the specimen and obtain an adequate (a 0.1 cm cube) size sample from the center. The weight of this cracked piece was between one and three grams.

After the sample was weighed in an analytical balance, it was placed in the porosimeter penetrometer and the cap was sealed with high-vacuum grease. The penetrometer was then placed in the filling device and this connection was sealed by fitted O-rings. The high vacuum pump was used to create a vacuum in the system of at least 0.02 mm. of Hg from absolute. If this vacuum level could be reached within 30 minutes, a small leak in the system was likely present and the equipment was disassembled and checked.

The filling device must be filled with sufficient mercury to cover the penetrometer and fill it. When the filling device is tilted to its filling position the chamber of the penetrometer should be tapped with a pencil to assure that the mercury intrudes all the voids at this pressure level. The filling device was then brought to its normal position and the first reading from the penetrometer was obtained. After each increment of pressure, tapping with a pencil is required until the reading on the penetrometer is constant.

This study required a close look at the large pore structure. More increments than usual were performed during intrusion, to produce the typical result shown in Figure 3.2. Only low pressure intrusions were done because the interest of the project is in the larger fabric framework. The compressibility of the asphaltic binder is not affected by this applied change of pressures. If penetrations at higher pressures are to be performed in the future, compensations for compressibility of the asphalt would be required.

Washburn (1921) pointed out that mercury will not voluntarily enter the pores in most materials and that pressure is required to induce it to do so. He derived a simple equation, the Washburn equation, that relates the required pressure and the size of pore being entered. He used a cylinder as a geometric model of a pore.

$$P = \frac{-2\gamma\cos(\theta)}{r}$$

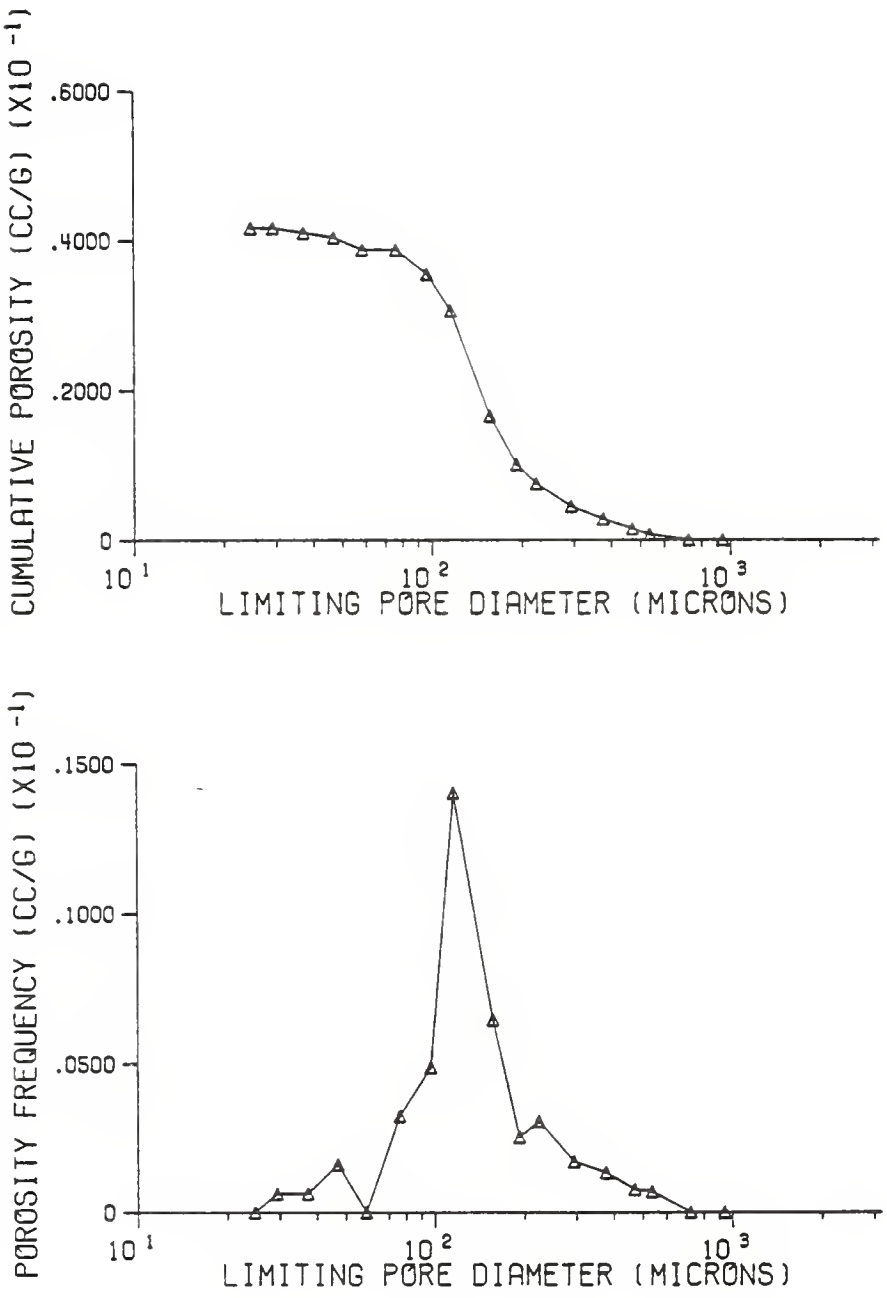

Figure 3.2 Typical Pore Size Distribution Curves.

where,

P = pressure causing the intrusion.
r = radius of cylindrical pore.
γ = surface tension of mercury.
θ = contact angle between mercury and pore wall.

Because most porous materials do not have cylindrical pore geometries, this equation yields only the diameter of an equivalent cylindrical pore that would be intruded at the given pressure.

The increments of pressure applied to a sample immersed in mercury relate to the size of the pores. These increments were calculated by an exponential equation that will give an even spacing of data points along the logarithmic x-axis.

$$\frac{P_i}{P_{i-1}} = 10^c$$

where,

P_i = ith increment of pressure.
P_{i-1} = increment of pressure before i.
c = constant of increment

Small increments were desired in this study; a magnitude for c of 0.0989 was used, based on experience of investigators on similar projects.

The porosimetry results in differential and cumulative distribution curves (Figure 3.2). To describe these curves various possible descriptors have been used, as shown in Table 3.1. The descriptors used for this study were selected from those shown.

In addition, "LD" represents the logarithm of the diameter at which peak pore frequency occurs. The term "V/T" is the ratio

of the volume intruded at the peak frequency to the total intruded volume. The terms "AI" and "AD" are the onset and offset angles, respectively, to the peak of the differential curve. The term "LD_{50}" is the logarithm of the diameter at which 50% of the intruded volume is in larger pores. Finally, the term "T/P" was created as the ratio of total volume of voids intruded to the total volume of voids.

The descriptors are shown in Figures 3.3 and 3.4

Table 3.1 Compilation of Commonly Used PSD Curve Descriptors

M1	maximum porosity frequency
L1	log of diameter having maximum porosity frequency, "peak"
L2	log of diameter of "inflection point" where increase in porosity frequency to peak begins
A1	onset angle to peak on differential plot
A2	total angle difference at peak
P1	total porosity
P2	percentage of total porosity intruded
D2	log of diameter where 25% of intruded volume is in larger pores
D3	log of diameter where 50% of intruded volume is in larger pores
D4	log of diameter where 75% of intruded volume is in larger pores
D5	log of diameter where 10% of intruded volume is in larger pores
D6	log of diameter where 60% of intruded volume is in larger pores
R1	ratio of 60% diameter/25% diameter
R2	ratio of 75% diameter/50% diameter
R3	ratio of 75% diameter/25% diameter
R4	ratio of 50% diameter/25% diameter
R5	L1 + R1

Table 3.1 (continued)

R6	ratio of inflection point diameter/peak diameter
R7	(50% diameter + 60% diameter)/25% diameter
X1	arithmetic value of L1,(10^{L1})
X2	arithmetic value of D2
X3	arithmetic value of D3
X4	arithmetic value of D4
X5	arithmetic value of D5
X6	arithmetic value of D6
X7	arithmetic value of L2
PC1	percentage of intruded volume in pores larger than peak diameter
PC2	percentage of intruded volume in pores larger than the inflection diameter
PC3	percentage of intruded volume in pores larger than 1 micron
S1	PC1 - PC3
S2	PC2 - PC3
S3	X3 + X6
S4	X1 + R2
S5	P2 + PC1
S6	P2 + PC2
S7	P2 + PC3

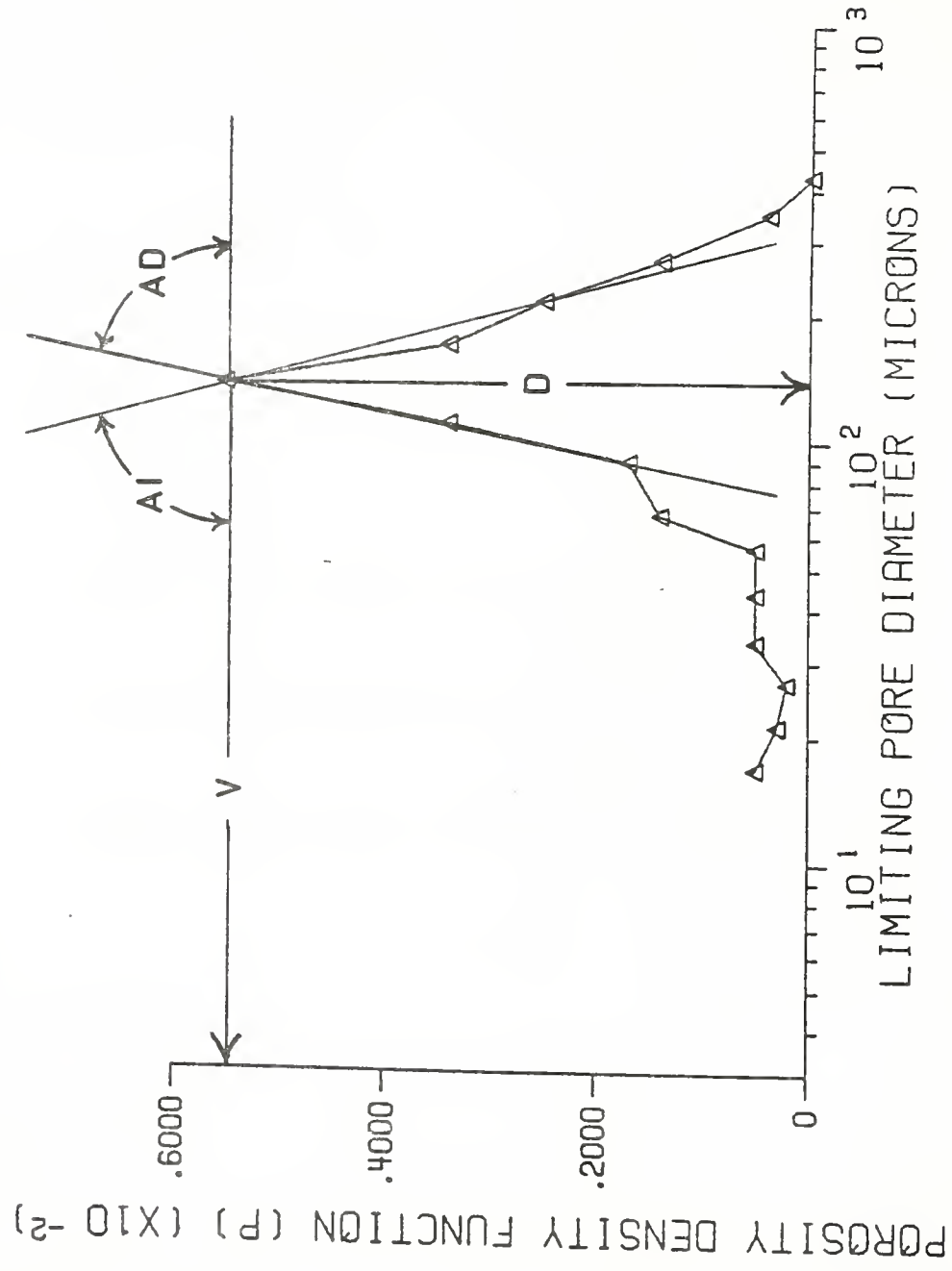

Figure 3.3 Differential PSD Curve and Descriptors.

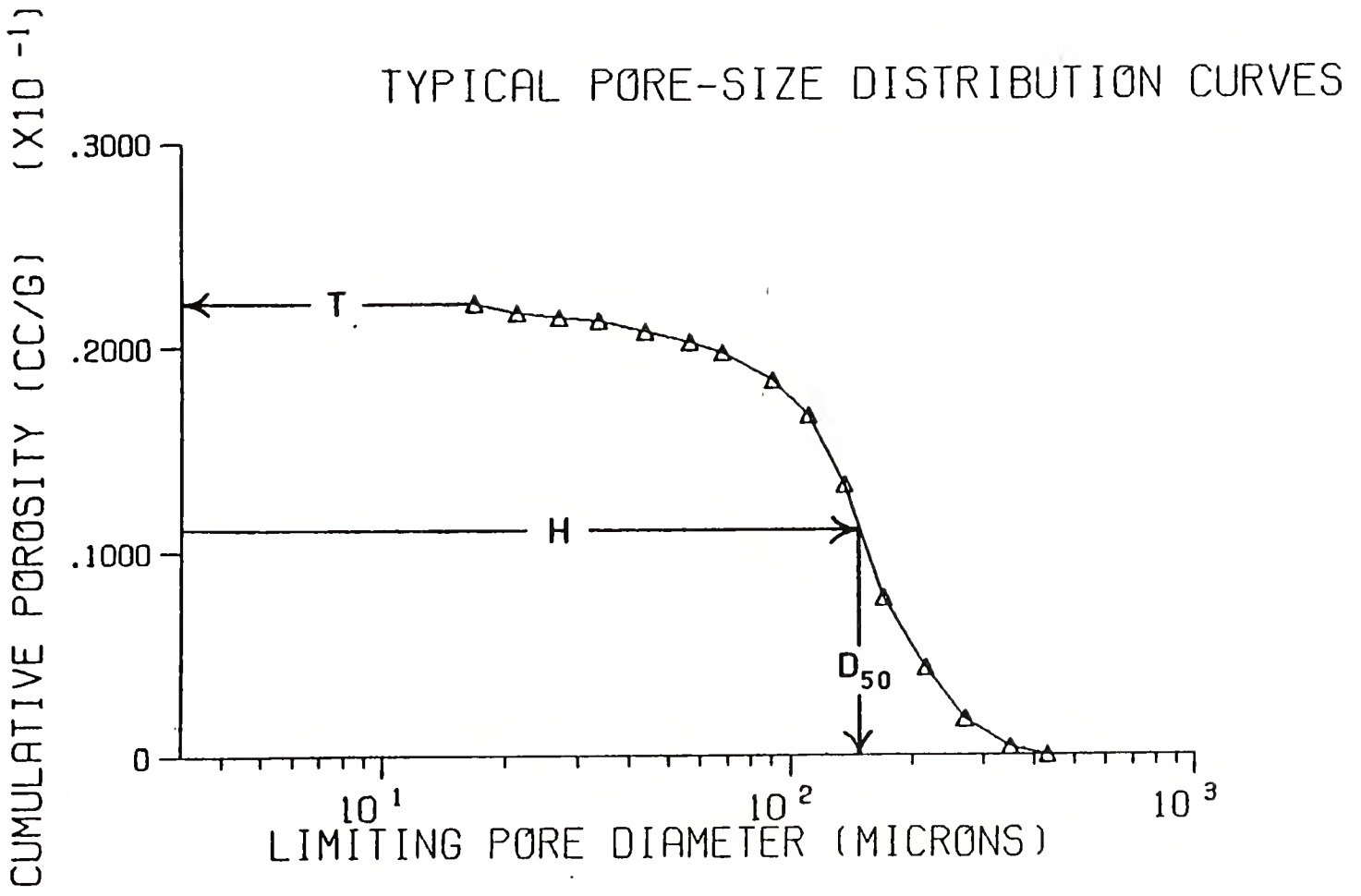

Figure 3.4 **Cumulative PSD Curve and Descriptors.**

CHAPTER 4

ANALYSIS OF RESULTS

4.1. Pore Size Distributions

A set of 6 specimens were taken from each compacted sample or field core for pore size distributions. Means and standard deviations were obtained for each set of the descriptors that were useful in comparisons. Tables 4.1, 4.2, and 4.3 contain data for comparable laboratory samples and field cores. The underlined data indicate an equivalence in that descriptor between the laboratory and field state (i.e., similarity in fabrics as indicated by that descriptor).

Tables 4.4, 4.5, 4.6 contain data for laboratory samples only. There were available no field cores of comparable material. These data allow an examination of the effects of aggregate and compaction temperature upon the fabric.

Table 4.3 has very few laboratory data because of the inability in the laboratory to create samples to the field density.

An examination of these data suggests that the gyratory testing machine offers the closest replication of the field fabric.

Table 4.1 Results of Local G2 Curve Descriptors.

	LD	V/T	AI	AD	LD_{50}	T/P
Field Cores	2.122	0.215	65.5	65.2	2.164	0.752
	(.106)	(.022)	(6.72)	(9.16)	(.069)	(.084)
Gyratory 230 F						
20 psi for 35 revs	1.984	0.221	37.8	44.5	2.082	0.427
	(0.126)	(0.026)	(14.72)	(21.16)	(.046)	(.066)
30 psi for 20 revs	2.130	0.244	53.2	65.2	2.129	0.457
	(0.065)	(0.022)	(11.65)	(6.89)	(.118)	(.122)
500g sample 30 psi	1.919	0.165	53.7	56.9	2.016	0.674
	(0.106)	(0.019)	(14.60)	(10.50)	(.084)	(.088)
Kneading 230 F						
90 psi for 3 min.	1.913	0.224	46.3	39.6	1.979	0.395
	(0.136)	(0.047)	(7.61)	(16.90)	(.076)	(.086)
Kneading 180 F						
90 psi for 3 min.	2.047	0.216	42.4	43.3	2.112	0.459
	(0.107)	(0.019)	(19.19)	(18.70)	(.057)	(.115)
Vibratory 230 F						
15000 lb .25 in/min	2.102	0.143	38.6	23.8	2.055	0.671
	(0.096)	(0.021)	(24.30)	(13.40)	(.040)	(.153)
Marshall 230 F						
25 blows/side	2.040	0.228	49.2	52.1	2.108	0.553
	(0.056)	(0.043)	(9.40)	(16.20)	(.038)	(.051)

( ) - Standard Deviation

_____ - Equivalent to field mean within a 95% confidence interval

Table 4.2 Results of 90-10 G2 Curve Descriptors.

	LD	V/T	AI	AD	LD_{50}	T/P
Field Cores	2.069	0.222	57.3	55.9	2.110	0.674
	(0.069)	(0.030)	(11.86)	(15.80)	(.051)	(.149)
Gyratory 230 F						
20 psi for 35 revs	2.034	0.200	44.0	51.4	2.070	0.486
	(0.110)	(0.024)	(10.59)	(9.23)	(.072)	(.040)
30 psi for 20 revs	2.019	0.196	39.8	41.9	2.050	0.484
	(0.115)	(0.022)	(21.19)	(18.51)	(.052)	(.075)
70 psi for 15 revs	1.969	0.197	32.8	26.1	2.030	0.430
	(0.110)	(0.026)	(12.10)	(11.35)	(.061)	(.080)
Gyratory 180 F						
20 psi for 35 revs	1.927	0.174	46.2	41.9	1.907	0.530
	(0.155)	(0.028)	(15.02)	(19.47)	(.096)	(.029)
Kneading 230 F						
90 psi for 3 min.	1.870	0.150	44.6	44.7	1.908	0.563
	(0.095)	(0.014)	(11.14)	(11.70)	(.087)	(.046)
60 psi for 5 min.	1.883	0.152	45.7	32.6	1.889	0.572
	(0.092)	(0.014)	(11.90)	(13.15)	(.064)	(.031)

( ) - Standard Deviations

_____ - Equivallent to field mean within a 95% confidence interval

Table 4.3 Results of Local FM Curve Descriptors.

	LD	V/T	AI	AD	LD_{50}	T/P
Field Cores	1.934	0.227	52.3	62.3	2.010	0.568
	(.090)	(.036)	(14.59)	(9.35)	(.044)	(.058)
Gyratory 230 F						
20 psi for 35 revs	1.706	0.124	19.8	17.9	1.785	0.306
	(.138)	(.028)	(14.24)	(13.36)	(.042)	(.045)

( ) - Standard Deviations

_____ - Equivalent to field mean within a 95% confidence interval

Table 4.4 Results of Local, G2, AC-20 Curve Descriptors.

	LD	V/T	AI	AD	LD_{50}	T/P
30 psi for 20 revs						
Gyratory 230	1.936	0.229	53.6	56.6	1.737	0.563
	(.107)	(.028)	(12.23)	(19.48)	(.675)	(.080)
Gyratory 180	2.069	0.207	47.4	55.9	2.106	0.465
	(.091)	(.012)	(7.66)	(6.68)	(.055)	(.039)
Gyratory 150	2.022	0.217	46.9	46.1	2.082	0.592
	(.092)	(.028)	(16.16)	(17.16)	(.037)	(.127)
90 psi for 3 min.						
Kneading 230	2.013	0.191	33.8	37.2	2.063	0.385
	(.089)	(.044)	(11.54)	(15.66)	(.063)	(.051)
Kneading 180	1.961	0.218	57.5	65.5	2.006	0.646
	(.139)	(.072)	(14.59)	(7.84)	(.077)	(.156)
Kneading 150	2.053	0.211	57.8	57.3	2.100	0.662
	(.061)	(.026)	(12.15)	(8.69)	(.085)	(.120)
70 psi for 15 revs						
Gyratory 230	2.130	0.185	49.9	38.6	2.081	0.529
	(.070)	(.079)	(17.65)	(25.19)	(.096)	(.133)

( ) - Standard Deviations

Table 4.5 Results of 70-30, G2, AC-20 Curve Descriptors.

	LD	V/T	AI	AD	LD_{50}	T/P
30 psi for 20 revs						
Gyratory 230 F	1.907	0.259	64.0	64.8	1.936	0.633
	(.120)	(.046)	(7.39)	(12.42)	(.112)	(.149)
Gyratory 180 F	2.001	0.217	58.4	65.2	2.072	0.613
	(.085)	(.041)	(9.07)	(6.94)	(.068)	(.071)
Gyratory 150 F	2.084	0.213	61.2	54.4	2.113	0.643
	(.048)	(.027)	(7.81)	(15.23)	(.047)	(.116)
90 psi for 3 min.						
Kneading 230 F	2.105	0.210	42.2	39.6	2.105	0.431
	(.088)	(.050)	(13.62)	(12.52)	(.043)	(.096)
Kneading 180 F	2.035	0.220	60.2	60.2	2.073	0.618
	(.113)	(.056)	(14.84)	(17.90)	(.117)	(.130)
Kneading 150 F	2.084	0.243	66.0	72.6	2.136	0.701
	(.048)	(.019)	(9.97)	(3.79)	(.040)	(.086)

( ) - Standard Deviations

Table 4.6 Results of Crushed, G2, AC-20 Curve Descriptors.

	LD	V/T	AI	AD	LD_{50}	T/P
30 psi for 20 revs						
Gyratory 230 F	2.131	0.269	77.7	77.8	2.168	0.818
	(.083)	(.015)	(5.47)	(1.92)	(.066)	(.068)
Gyratory 180 F	2.193	0.262	75.7	76.5	2.217	0.765
	(.050)	(.016)	(1.16)	(3.07)	(.063)	(.071)
Gyratory 150 F	2.128	0.201	64.7	70.8	2.176	0.725
	(.000)	(.019)	(8.81)	(7.57)	(.019)	(.112)
90 psi for 3 min.						
Kneading 230 F	2.090	0.249	68.2	69.4	2.142	0.758
	(.047)	(.039)	(6.58)	(9.55)	(.033)	(.111)
Kneading 180 F	2.143	0.249	75.8	74.1	2.170	0.787
	(.081)	(.030)	(4.77)	(7.39)	(.061)	(.068)
Kneading 150 F	2.209	0.237	67.8	73.8	2.256	0.727
	(.040)	(.024)	(7.65)	(3.90)	(.027)	(.125)

( ) - Standard Deviations

4.2. Effect of Compaction Temperatures.

The compaction temperatures for the specimens in this study was kept within the range of field compaction that IDOH specifies (i.e. 145°F to 230°F). This range of temperatures did not produce large variations in the final compacted mix.

Because results were more sensitive to changes than at lower temperatures, this suggests that if the mix is compacted at lower temperatures (150°F) in the field, the compacted layer would be more susceptible to changes in performance.

4.3. Effect of the Aggregate Types.

The densities increased as the aggregate types were varied in the following order: 70% sand and 30% crushed limestone, pit-run sand, crushed sand. It was thought that the changes in density were produced by the shape of the particles in the aggregate. Even though the densities varied with the types of aggregates used the stability values and the resilient modulus were not strongly affected.

The effect of aggregate angularity on pore size distribution, however, is very noticeable and consistent for all sets of compaction parameters. The more angular the aggregate, the larger the peak and 50^{th} percentile pore diameters. Furthermore, samples with higher percentages of angular aggregate had a larger

percentage of pores intruded. This means there is increased interconnection of voids.

4.4. Effect of the Gradations.

The Fineness Modulus design gradation produced laboratory samples of higher density than samples with aggregate gradation G2, (142 pcf versus 135 pcf) although subjected to the same compactive effort. The reduction in the average peak pore diameter and 50^{th} percentile diameter are thought to be a direct result of this increased density. There is slightly less pore volume concentrated about the peak frequency diameter for FM Gradation specimens, probably due to the deliberate grading characteristics on the lower sieves which also produced a "tighter" fabric; a tight fabric is one in which the pores are of smaller sizes and more often isolated as compared to the G2 Gradation.

4.5. Effect of Binder Type.

The two binders used were Asphalt Emulsion (AE-60) and Asphalt Cement (AC-20). As a result of the different specific gravities of these binders the densities of the specimens varied as well No major differences were found in the stability or strength properties for the different binders were used. In addition, it was observed that coating for both binders was acceptable when the appropriate mixing procedures were followed

4.6. Comparison of Stabilities between the Different Laboratory Compaction Methods.

The Hveem stability S-values were performed on all the compaction methods. Marshall compaction produced the most stable specimens in all the different materials used, even though the densities were the same as the specimens produced with the gyratory and kneading compactors. For gyratory and kneading compaction methods, the stability values were of similar magnitude in most cases. The vibratory compactor always resulted in the lowest stability values due to the lack of ability to compact to the desired density with effective vibrating load. For all compaction methods, Hveem S-values of 15 to 20 for the laboratory specimens showed good field performance.

4.7 Other Relationships.

The results of samples having a 90-10 combination of aggregate and AE-60 as a binder indicate that as the applied pressure is reduced and the time of compaction increased, the fabric obtained approaches that of the field cores. This is true for both the Gyratory and Kneading Compactors with the first being more sensitive. The trend is not followed, however, for the compacted samples containing only local material and is, in fact, reversed.

One definite trend observed from the results is that when the peak pore diameter is decreased, the 50^{th} percentile diameter

reacts similarly. Both of these result in less percentage of pore volume being intruded.

A consistent and important observation made from the results is that when the pores are concentrated about the peak there is a higher percentage of voids intruded. This trend is consistent for compaction temperatures, compactors, and pressure-time relationships and is more influential than the effects of LD and LD_{50}. When AC-20 is the binder, this tendency is more closely followed that when AE-60 was used.

Tests previously conducted on cores from good and poor performing pavement surfaces indicate that the poor performing pavements had larger volumes of pores at the peak. The set of samples obtained from good performing areas had pores more evenly distributed among the various pore diameters. On the basis of these limited results, it is believed that the FM Gradation could prove to be stable when subjected to service loads.

4.8 Compaction Time.

One facet of the bituminous pavement construction process which influences performance is the allowable compaction time (the "Compaction Time Window"). Compaction performed while the mixture is too hot will result in "shoving" of the material. Compaction performed after the mixture has cooled excessively will result in the required density not being achieved. These pavements compacted outside the "Compaction Time Window" are

unstable under further traffic loading resulting in unsatisfactory performance.

4.8.1 Heat Transfer Mechanisms.

Natural convection, or the transfer of heat from a solid to a fluid of a different temperature causes fluid motion near the surface of the solid. A hot-laid bituminous mixture creates a gradient which causes heat to flow from the mixture to the surrounding air. Gravity is the driving force producing this fluid motion which maintains the convective process. The rate of this transfer depends upon the ambient air temperature, initial mix temperatures, and wind velocity as well as less significant factors such as solar radiation and the heat transfer coefficient, h, of the sand mix.

The development of equations relating temperature to time for the free convective process are shown in heat transfer books (5,28). The equation used for practical application is one developed by Newton,

$$dq = (h_c)(dA)(T_s - T_\infty) \qquad (4.1)$$

where

dq = rate of heat transfer of convection

h_c = convective heat-transfer coefficient

dA = differential surface area

T_s = temperature of solid

T_∞ = fluid temperature far from the solid

4.8.2 Conductive Heat Transfer

The mechanism controlling the transfer of heat within the mixture and to the base material, conduction, has been determined to be a significant factor in the cooling of an asphalt pavement (40).

Again the derivation of transient conductive heat-transfer equations can be found in various publications (5,28,49). The general heat conduction equation which governs the temperature distribution and the conduction heat flow in a solid having uniform physical properties is

$$\frac{\partial^2 T}{\partial x^2} + \frac{\partial^2 T}{\partial y^2} + \frac{\partial^2 T}{\partial z^2} + \frac{\dot{q}}{k} = \frac{1}{\alpha}\frac{\partial T}{\partial \theta} \qquad (4.2)$$

where

T = initial fluid-solid temperature difference

k = thermal conductivity, assumed uniform and constant

α = thermal diffusivity

$\theta = t - t_f$ = temperature difference variable

t = temperature of the asphaltic mat

t_f = temperature of the surrounding air

For one-dimensional heat conduction with no internal heat source, Equation 4.2 becomes

$$\frac{\partial^2 T}{\partial z^2} = \frac{1}{\alpha}\frac{\partial T}{\partial \theta} \qquad (4.3)$$

where z is the vertical direction. The cooling of an asphaltic roadway can be approximated by this equation.

4.8.3 Influence of Thermal Properties

The thermal conductivity and diffusivity appear in all transient heat conduction problems; thus, the numerical values of these two properties influence the time-rate of temperature change within the mixture. The thermal diffusivity, however, depends upon the thermal conductivity, specific heat, and density of a material. Since the density of a bituminous mixture increases with compaction, the diffusivity and conductivity vary. Density changes due to compaction do not significantly affect the diffusivity and conductivity since density upon leaving the spreader is 85% of the compacted density. The effect of temperature on these properties is not influential either. Thus, the diffusivity and conductivity, for the purposes of this study, are assumed constant.

The convective heat-transfer coefficient is a complicated function of the fluid flow, the thermal properties of the fluid medium, and the geometry of the system. An exact evaluation of the heat transfer coefficient for natural convection from the boundary layer is difficult. Therefore, it was decided that only the influence of the thermal conductivity could properly be

accounted for and was the only thermal property measured. The convective heat-transfer coefficient was back-calculated using the cooling curves of Wolfe and Colony (49) and a chart relating temperatures at the center of a solid to the F_o and B_i.

4.8.3.1. Sample Preparation for Thermophysical Properties Testing

Thermophysical test specimens required special preparation in order to obtain the required properties. Three test specimens were compacted to thicknesses of approximately 0.2 inches using the Riehle "Static" Compactor. Achievement of this small thickness required that the 3% of No. 4 material normally used be eliminated. This procedure produced the two relatively smooth, parallel surfaces required to obtain accurate results from the laser flash diffusivity test method. Three one-centimeter square samples were cut from each of these statically compacted disks and submitted for testing.

4.8.3.2 Determination of Thermal Conductivity

Since the thermal conductivity plays a fairly significant role in the cooling of an asphaltic mat, this property was determined for the HAE Type IV Surface Sand Mix. Tests were performed by the Thermophysical Properties Research Laboratory (TPRL) at Purdue University. The properties determined were density, specific heat, and thermal diffusivity. From these measurements, the thermal conductivity was calculated. The results are

summarized below.

Thermal Conductivity: $0.0179 \frac{W}{(cm)(K)}$

Thermal Diffusivity: $0.0101 \frac{cm^2}{sec}$

Specific Heat: $0.9140 \frac{(W)(sec)}{(gm)(K)}$

Density: $1.936 \frac{gm}{cm^3}$

Values typically used for the thermal conductivity and thermal diffusivity of bituminous mixtures are as follows:

Thermal Conductivity: $0.0125 \frac{W}{(cm)(K)}$

Thermal Diffusivity: $0.00575 \frac{cm^2}{sec}$

4.8.4 Evaluation of Sand Mix Cooling Rate

The Fourier and Biot Numbers are important measures of how a body responds to temperature changes. The Fourier Number, F_o, is a measure of the time required to transfer heat within the body; bodies with high diffusivities and large bodies respond more slowly than small bodies. The Biot Number, B_i, plays a fundamental role in conduction problems that involve surface convection effects. This number measures the temperature drop in solid relative to the temperature difference between the surface and the fluid. When the Biot Number is significantly less than one it is sufficient to assume uniform temperature distribution within the solid at any time during a transient process. As will be seen, however, this is not the case for thin Sand Mix Surface

Courses; therefore, only average mat temperatures at any time during the transient heat process will be obtained. In this study, the average mat temperature was assumed to be located at the mid-depth.

The Fourier and Biot Numbers are given by the following equations:

$$F_o = \frac{\alpha \tau}{L^2} \tag{4.4}$$

where τ = time

α = thermal diffusivity L = half the thickness of the solid

and

$$B_i = \frac{(h)(L)}{k} \tag{4.5}$$

where h = convective heat-transfer coefficient

k = thermal conductivity of the solid

It can be shown (5) that

$$\frac{t-t_f}{t_i-t_f} = 2 \sum_{n=1}^{\infty} e^{-\partial_n^2 o} \frac{s \ \delta_n}{\delta_n + \sin\delta_n \cos\delta_n} \cos\delta_n \ \xi \tag{4.6}$$

where

δ_n = n^{th} root of $\delta_n \tan\delta_n - B_i = 0$

ξ = location within the half-mat

Equation (4.6) has been evaluated numerically by a number of

investigators for various ranges of ξ (position), F_o, and B_i allowing this equation to be solved through the use of Figure 4.1.

Cooling curves for various mat thicknesses, base and air temperatures, and wind velocities had previously been generated by a finite element analysis (49). Using the finite element results for a one half inch overlay, shown in Figure 4.2, the Biot Number for that mixture was determined from Figure 4.2. From this, the heat-transfer coefficient was calculated. Next, the thermal conductivity and Fourier Number for the Sand Mix were inserted and, using the heat-transfer coefficient back-calculated from the finite element analysis values, Figure 4.2 was used to determine the time-temperature relationship for the Type IV Sand Mix. A sample calculation of this process will be presented next.

From Figure 4.2 the temperature of a 1/2 inch mat is seen to be 179°F for air and base temperatures of 90°F 4 minutes after being spread. The Fourier Number for this mixture is:

$$F_o = \frac{(5.55*10^{-7})(4*60)}{0.00635^2} = 3.30 \qquad (4.7)$$

where the thermal conductivity is in BTU units.

The temperature, in percent of initial temperature, is found to be:

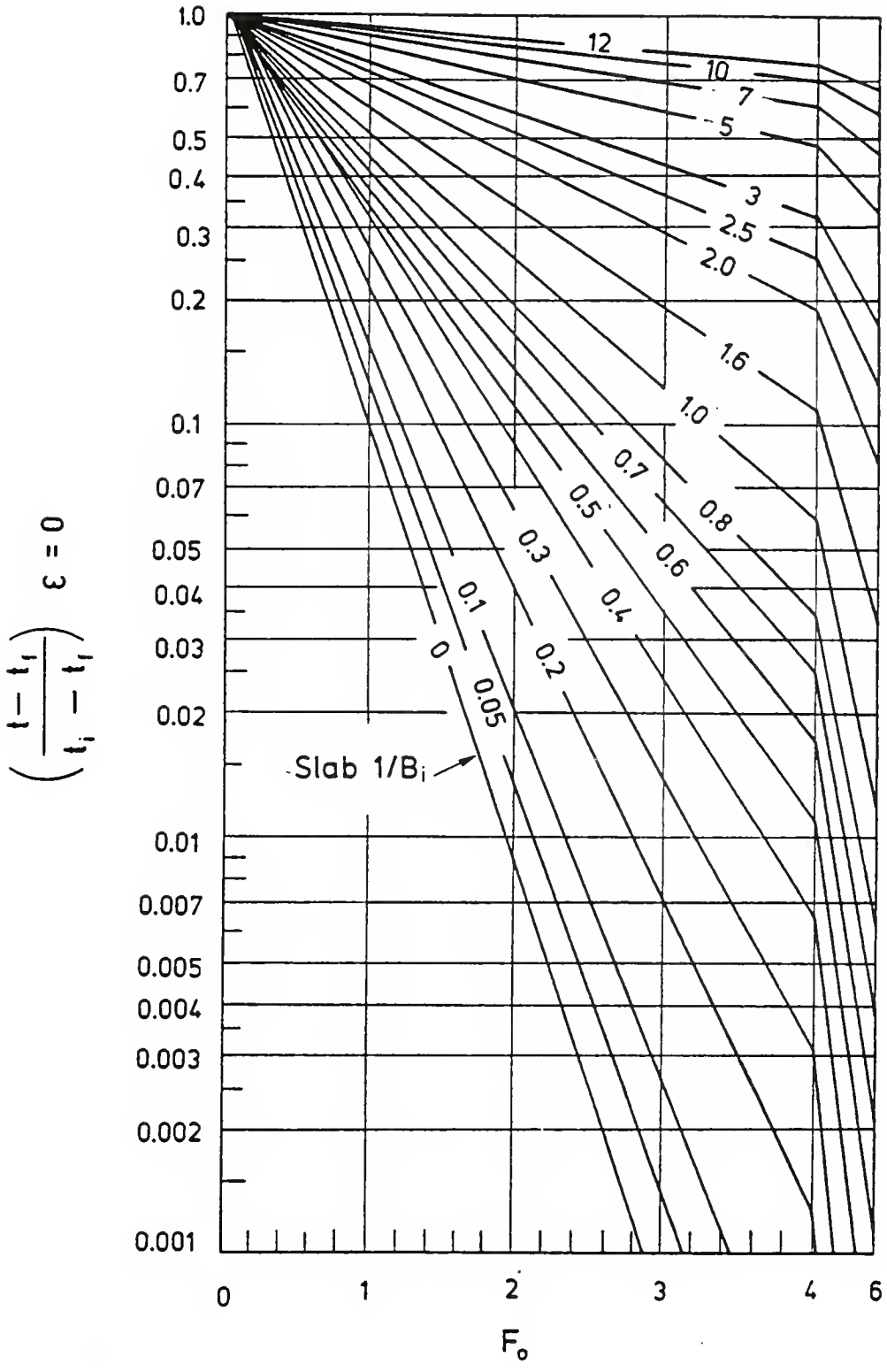

Figure 4.1 Percent of Initial Mixture Temperature Relative to Material Properties (from 5).

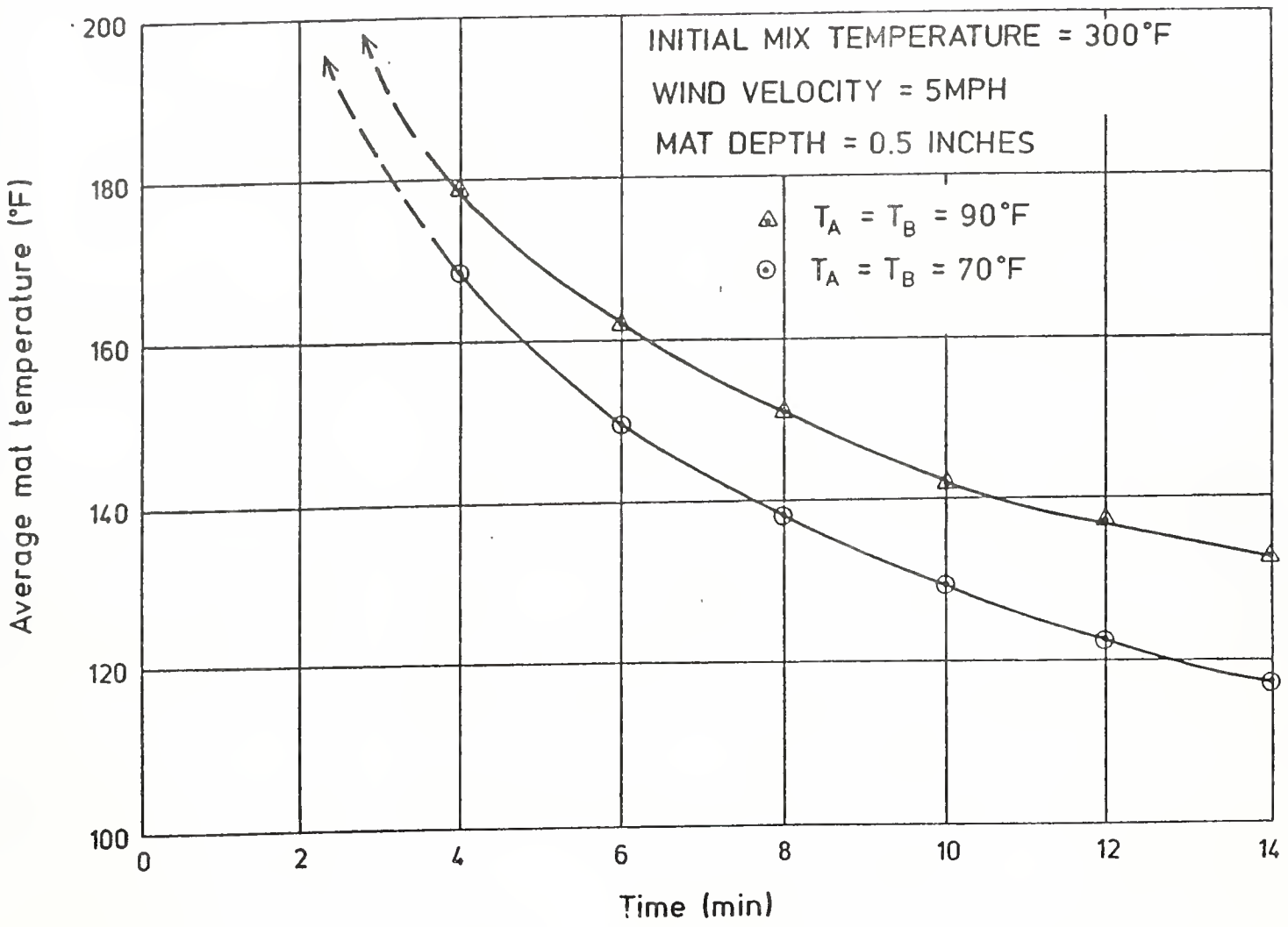

Figure 4.2 Cooling Curves from FEM Study (from 48).

$$\frac{(t-t_f)}{(t_i-t_f)} = \frac{(179-90)}{(300-90)} = 0.424 \qquad (4.8)$$

Then, using Figure 4.1, the inverse of the Biot Number can be found by interpolation. In this case, $1/B_i$ is approximately 3.4 and B_i is 0.294. The heat-transfer coefficient is then determined to be:

$$h = \frac{B_i(173.219)}{0.00794} = 6414 \qquad (4.9)$$

The diffusivity, thickness, and thermal conductivity values determined for the Sand Mix result in Fourier and Biot Numbers as follow,

$$F_o = \frac{(1.01*10^{-6})(\tau)}{(5/16)(2.54)(0.01)^2} = 0.01603(\tau) \qquad (4.10)$$

and

$$B_i = \frac{(h)(.00794)}{173.219} = \frac{h}{21816} \qquad (4.11)$$

at the centerline of the overlay.

The Fourier Number for the Sand Mix at 3.85 while the Biot Number is 0.294 and $1/B_i$ is 3.40. These numbers are then inserted into Figure 6.1 to obtain the temperature of the 5/8 inch Sand Mix overlay 4 minutes after the initial placement at 90^oF. Coincidentally, the increased thermal conductivity of the Sand Mix just offsets the increase in thickness of the finite element mixture properties and thickness.

Base and air temperatures of 90, 70, and 50 degrees Farenheit were examined with the resulting cooling curves shown in Figure 4.3.

4.8.5 Determination of Minimum Compaction Temperature

Most studies use a minimum compaction temperature of 175° Farenheit. IDOH field procedures require rolling to be complete before the average mat temperature reaches 180° F for AC-20 mixes and 145° F when the binder is AE-60. An investigation was undertaken to determine if the minimum allowable compaction temperature was lower than these temperatures used by the IDOH. Samples were batched by G2 gradation. Compaction temperatures of 180, 155, 145, 135, 120, and 100° F were used for the AE-60 samples while 200, 180, 160, 150, 140, and 120° F were used for the AC-20 samples. The densities obtained by compacting these samples using the Gyratory Testing Machine with a vertical ram pressure of 20 psi and 35 revolutions of the upper compaction head are shown in Figure 4.3. The compaction temperature-density curves of Figure 4.3 show a tendency for slight decrease in density with decreasing temperature. At a temperature below 140° F for the AC-20 and 120° F for the AE-60 there is seen to be a significant decrease in density for the same compactive effort. This indicates that the minimum allowable compaction temperature is 140° F for AC-20 and 120° F for AE-60. However, while the mixture was being placed into the mold, it was observed that the mix did not act as a particulate material, rather as large clumps of

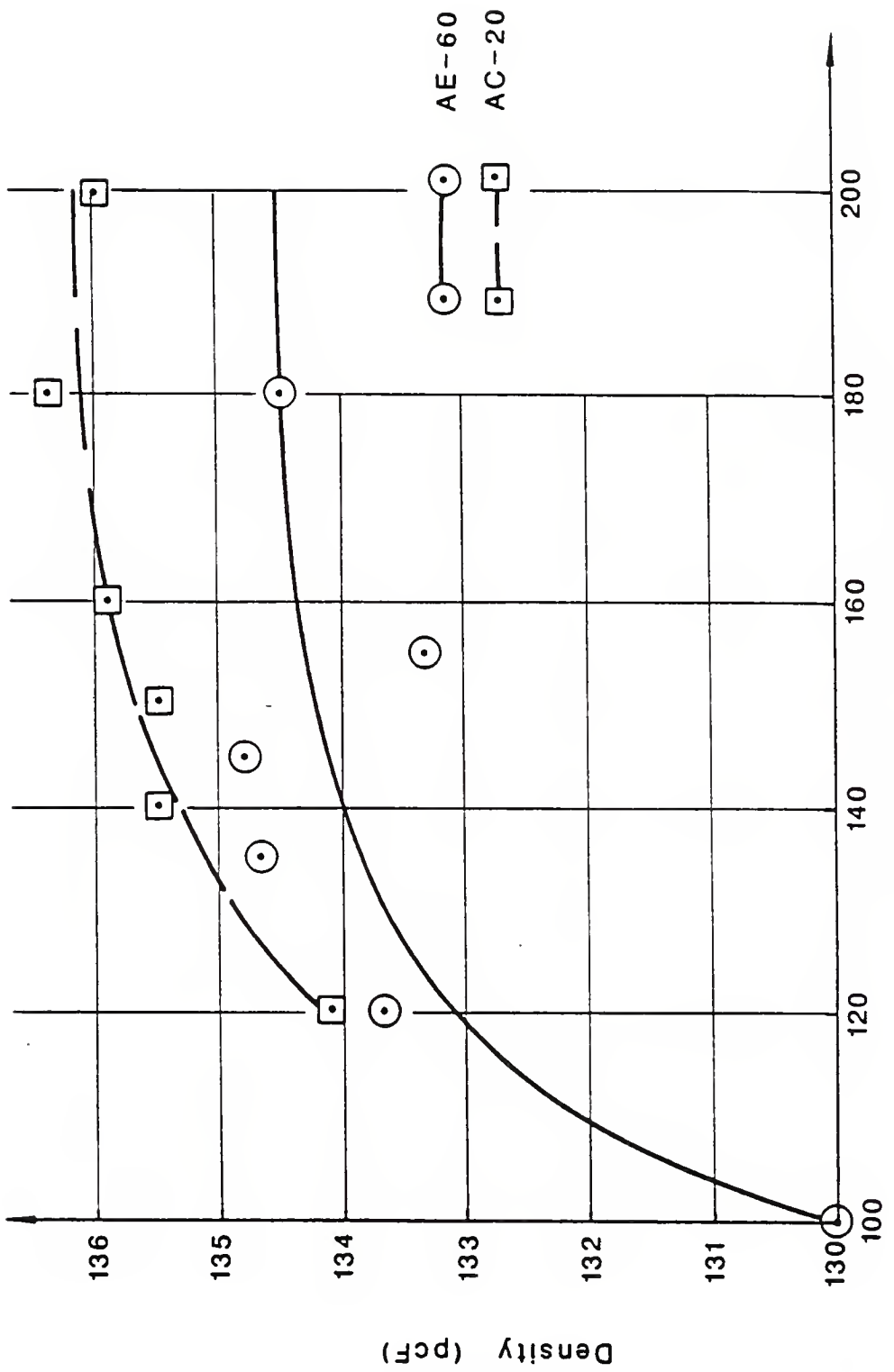

Figure 4.3 Compaction Temperature versus Density Curves.

material, up to temperatures of 160° F for the AC-20 and 135° F for the emulsion. The asphalt was sufficiently fluid at these temperatures to allow the mixtures to act mostly as individual particles. At the next higher temperature investigated, 180° F for AC-20 and 145° F for AE-60, it was observed that the mixture acted completely as discrete particles. This criterion indicates the currently used minimum allowable compaction temperatures are approximately correct.

Figure 4.4 shows the allowable compaction time related to the ambient air temperature. Figures 4.5 and 4.6 show the effect of base temperature and wind velocity, respectively, on the cooling rate; both these effects tend to reduce the allowable compaction time. It is seen from these figures that the effect of wind velocity is minor, but base temperature can play a significant role in the cooling rate of a thin sand mix overlay.

The air temperatures are intentionally made high: 90 F to illustrate that, even under favorable conditions, the cooling curve for the 5/8 inch sand mix wearing coarse shows that compaction must be completed within the first 4 minutes for AC-20 mixtures and within 9.5 minutes for AE-60 samples. Under less favorable conditions such as 50° F the temperature-allowable compaction time relationship is such that rolling must be completed within 2.5 minutes and 5 minutes, respectively, for AC-20 and AE-60 samples.

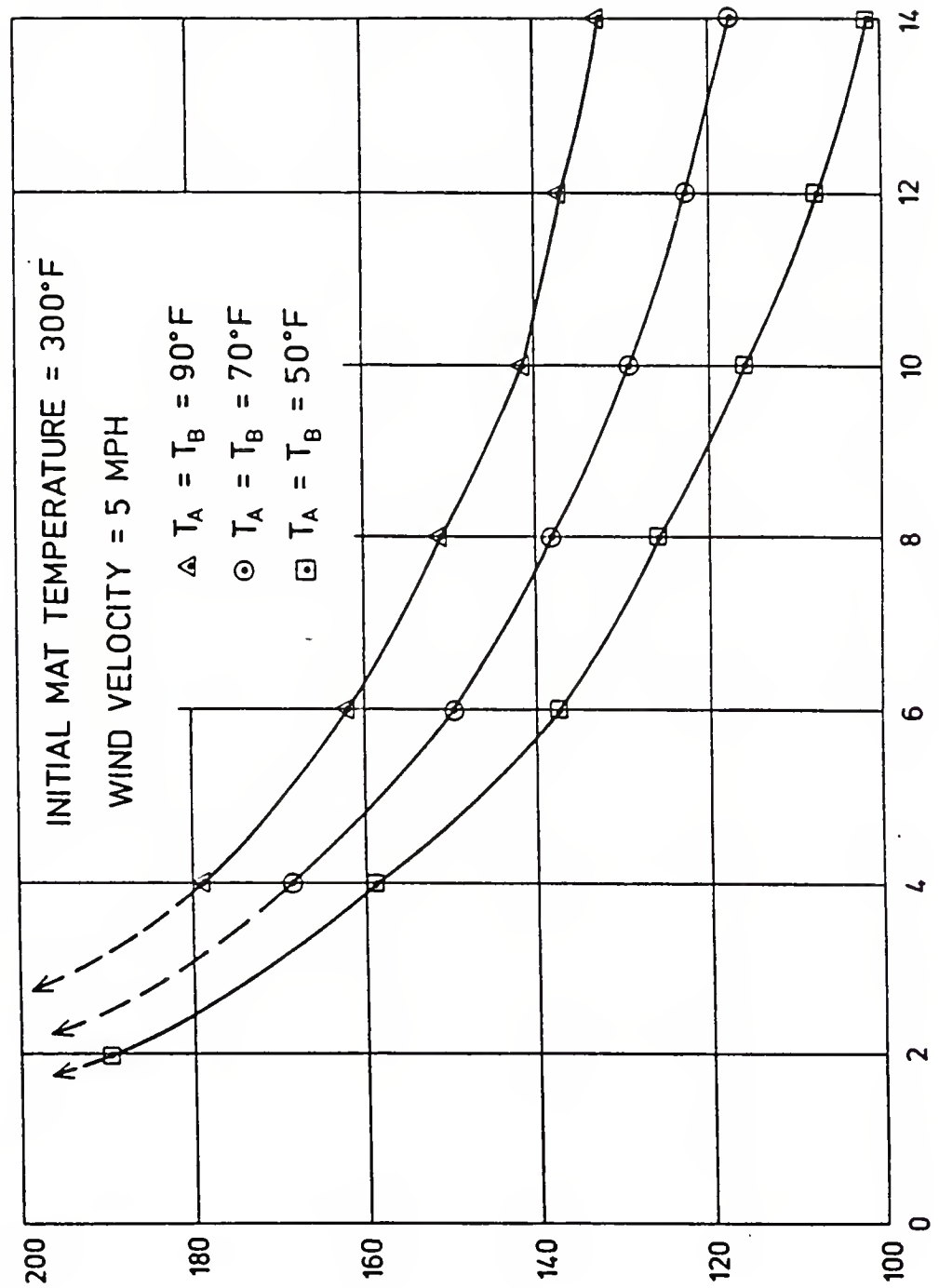

Figure 4.4 5/8 Inch Sand Mix Cooling Curves.

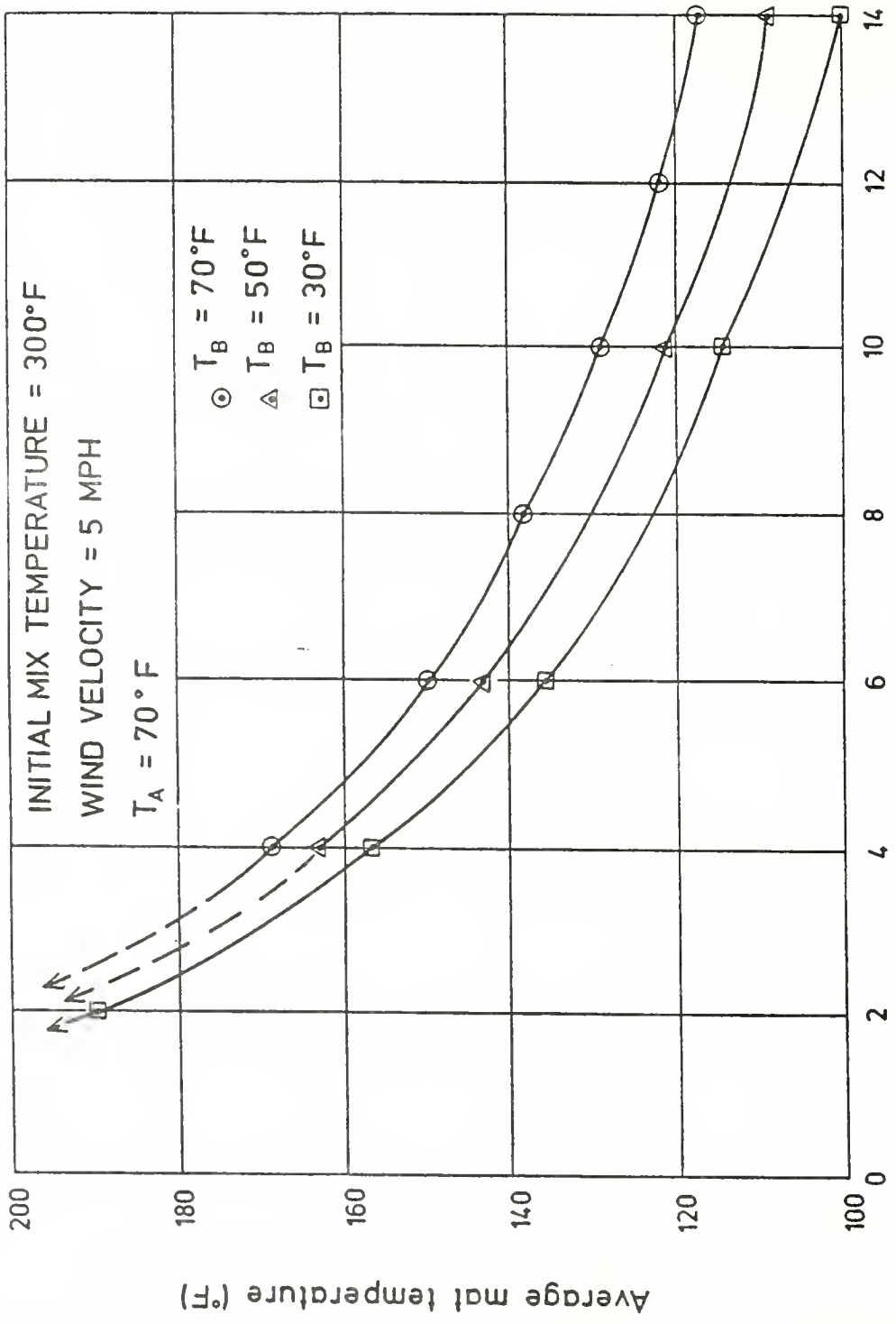

Figure 4.5 Cooling Curves Showing the Effects of Base Temperature.

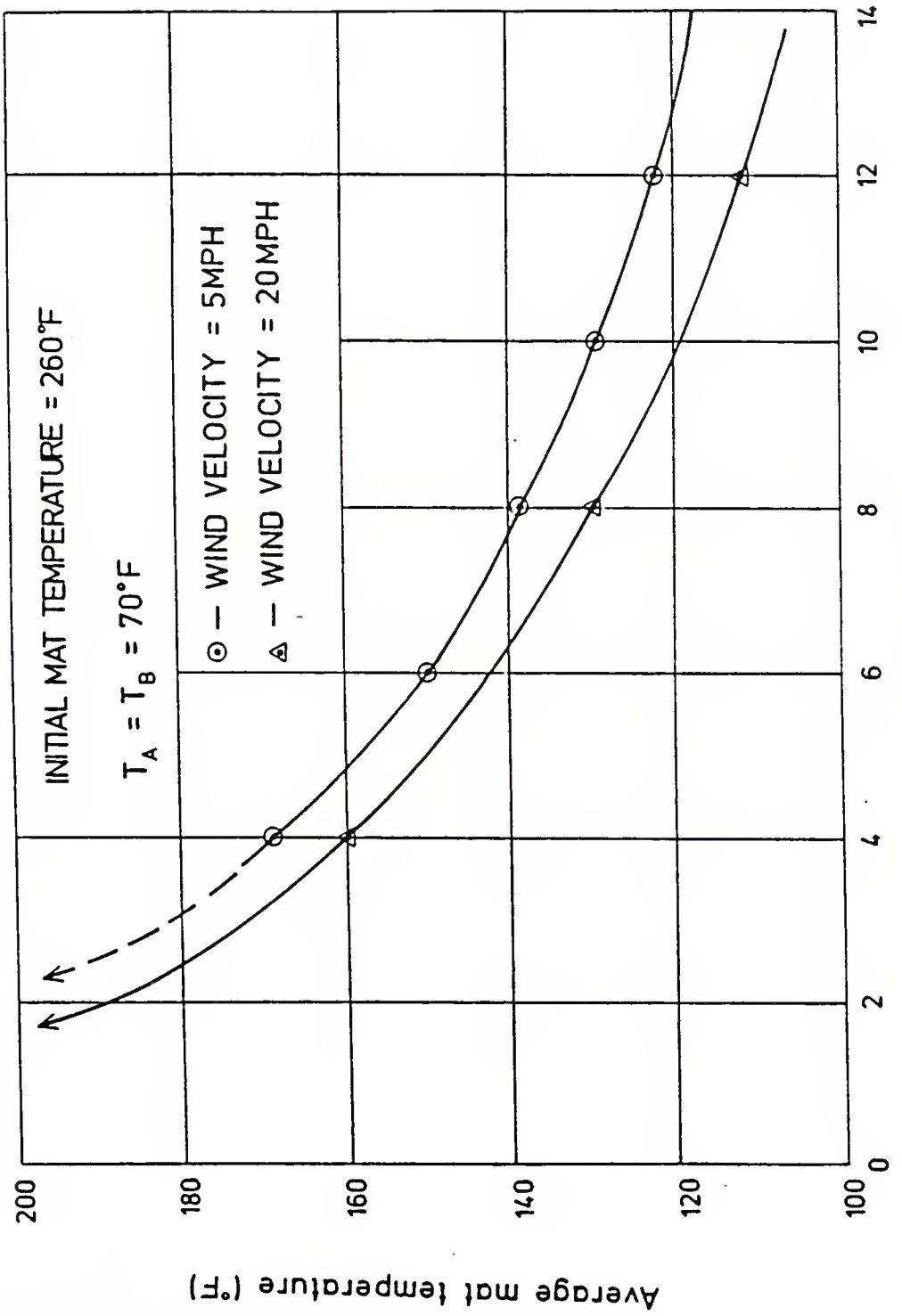

Figure 4.6 Cooling Curves Showing the Effects of Wind Velocity.

CHAPTER 5

SUMMARY AND CONCLUSIONS

This study had the overall objective of improving the performance of those asphalt paving mixtures used especially as thin surface courses. The aim was to learn if one of the available laboratory techniques for compaction offers a good characterization of the field compacted sand mix surface courses. Two thin surface course mixtures were studied: HAE Type IV and HAC Type D. Four aggregate combinations were used: local gravel-sand, sand with crushed agglime in blends of 90%-10% and 70%-30%, and 100% manufactured aggregate. The 2 binders used were AC-20 and AE-60. Two commonly used IDOH gradations were examined, G2 and FM. The G2 has shown good performance on pavement sections, and the second is based on the Fineness Modulus concept. The laboratory compaction of these mixtures was performed by varying the compaction parameters of four different compaction methods: Gyratory, Marshall, Kneading, and Vibratory.

Field cores were obtained from newly constructed overlays in Indiana for comparison purposes. Mercury-intrusion porosimetry was used to obtain pore-size distribution (PSD) curves. This

allowed comparison of the fabrics of the laboratory and field compacted material.

The following conclusions are based on the data in light of the objectives of the study and the constraints created by the details of the IDOH construction program.

1. Due to the lateral confinement of the mold, which is not present with field compaction, less than standard compactive effort is required in the laboratory to achieve the target density in thin asphaltic layers. The thin asphaltic layers compacted in the laboratory exhibit low Hveem stability values. When corrected to match standard specimen thickness, values in the range of 15 to 20 are satisfactory for field performance of the mixtures.

2. Compaction procedures determine the distribution of pores near the peak frequency diameter. Using this as a measure of a fabric's characteristics, the Gyratory Test Machine GTM best duplicates the pore that is produced by field rolling procedures. The Gyratory Compactor with a 20 psi vertical ram pressure for 35 revolutions at a 1 degree angle of inclination plus 5 leveling revolutions (no gyratory angle) best duplicates the fabric obtained by the field compaction procedures currently in use with Gradation 2 mixes. The Kneading Compactor produces some fabric characteristics not too far removed from field fabric as well. Although the

Fineness Modulus Gradation fabric was not matched as well by the GTM procedure, used at low vertical ram pressures, it offers the best opportunity to reproduce Sand Mix fabric for a range of gradations.

3. Newly paved G2 gradation surface courses have displayed mixed performances in the field. In some cases, additional compaction from the action of traffic can cause a redistribution of pore size frequencies, as measured on Pore Size Distribution (PSD) curves by a concentration of relatively large voids near the peak frequency diameter. The differential PSD curve obtained in this situation most likely represents a fairly stable void configuration, and is associated with good performing pavements. A sharp-peaked differential PSD curve, however, shows no redistribution of pore sizes caused by traffic, and is indicative of poor performance of pavements.

4. Tests on newly paved Sand Mix overlays consisting of the FM Gradation revealed less pore volume located near the peak frequency diameter. This more evenly distributed volume of pore sizes creates a more stable pavement structure which should have less variability in fabric after compaction by traffic, and good performance in the field. (One note of caution is required; the number of test results upon which the good- and poor- performing characteristics is based is limited.)

5. The validity of conclusions 3 and 4 lead one to question the hypothesis that permeability greatly influences the performance of thin overlays. While permeability is likely to be influential in obtaining good Friction Numbers, it may not be as important with regard to delamination, rutting, or blistering problems. Good- and poor- performing sections of pavement had PSD curves with similar peak frequency diameters, but good- performing sections had fewer large pores and more smaller pores. Other variables being neglected, this would indicate lower permeabilities for good-performing sections.

6. The minimum allowable compaction temperatures presently used: 145° F for AE-60 and 180° F for AC-20 samples, is suggested based upon the greatly reduced workability of the mix at lower temperatures. Compaction must occur within 4 minutes for a mix containing AC-20 as the binder and when the ambient air and base temperatures are at 90° F. Samples with AE-60 as the binder must be compacted within 9.5 minutes after spreading. These times are reduced greatly when the ambient air and base temperatures fall to 50° F AC-20 and AE-60 mixtures must be compacted within 2.5 and 5 minutes, respectively. This time is not sufficient for normal compaction procedures to be utilized, however, the use of three-roller trains following closely behind the spreader could be used to meet this time constriction. The

allowable compaction time must be determined and adhered to in order to create overlays consisting of the desired pore size distributions.

7. During field compaction, attention must be given to the base temperature while the wind speed can be neglected without excessive errors being introduced. Construction projects being accomplished in the early spring and late fall should use only AE-60 as the binding agent to allow additional time for compaction to occur. Although mixes using other binders may achieve higher densities in the lab, field cooling may not allow sufficient time for these densities to be attained by compactors.

PART II

HIGH PRESSURE-GEL PERMEATION CHROMATOGRAPHY OF BLENDED ASPHALTS

Contribution from the
work of N. Garrick (1986)

CHAPTER 1

INTRODUCTION

There have been many reports of an increasing problem with premature failure of asphalt pavements. Some researchers cite such reports as evidence that the refineries are supplying an increasing amount of inferior asphalt. This in turn is blamed on the more widespread use of non-traditional methods of asphalt production. However, there is no documented evidence concerning the adequacy or inadequacy, for paving purposes, of asphalts produced by these new methods of processing. Consequently, one objective of this project was to evaluate the products of one non-traditional asphalt production process, the residuum oil supercritical extraction (ROSE) process.

In addition to the changes in the asphalt that were discussed previously, there have been many other changes in the asphalt industry over the last decade. These include new technology for asphalt paving mix production and for pavement construction. Furthermore, greater demands have also been placed on the pavements by significant increases in vehicle load, in tire pressure, and also in traffic volume. It is increasingly apparent that current methods of specifying and characterizing asphalts

are inadequate in light of the rapid changes that have recently taken place in the industry. Consequently, the second objective of this project was to investigate and evaluate a new procedure for characterizing asphaltic materials.

A third objective of this study was to develop a suitable procedure for characterizing the chemical composition of asphaltic material. If this goal was successful an additional objective was to develop relationships between chemical composition of the asphalts and their physical properties. To this end, high pressure-gel permeation chromatography was selected for evaluation as a tool for characterizing the chemical composition of asphalt.

The asphalts tested in this project were from two different ROSE sources and from four other sources. However, a significant proportion of the tests were conducted on asphalts from one ROSE source and one conventional source only. The tests on asphalt mixes were conducted primarily for a sand mix gradation of a local aggregate. However, some tests were also conducted for a base course gradation with aggregate from this same local source. All of the tests were conducted on laboratory samples only.

CHAPTER 2

TEST MATERIALS

The asphalts used in this study were from six separate sources. Two groups of asphalts were blended from the products of residuum oil supercritical extraction (ROSE) plants, Pester (Plant A) in Kansas and Kerr-McGee (Plant B) in Oklahoma. The third asphalt is a commercial AC-10 grade material from Amoco Refinery (Plant C) in Indiana. The last three groups of asphalts (D, E, F) are from various facilities in Indiana.

2.1 - Asphalts from ROSE Plants A and B

2.1.1 - ROSE Products from Plant A

The ROSE products from this plant were an asphaltene-rich fraction, a resin-rich fraction, and deasphalted oil (DAO). A Strieter chemical analysis of the fractions was provided by the manufacturers and is shown in Table 2.1. This table shows that the asphaltene-rich fraction contains 40.8% asphaltene; however, it also contains a significant amount of resin and oil. The resin fraction consists mostly of resin but also has a relatively large amount of oil. Deasphalted oil contains 79.5% oil; much of the remaining component is resin.

Table 2.1 - Strieter Analysis of ROSE Products from Plant A

Fraction	Asphaltene(wt%)	Resin(wt%)	Oil(wt%)
Asphaltene-rich	40.8	26.8	32.4
Resin-rich	6.5	54.6	38.9
DAO	1.1	19.4	79.5

The asphaltene fraction is a black, friable, solid at room temperature. It has a ring and ball softening point of 212° F (100° C). In addition the viscosity is 420 centistokes at 390° F (199° C). This material has no melting point, and, instead, it swells and decomposes with intense heating.

The resin fraction is a black, semi-solid at room temperature. It has a viscosity of approximately 300 centistokes at 284° F (140° C). The rheological and other physical properties of the resin fraction are similar to those of a typical AC-10 asphalt.

Deasphalted oil is a brown viscous fluid at room temperature. This material typically has a viscosity of about 79 centistokes at 199° F (93° C); thus, it is appreciably less viscous than the resin fraction, and is sufficiently fluid to be poured from its container. The specific gravity of the three fractions decreases in the order asphaltene, resin, and deasphalted oil.

2.1.2 - ROSE Products from Plant B

Plant B produces only two ROSE products, an asphaltene and a resin fraction. The physical properties of these materials are slightly different from that described above for the Plant A products. The asphaltene is less friable, and hence, less easily pulverized for blending than the Plant A material. The consistency of the resin fraction is intermediate between the Plant A resin and deasphalted oil. It has a viscosity of 400 poises at 140° F (60° C) which is about half that of the Plant A resin fraction.

2.1.3 - Blending Process for Plant A and B ROSE Products

The procedure used in blending the ROSE products to produce asphalt was the same for material from both plants. This procedure is outlined below:

i) The required amounts of deasphalted oil and resin fractions were heated to approximately 150° F (66° C), at which point

ii) A small proportion of the required amount of asphaltene fraction was then added and the mixture stirred with a spatula. Stirring was continued until all traces of the solid asphaltene dissolved.

iii) The second step was repeated until all the asphaltene had been added. The maximum temperature attained was 250° F (121° C).

Asphalts were blended in batch sizes of approximately 1000 grams for the tests on asphalt cements. Asphalts were produced in batch sizes of 2000 grams for the second section of the project which called for tests on asphalt mixtures. The total time for blending these batches was from two (2) to three (3) hours. Blending time increased with batch size and with the proportion of asphaltene in the blend.

2.1.4 - Blend Proportions for Plant A ROSE Products

Each set of ROSE products required preliminary tests in order to determine the nature of the relationship between the proportion of ROSE products in an asphalt blend and the viscosity (140° F) of the blend. This information was used to predict the combination of ROSE products which gave asphalts of a certain viscosity or range of viscosities. The blends selected were those which would meet the viscosity requirements for AC-10 and AC-20 grade asphalt.

It was determined in the preliminary investigations that asphalts with the same viscosity at 140° F (60° C) could be produced from many different combinations of ROSE products. Furthermore, it was shown that difference in temperature susceptibilities among the various blends was small. Thus it was possible to

define a range of combinations of ROSE products which gave asphalts of a particular grade.

Six different composition were blended in this project. Three of these blends were in the AC-10 asphalt range and three were in the AC-20 range. The blends selected represented the extremes and middle combinations from the range of possible values for each grade. These combination can be considered to be the low, middle, and high blends respectively, where the terms low, middle, and high signify blends with the minimum, middle, and maximum proportion of asphaltene for blends of that grade. The combinations that were blended for each grade are shown in Table 2.2.

2.1.5 - Blend Proportions for Plant B ROSE Products

Since there were only two ROSE components, it was not possible to produce two blends with the same viscosity. However, viscosity was found to increase with the proportion of asphaltene in the blend. Thus, two separate combinations of ROSE products were blended from the Plant B resin and asphaltene for this study. One of the blends gave an AC-10 grade asphalt and the other an AC-20 grade. In addition, an AC-10 asphalt was blended from a combination

Table 2.2 - Proportion of Plant A ROSE Products in Blends

Composition	Grade	Proportion of ROSE Products		
		Asphaltene	Resin	Deasphalted Oil
LAC	AC-10	3.3	96.7	0.0
MAC	AC-10	24.2	48.4	27.5
HAC	AC-10	42.1	0.0	57.9
LAC	AC-20	11.5	88.5	0.0
MAC	AC-20	29.3	44.3	25.5
HAC	AC-20	44.8	0.0	55.2

LAC, MAC, and HAC are blends with low, middle and high asphaltene content respectively

Table 2.3 - Proportion of Plant B ROSE Products Asphalt in Blends

Composition Number	Grade	Proportion of ROSE Products		
		Asphaltene Plant B	Resin Plant B	Deasphalted Oil Plant A
700	AC-10	27.0	73.0	0.0
800	AC-10	40.0	35.0	25.0
900	AC-20	19.0	81.0	0.0

of the Plant B asphaltene, and resin, and the Plant A deasphalted oil. The proportion of the different ROSE products in these blends are given in Table 2.3.

2.2 - Asphalts from Sources C, D, E, and F

The third type of asphalt that was used extensively in this study is a commercial AC-10 asphalt from AMOCO Refinery (Plant C) in Indiana. This asphalt was used as a control for comparison with the ROSE asphalts. The rheological properties of this asphalt and of those from sources D, E, and F are given in Table 2.4.

The asphalts from the three other sources were only used for a few tests because they are available in very limited quantities. Three forms of the asphalt from Source D were evaluated. These were the original asphalt, a thin film oven test residue, and the residue extracted from a pavement section. The original asphalt and the thin film oven residue for the Source E material were tested. The material from Source F was the residue from a pavement section.

Table 2.4 Rheological Properties of Asphalts from Sources C, D, E and F

Plant	Type	Viscosity 140°F, p	Viscosity 275°F, cst	Penetration 77°F, 0.1mm
C	Original, AC-10	1103	293	79
D	Original	1993	391	-
D	TFOT Residue	4646	576	-
D	Road Residue	11832	1038	-
E	Original	2373	402	59
F	Road Residue	34397	1446	-

2.3 - Aggregate

A local pit-run gravel was used to make asphalt mixes for this study. This material is a terrace gravel-sand that was deposited by the Wabash River. The physical properties of this aggregate are summarized in Table 2.5.

Two different gradation of this aggregate was used. One was a sand mix and the second was a No. 11 mix (Indiana Department of Highways (IDOH) designation). The gradation for the sand mix and the No. 11 mix are shown in Figures 2.1 and 2.2 respectively.

IDOH specifications for these gradations are also shown on the figures. The fineness modulus is 2.89 for the sand mix and 3.65 for the No. 11 mix.

Table 2.5 Physical Properties of Aggregate (from Ref. 58)

Apparent Specific Gravity	2.66
Bulk Specific Gravity	2.62
Absorption, %	1.08
Florida Bearing Value, G1	26.00
Florida Bearing Value, G2	64.00

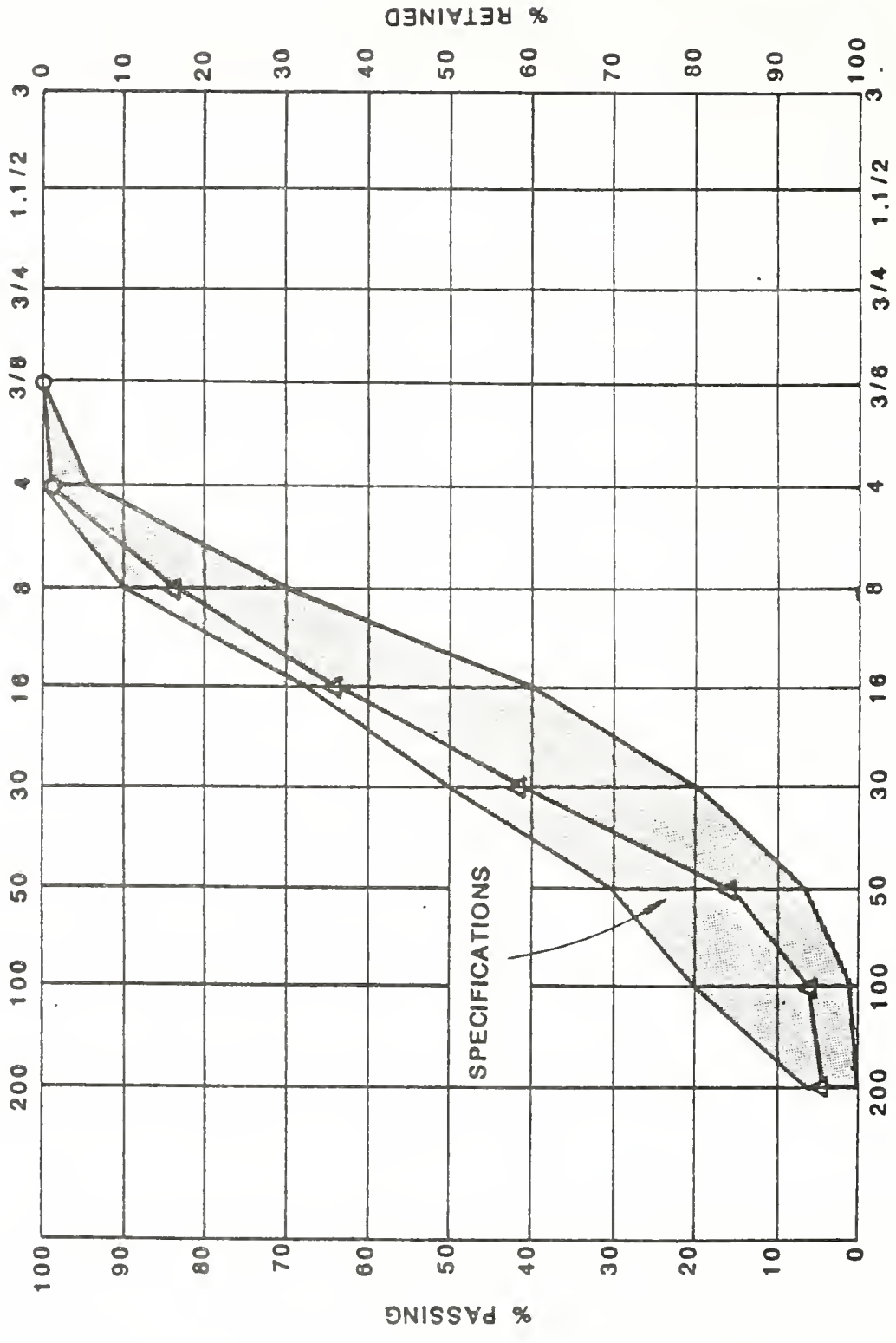

Figure 2.1 Gradation for Sand Mixes

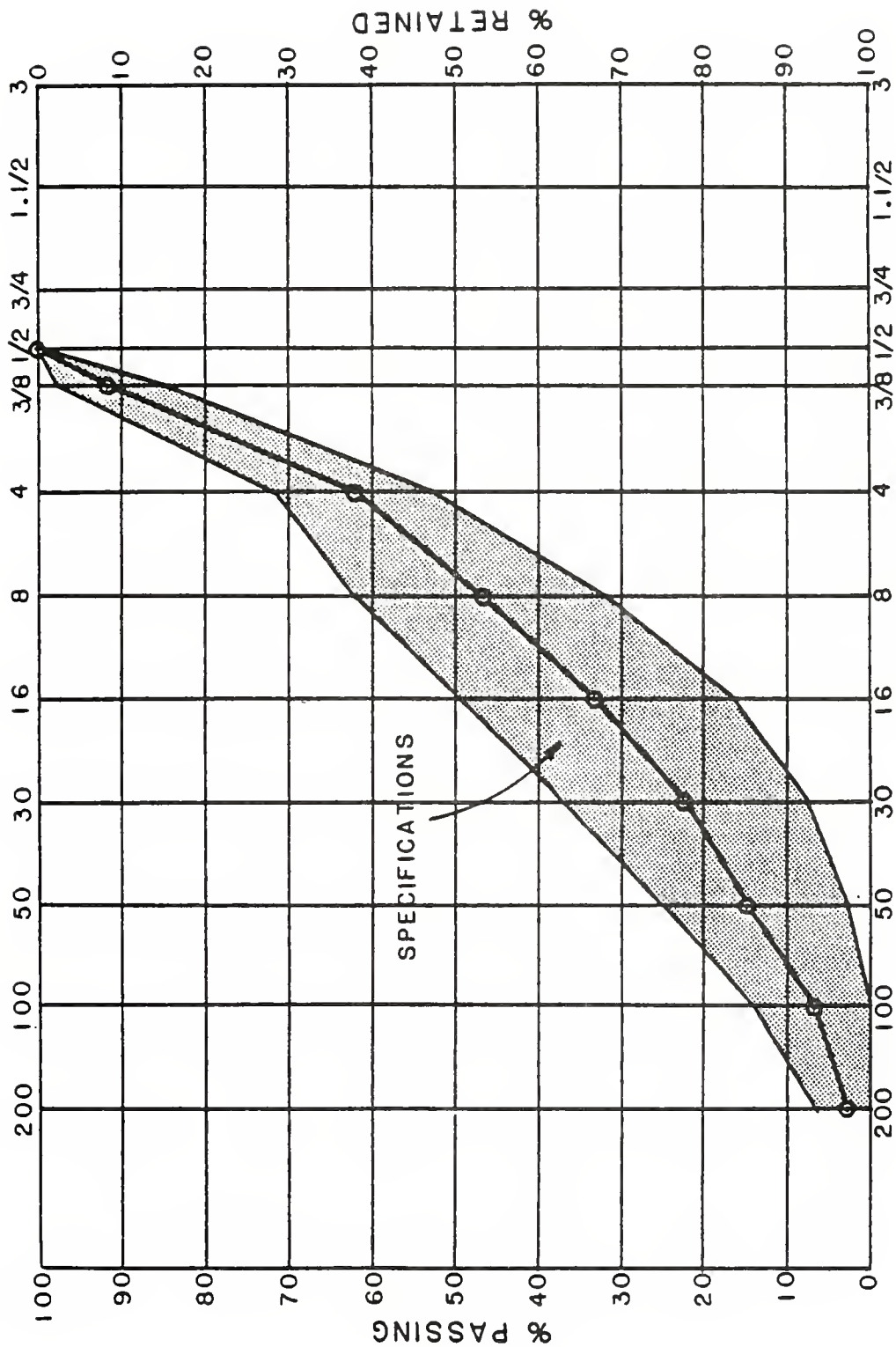

Figure 2.2 Gradation for Number 11 Mixes

CHAPTER 3

OUTLINE OF EXPERIMENT

The laboratory work for this study was divided into two sections i) tests on asphalt cements, and ii) tests on asphalt concrete mixes.

3.1 - Statistical Design of Experiment for Plant A Asphalts

A nested statistical design was used in this project for tests on the Plant A asphalt cements and asphalt mixes. In this design, tests were conducted for asphalts of two different asphalt grade, AC-10 and AC-20. Three different compositions in each grade were used for tests on asphalt cements. These were the low, middle, and high asphaltene content (LAC, MAC, and HAC) asphalts respectively. However, only LAC and HAC asphalts in each of the two grades were used for tests on asphalt mixes. Two separate batches were blended for each of the asphalt compositions used. All tests were conducted on two specimens from each batch; thus a total of four specimen were tested for each asphalt composition.

3.2 - Tests on Asphalt Cements

3.2.1 - Physical Properties

The tests of physical properties of asphalt cements included the following: specific gravity (ASTM D70), viscosity (140° F and 275° F) (ASTM D2170 and D2171), penetration (39.2° F and 77° F) (ASTM D5), and thin film oven test (TFOT) (ASTM D1754). The TFOT residues were tested for viscosity (140° F and 275° F) and penetration (39.2° F and 77° F). All of these tests were conducted in accordance with the ASTM procedures.

Most of the above tests were conducted for all the asphalts from Plants A, B, and C. Testing of the other three groups of asphalt was limited to the determination of viscosity (140° F and 275° F), and penetration (77°F). The data for these asphalts from Plants D, E, and F were used solely for regression analyses relating HP-GPC parameters and rheological properties of the asphalts.

The viscosity and penetration measures were used to calculate log-log temperature susceptibility, pene- tration-viscosity number, and penetration ratio. These three variables are used, respectively, as indicators of asphalt temperature susceptibility in the following temperature ranges: 140°F to 275°F, 77°F to 275°F, and 39.2°F to 77°F.

The amount of heat hardening in the TFOT was determined by calculating viscosity ratios (140°F and 275°F), and penetration retained values (39.2°F and 77°F) from the results for both the original and residual asphalt. Large values of viscosity ratio indicate a significant amount of heat hardening in the thin film oven. Large values for penetration retained values indicate little or no heat hardening.

3.2.2 - Chemical Characterization

High pressure-gel permeation chromatography (HP-GPC) was used in this project to characterize the chemical composition of the asphalt cements. This test was conducted on all asphalts from Plants A, D, E, and F. In addition, HP-GPC parameters were obtained for two of the three ROSE asphalts from Plant B. These results were used in developing regression functions relating HP-GPC data to i) properties of the asphalt cements, and ii) properties of the asphalt mixes.

3.3 - Tests on Asphalt Mixes

The following tests were conducted on asphalt mixes: resilient modulus (50° F and 72° F), indirect tensile strength, pulse velocity, stability (Hveem R-value and S-value), water sensitivity test, and artificial age hardening. All of these tests were conducted for both sand and No. 11 mixes with asphalts from Plant A and C. In addition, resilient modulus and indirect ten-

sile strength determinations were conducted for sand mixes with asphalts from sources B, D, and E.

One set of samples with asphalts from Plant A and C were used for pulse velocity, resilient modulus ($50^{o}F$ and $72^{o}F$), stability and indirect tensile strength. These tests were conducted in the order shown. A second set of samples was used for the water sensitivity test. Artificial age hardening tests were carried out on a third set of specially conditioned samples. Tests were conducted to determine the resilient modulus ($72^{o}F$ only) and indirect tensile strength of these samples.

The identical compaction condition was maintained in producing specimens for all of the above tests. Asphalt contents of 7.5 % and 7.0 % were used in the sand mixes and number 11 mixes respectively.

CHAPTER 4

DISCUSSION OF RESULTS

4.1 - Physical Properties of the Test Asphalts

The physical properties of the asphalts used in this study were compared to those of a representative sample of asphalts from across the United States. The objective of this was to identify any anomalous properties of the asphalts that were created from the ROSE process.

4.1.1 - Temperature Susceptibility

Figure 4.1 is a plot of viscosity at 140°F versus penetration at 77°F. It was determined that most commercial asphalts fall within the shaded region on this figure. The data-points for all the test asphalts are shown on the figure. In general, the Plant A asphalts fall close to the lower bound of the shaded region. Thus, these ROSE asphalts are more temperature susceptible than most commercial asphalts in the temperature range of 77°F to 140°F. Conversely, the temperature susceptibility of the Plant B ROSE asphalts are close to the average for commercial asphalts.

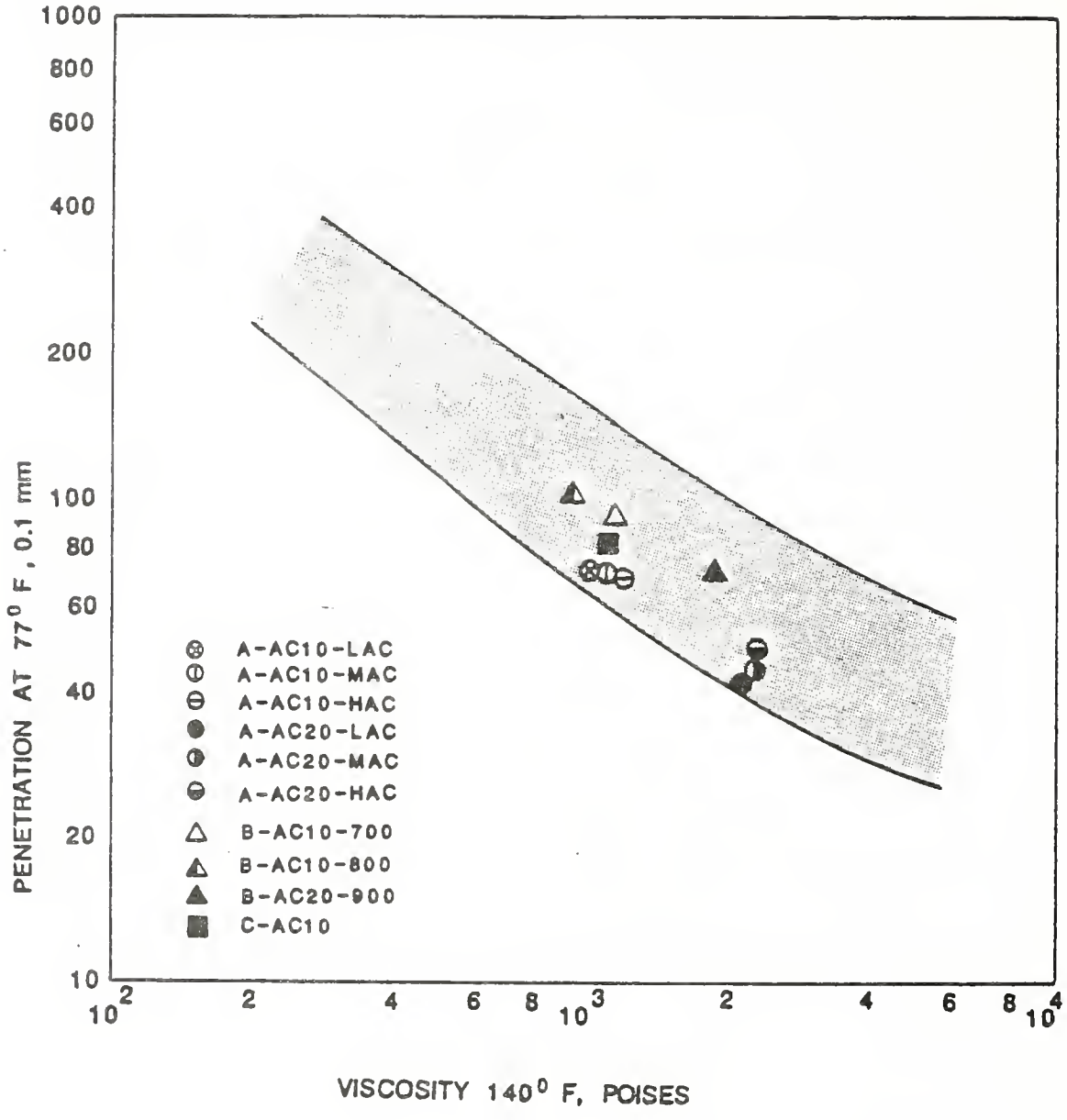

Figure 4.1 Relationship Between Viscosity at 140°F and Penetration at 77°F (from ref. 60)

Figure 4.2 shows the relationship between viscosity at 140°F and 275°F. In this case all of the test asphalts fall well within the region for commercial asphalts. In general, the temperature susceptibility of these asphalts, in the temperature range of 140°F to 275°F, are close to that of the average asphalt. However, the Plant A ROSE asphalts are slightly more temperature susceptible than the average asphalt.

In summary, the temperature susceptibility of the asphalts tested in this project are not significantly different from that of other commercial asphalts. At temperatures above 77°F, the Plant B asphalts have a lower temperature susceptibility than most commercial asphalts while the Plant A asphalts are more temperature susceptible than average. At temperatures below 77°F, all of the asphalts studied have lower temperature susceptibility than the average commercial product.

The temperature susceptibility of the hybrid Plant B AC-10 is very similar to those of the other two Plant B asphalts. This asphalt contained asphaltene and resin from Plant B, and deasphalted oil from Plant A. The addition of a sizable amount of DAO from Plant A did not have any noticeable effect on the temperature susceptibility of this hybrid.

4.1.2 - Heat Hardening

Figure 4.3 shows the relationship between the viscosity at 140°F for the original and heated asphalts. All of the test

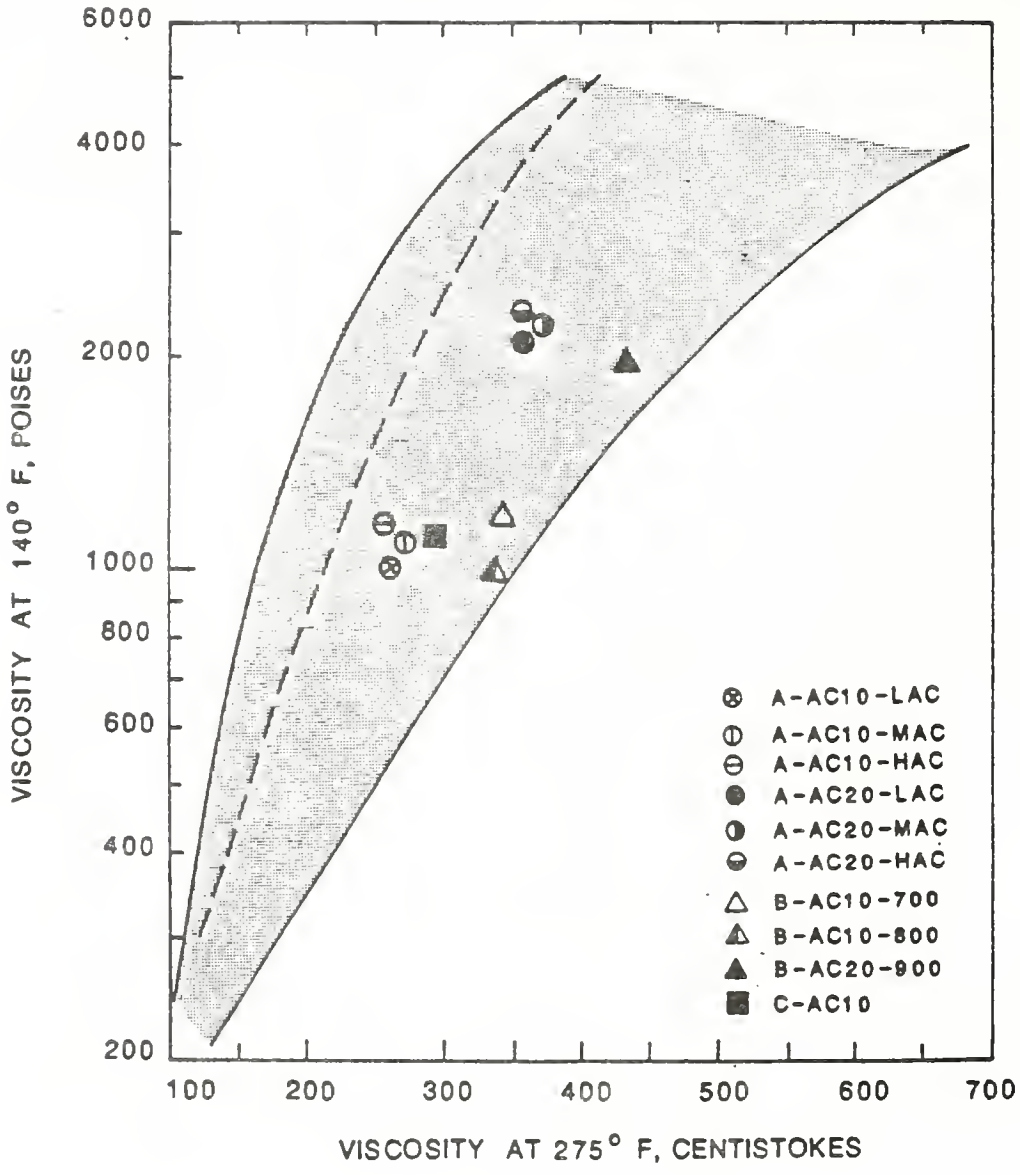

Figure 4.2 Relationship Between Viscosity at 140°F and Viscosity at 275°F (from ref. 60)

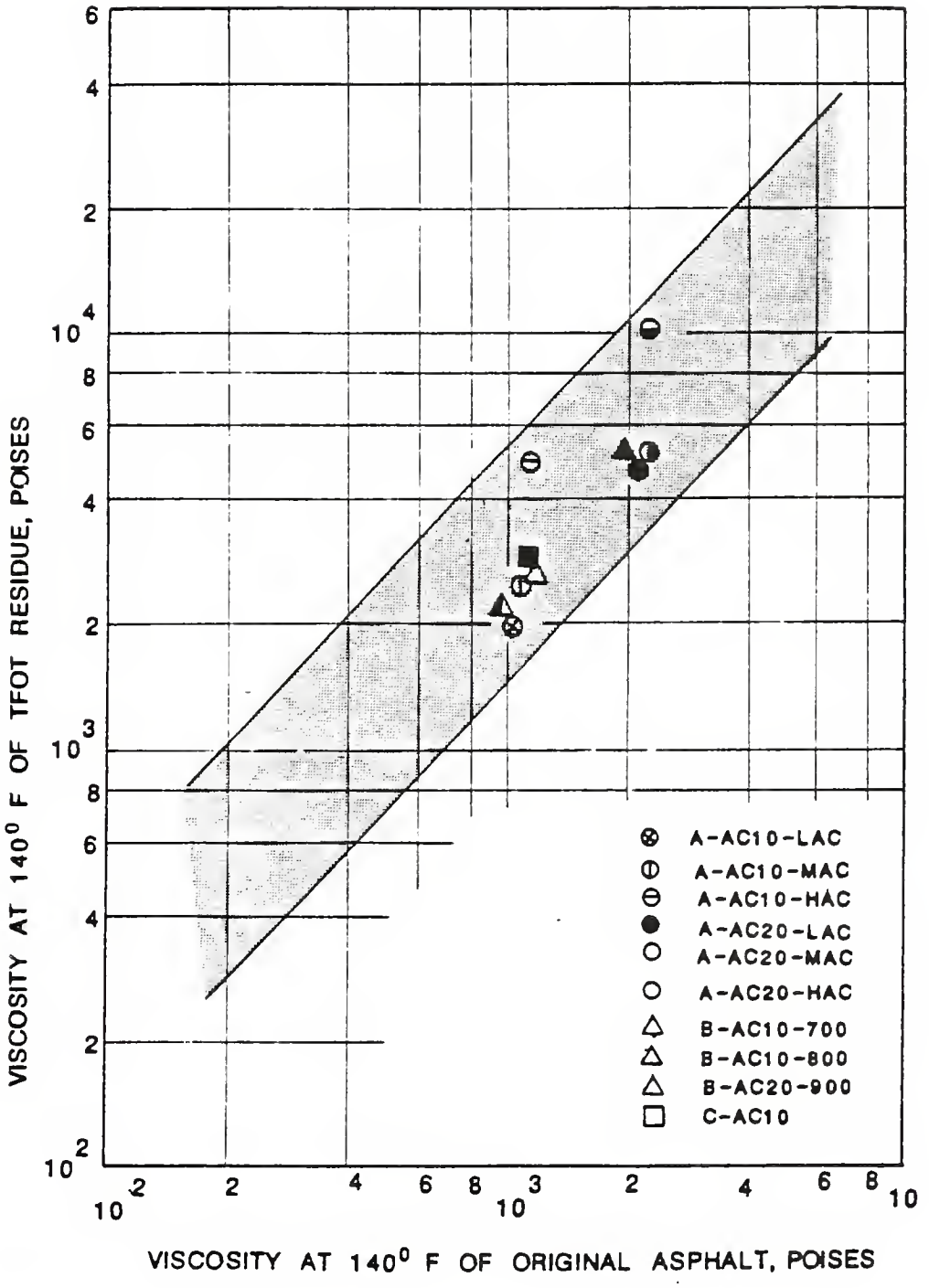

Figure 4.3 Effects of TFOT Heating on Viscosity at 140° F (from ref. 60)

asphalts in this project fall within this region. In general, variations in viscosity ratios between these asphalts are small, ranging from 1.89 to 2.66. The exceptions are the two Plant A, high asphaltene content asphalts which harden to a greater extent than any of the other asphalts.

Figure 4.4 depicts the relationship between the viscosity at 275°F of the original and heated asphalts. Again, all of the test asphalts fall with in the normal region for commercial asphalts.

The relationship between the penetration at 77°F for the original and heated asphalt is presented in Figure 4.5. All of the Plant B and Plant C asphalts fall within the region on the figure for commercial asphalts. However, the Plant A ROSE asphalts fall close to or outside the boundary of this region. Thus, the penetration of these asphalts decrease to a greater extent than do the majority of commercial asphalts. This behavior is particularly undesirable in these asphalts because of their low initial penetration.

Penn State data show that penetration retained values at 39.2°F range for 20 to 90 % while the average value is about 60 %. The values for asphalts tested in this project are given in Table 4.2. At this temperature, the degree of hardening of both the Plant A and Plant C ROSE asphalts are less than that for most other commercial asphalts.

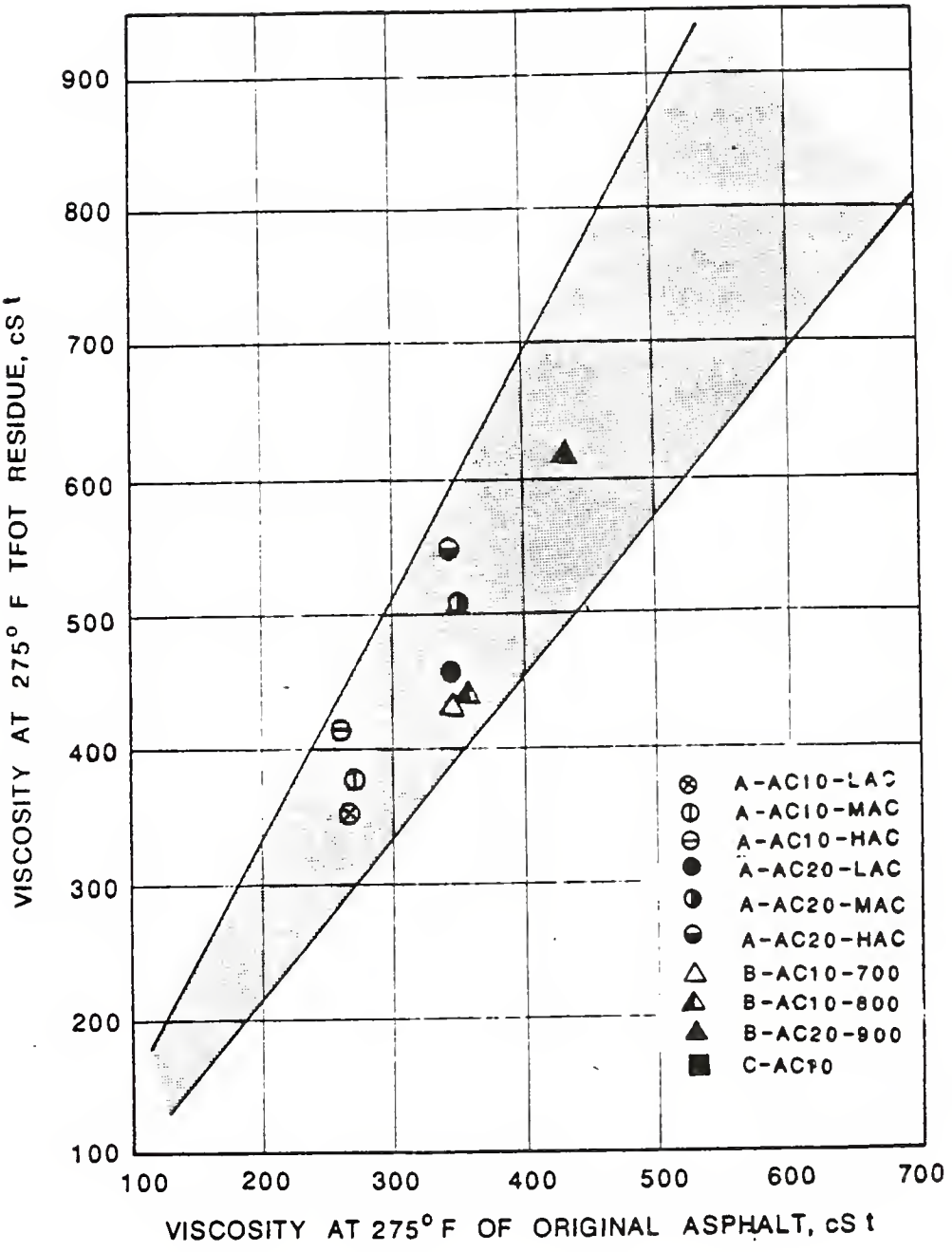

Figure 4.4 Effects of TFOT Heating on Viscosity at 275° F (from ref. 60)

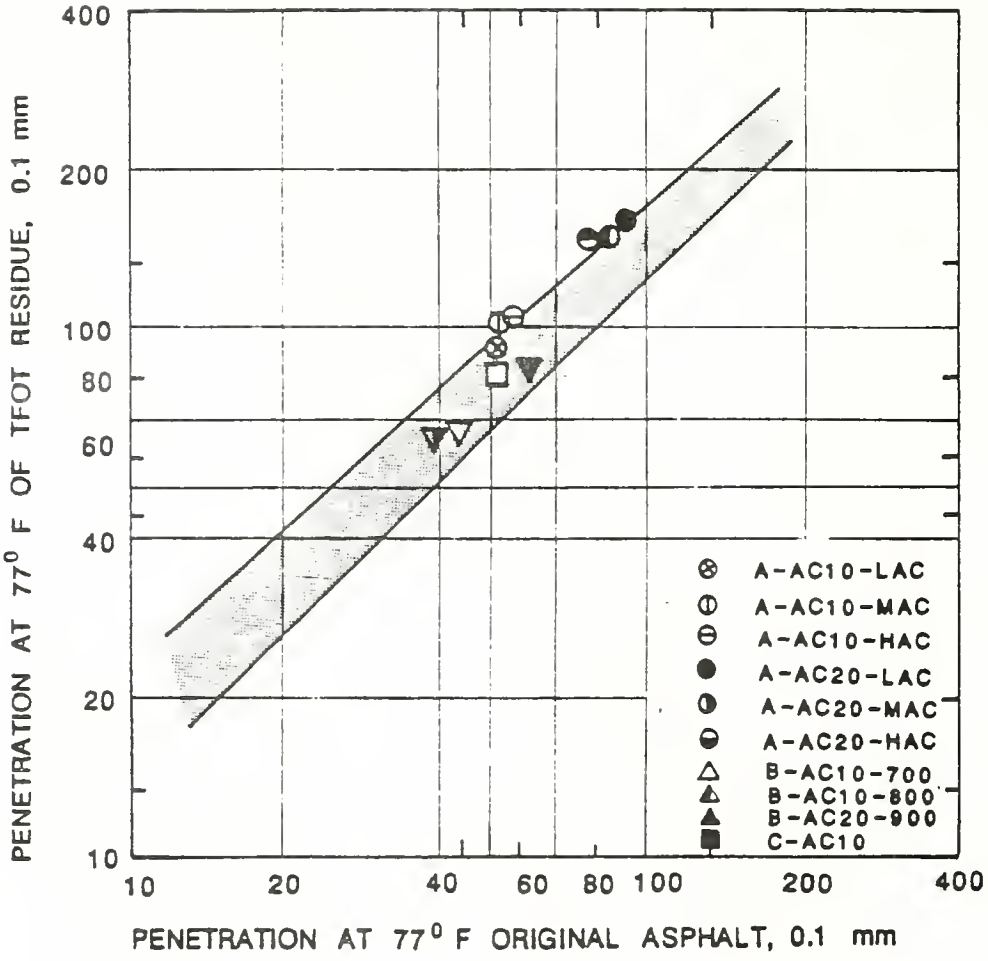

Figure 4.5 Effects of TFOT Heating on Penetration at 77° F (from ref. 60)

Figure 4.6 depicts log-log temperature susceptibility values before and after heating in the thin film oven. As shown, most commercial asphalts exhibit some increase in this variable after heating. This change is usually relatively small. Most of the asphalts tested in this project follow this pattern of little or no increase in log-log temperature susceptibility. However, the change for the two Plant A asphalts of high asphaltene content is greater than that for most other asphalts.

Table 4.2 TFOT: Penetration Retained at 39.2°F

Plant	Composition	Grade	Penetration Retained (39.2°F), %
A	LAC	AC-10	69
A	MAC	AC-10	81
A	HAC	AC-10	73
A	LAC	AC-20	60
A	MAC	AC-20	81
A	HAC	AC-20	80
B	007	AC-10	87
B	008	AC-10	81
B	009	AC-20	78
C	-	AC-10	59

Figure 4.7 shows pen-vis number before and after heating. For most asphalts, including the test asphalts, this variable

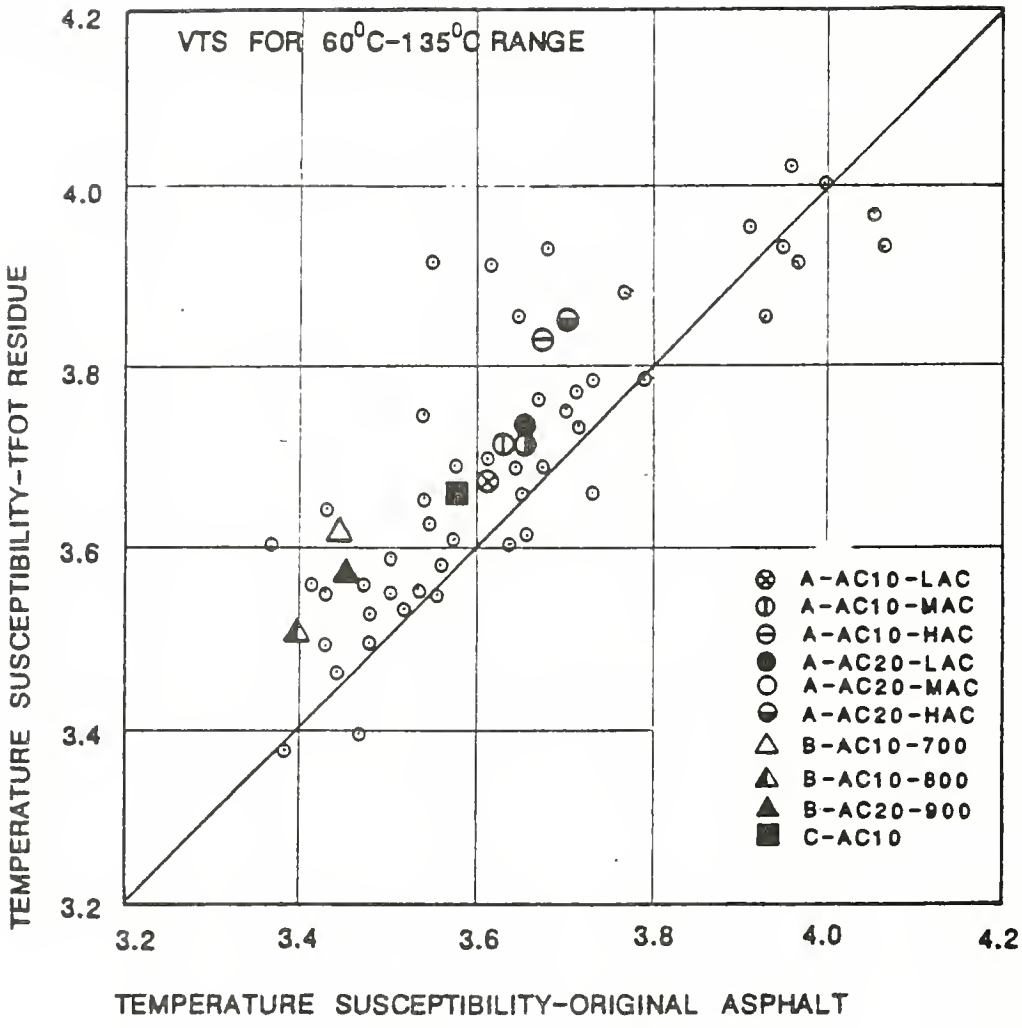

Figure 4.6 Effects of TFOT Heating on Log-log Temperature Susceptibility (from ref. 60)

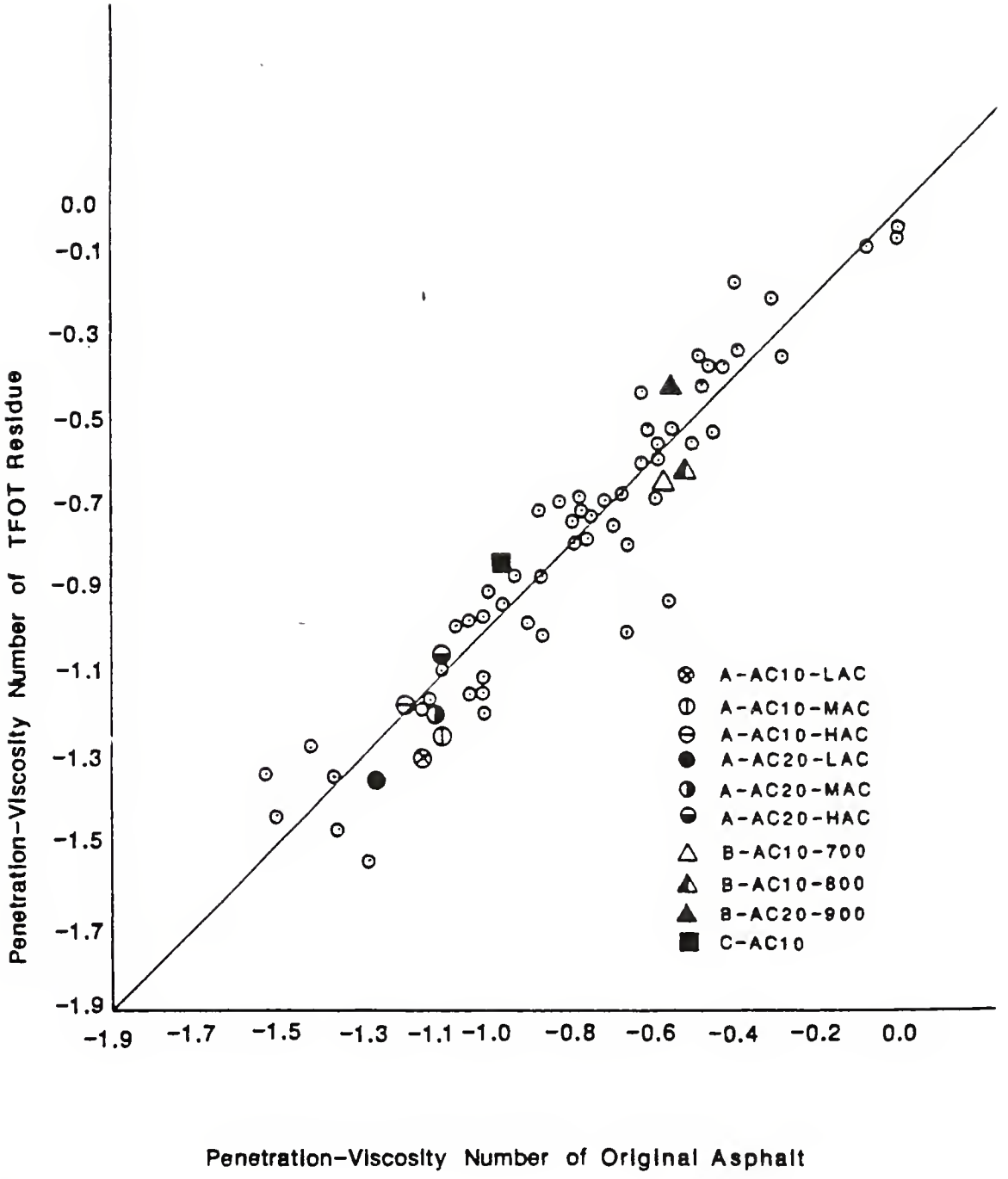

Figure 4.7 Effects of TFOT Heating on Penetration-viscosity Number (from ref. 60)

does not change significantly on heating. However, there are some variations among asphalts with different composition from the same source. For example, the high asphaltene content asphalts have the smallest changes in pen-vis number for asphalts from Plant A.

The change in penetration ratio with heating is presented in Figure 4.8. In most cases these changes are larger for the test asphalts than for the other commercial asphalts. In particular, the increase in penetration ratio is unusually large for the middle and high asphaltene content asphalts from Plant A.

These thin film oven test results show that, of the asphalts tested in this project, the high asphaltene content asphalts from Plant A exhibit the greatest degree of hardening at all temperatures, except 39.2°F. These HAC asphalts also contain the largest fraction of deasphalted oil of any of the blended asphalts. Thus, the high degree of hardening of these asphalts probably results from the loss of the volatiles that were contributed by the DAO fraction.

These HAC asphalts also have an unusually large change in log-log temperature susceptibility and penetration ratio. From these results it would appear that heat hardening properties are sensitive to changes in chemical composition. However, except in the few cases mentioned, the performance of the test asphalts on exposure to heat is not significantly different from that of other commercial asphalts.

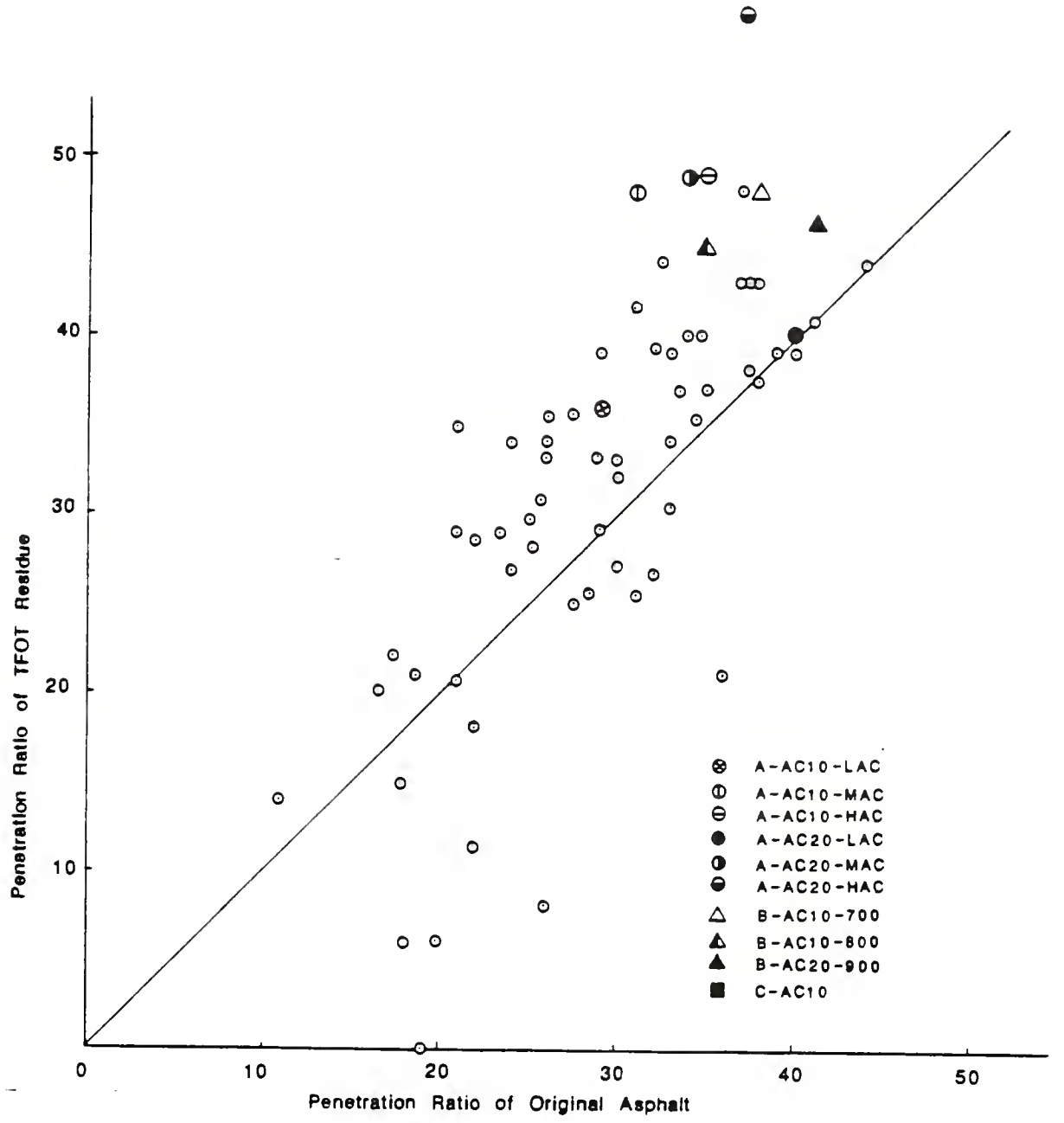

Figure 4.8 Effects of TFOT Heating on Penetration Ratio (from ref. 60)

4.2 - High Pressure-Gel Permeation Chromatography (HP-GPC)

Figure 4.9 presents the curves for the HAC, MAC, LAC AC-20 asphalts from Plant A. The LAC profile contains the least amount of both extremely large and extremely small molecules; conversely, the HAC contains the most amount of material in both categories. The asphaltene fraction is generally considered to contain most of the larger molecules in the asphalt while the DAO consists of the smaller molecules. Thus, the profiles reflect the fact that the HAC asphalt contains more asphaltene and also more deasphalted oil than the other two types of asphalts.

Figures 4.10 compares the AC-10 and AC-20 LAC asphalts. The differences between these profiles are small but significant. These differences are seen more clearly for the HP-GPC parameters in Table 4.4. These HP-GPC parameters result when the area under the profile are divided into 8 sections (see Fig. 4.11). The AC-10 asphalt contains fewer large molecules and more small molecules than the corresponding AC-20 asphalt. Similar results are obtained when the other two sets of asphalts are compared. These results show that asphalts with different rheological properties may have similar HP-GPC profiles. Conversely, asphalts with similar rheological properties may have different HP-GPC profiles.

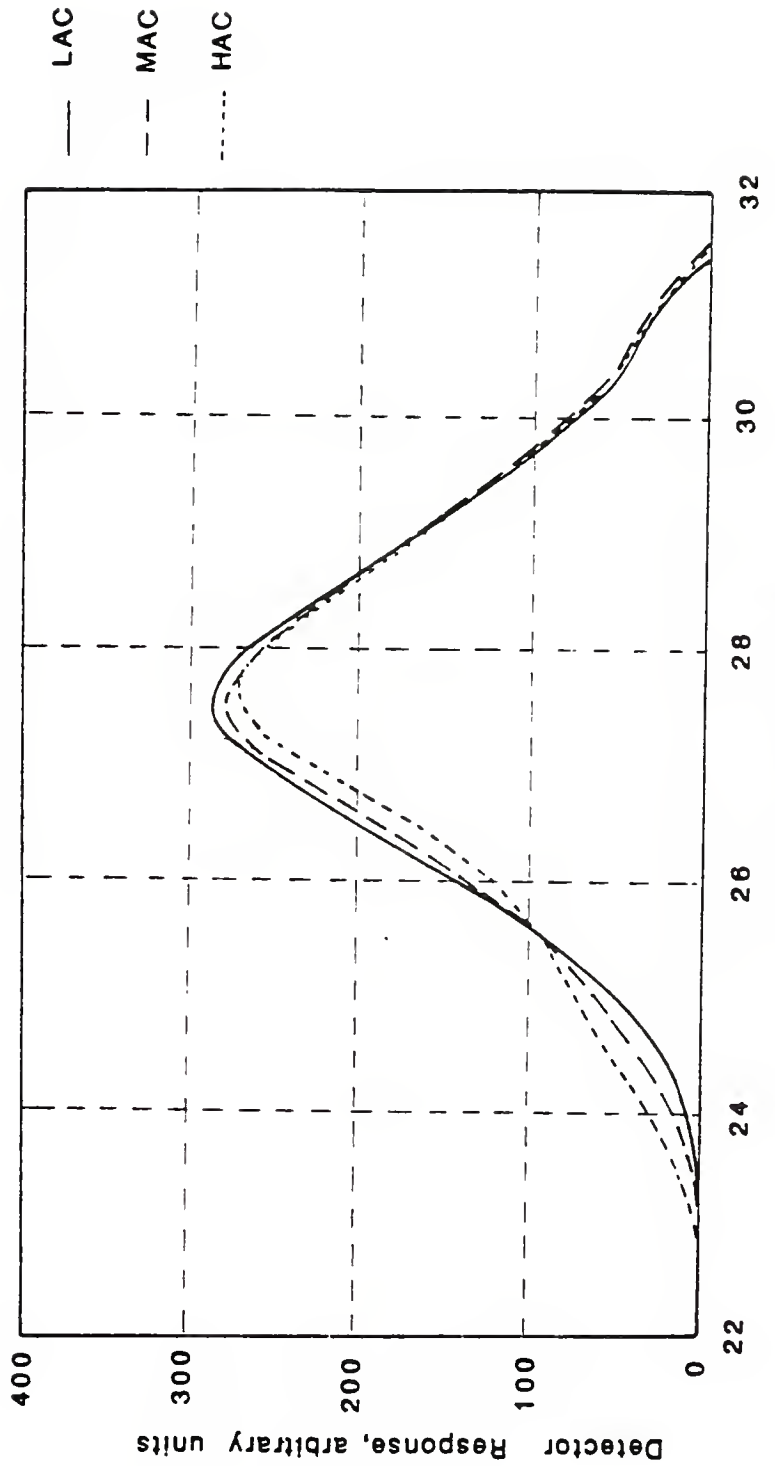

Figure 4.9 HP-GPC Profiles for Plant A AC-20 Asphalts

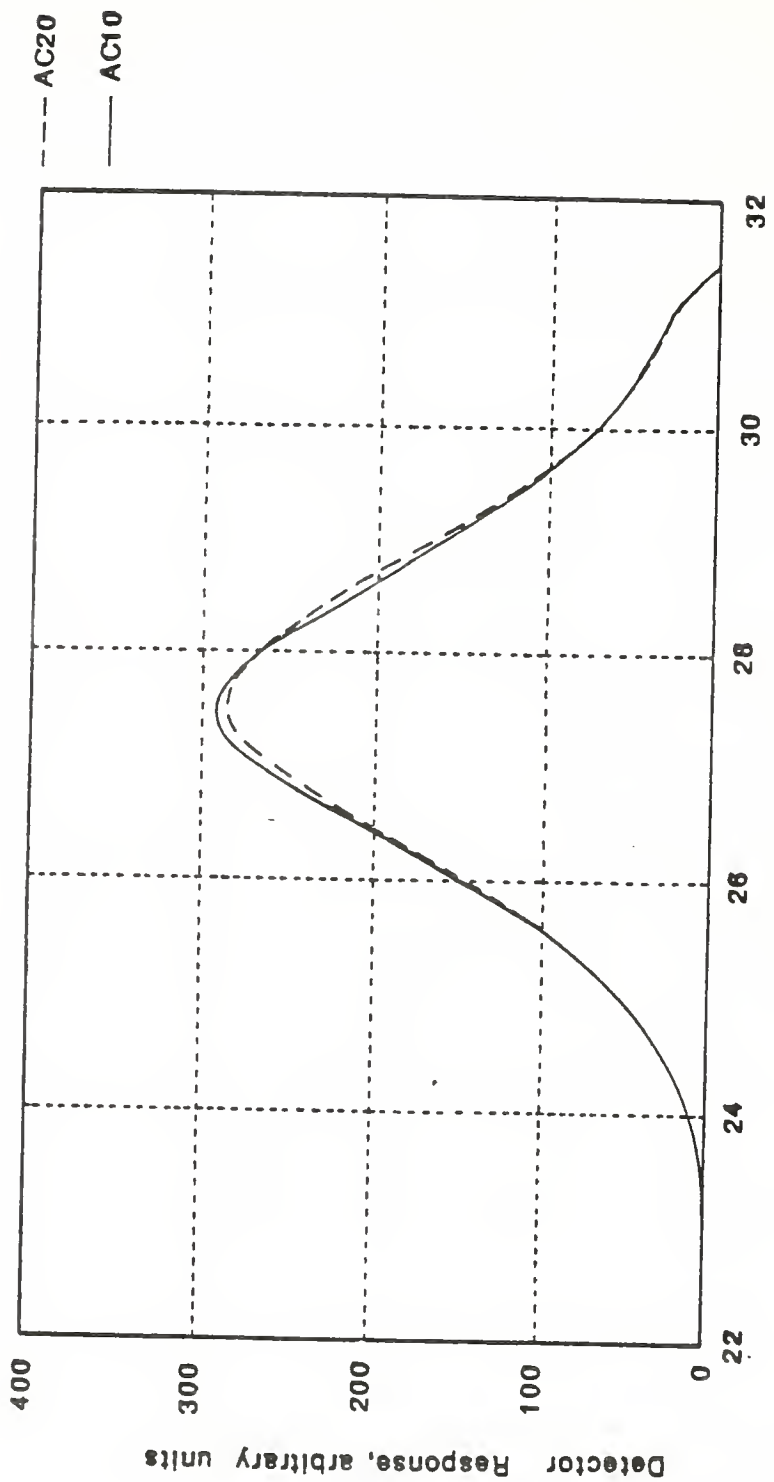

Figure 4.10 HP-GPC Profiles for Plant A AC-10 and AC-20 LAC Asphalts

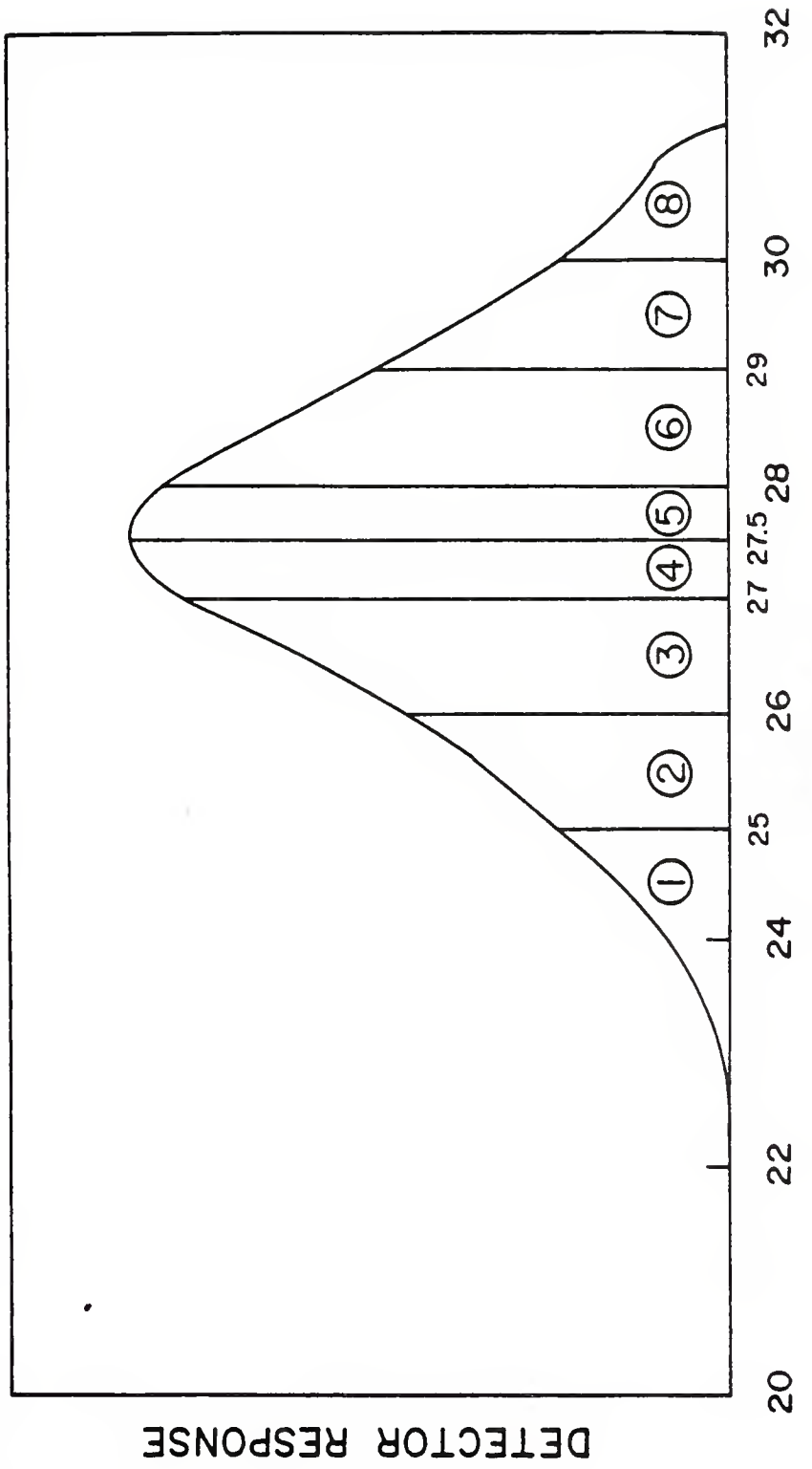

Figure 4.11 Typical HP-GPC Results

Table 4.4 HP-GPC Results for Two Plant A Asphalts

Composition and Grade	HP-GPC Parameters							
	X1	X2	X3	X4	X5	X6	X7	X8
LAC, AC-10	2.5	9.2	21.0	14.2	14.2	22.0	11.5	5.4
LAC, AC-20	2.9	9.4	20.4	13.8	14.0	22.2	11.9	5.5

Figure 4.12 further illustrates the situation in which asphalts of similar rheological properties have very different HP-GPC profiles. In this case, these AC-10 asphalts are from four different sources.

The many similarities among the profiles of the Plant A asphalts in Figure 4.9 suggest that these asphalts are related. On the other hand, the differences among the four profiles in Figure 4.12 seem to be more fundamental; thus, indicating that these asphalts are either from different crude sources or have been processed by different methods. From these results it appears that one potential use of HP-GPC is in identifying asphalts.

Figure 4.13 shows the profiles for the original and TFOT residue for the AC-20 LAC asphalt. The profile for the residue contains more large molecules and less smaller molecules than the

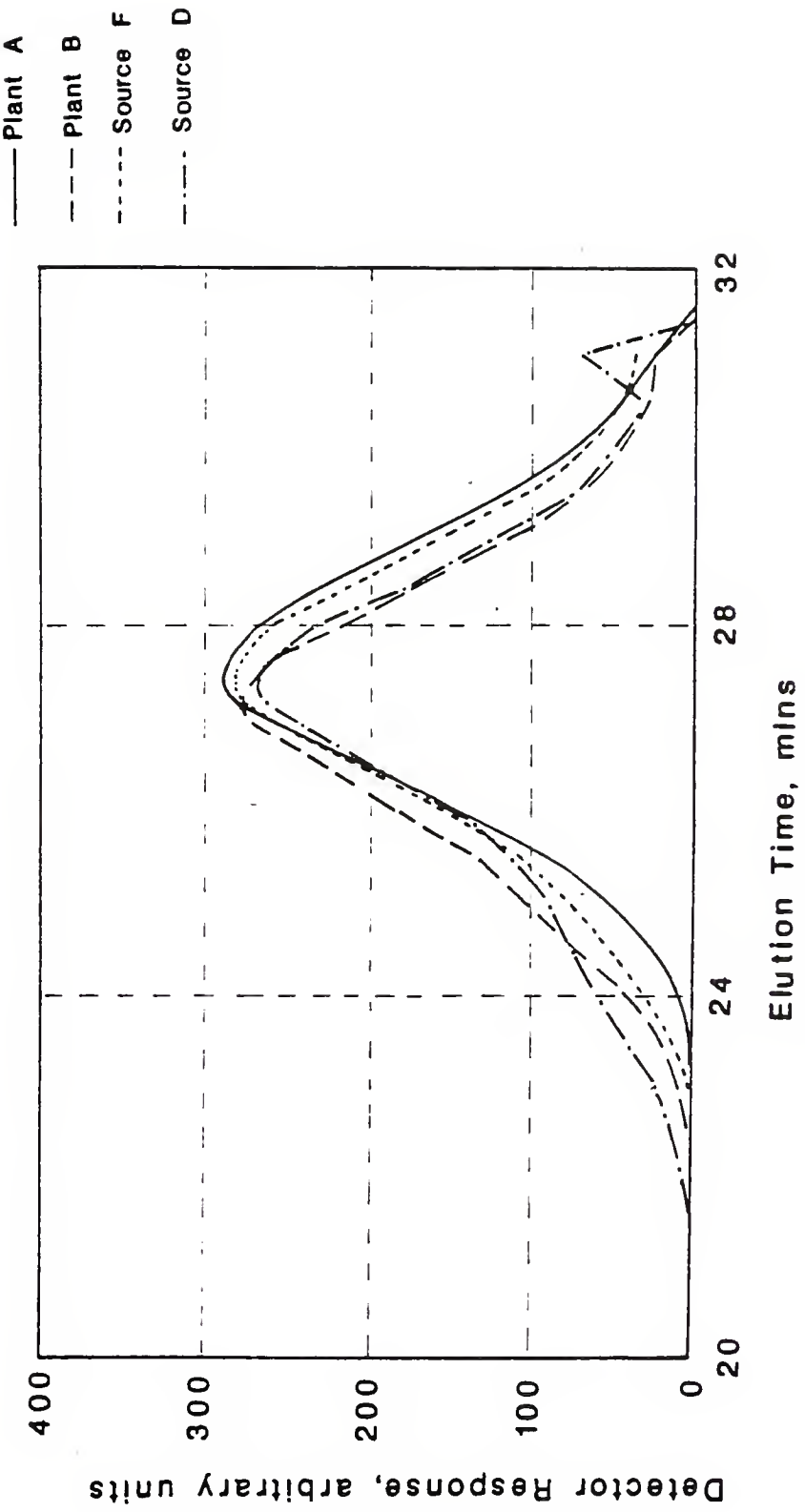

Figure 4.12 HP-GPC Profiles for AC-20 Asphalts from Four Sources

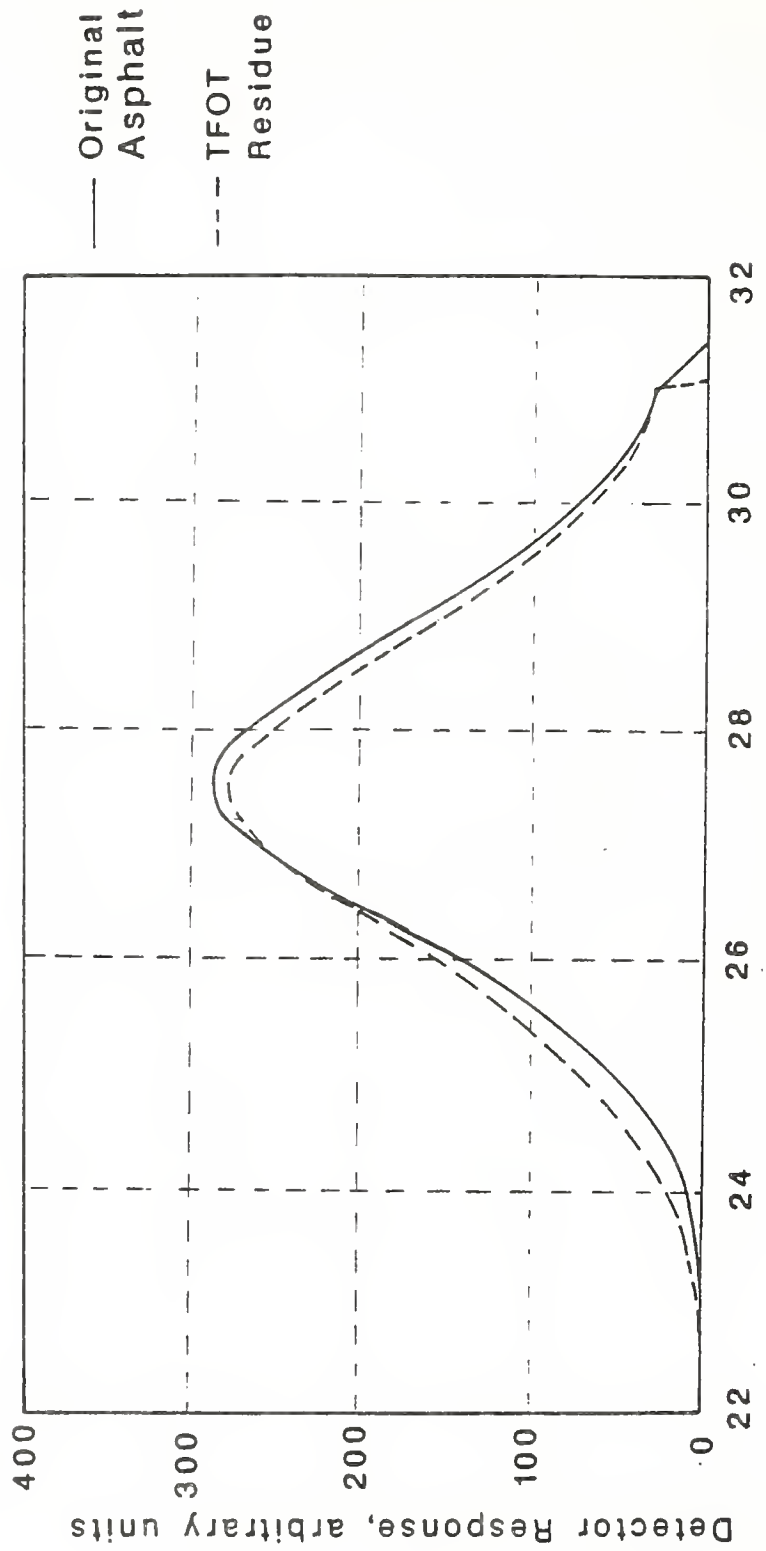

Figure 4.13 HP-GPC Profiles for Plant A AC-20 LAC Original and TFOT Residue

original asphalt. Similar results were found for all the asphalts tested; however, the amount of change varies with the asphalt. Figure 4.14 compares the profiles of an original asphalt, its TFOT residue, and its residue from the roadway. In this case, the roadway residue has significantly more large molecules than either the original asphalt or the TFOT residue. Research has shown that one of the major mechanisms causing age hardening is oxidation which results in an increase in the proportion of polar components. This is reflected in HP-GPC analysis as an increase in the large molecular area since polar molecules have a strong tendency to associate.

4.3 - Properties of Asphalt Concrete Mixes

4.3.1 - Asphalt Cement versus Asphalt Mix Properties

Figure 4.15 shows the relationship between temperature susceptibility of the asphalt cement and of the asphalt concrete sand mixes. The indicators used for temperature susceptibility of the asphalt cement and the concrete mixes respectively are the inverse of penetration ratio and the resilient modulus ratio. These two variables measure temperature susceptibility over roughly the same temperature interval. The plot shows little or no relationship between the two variables. There is also no discernible trend between the temperature susceptibility of the asphalts and that of the No. 11 concrete mixes.

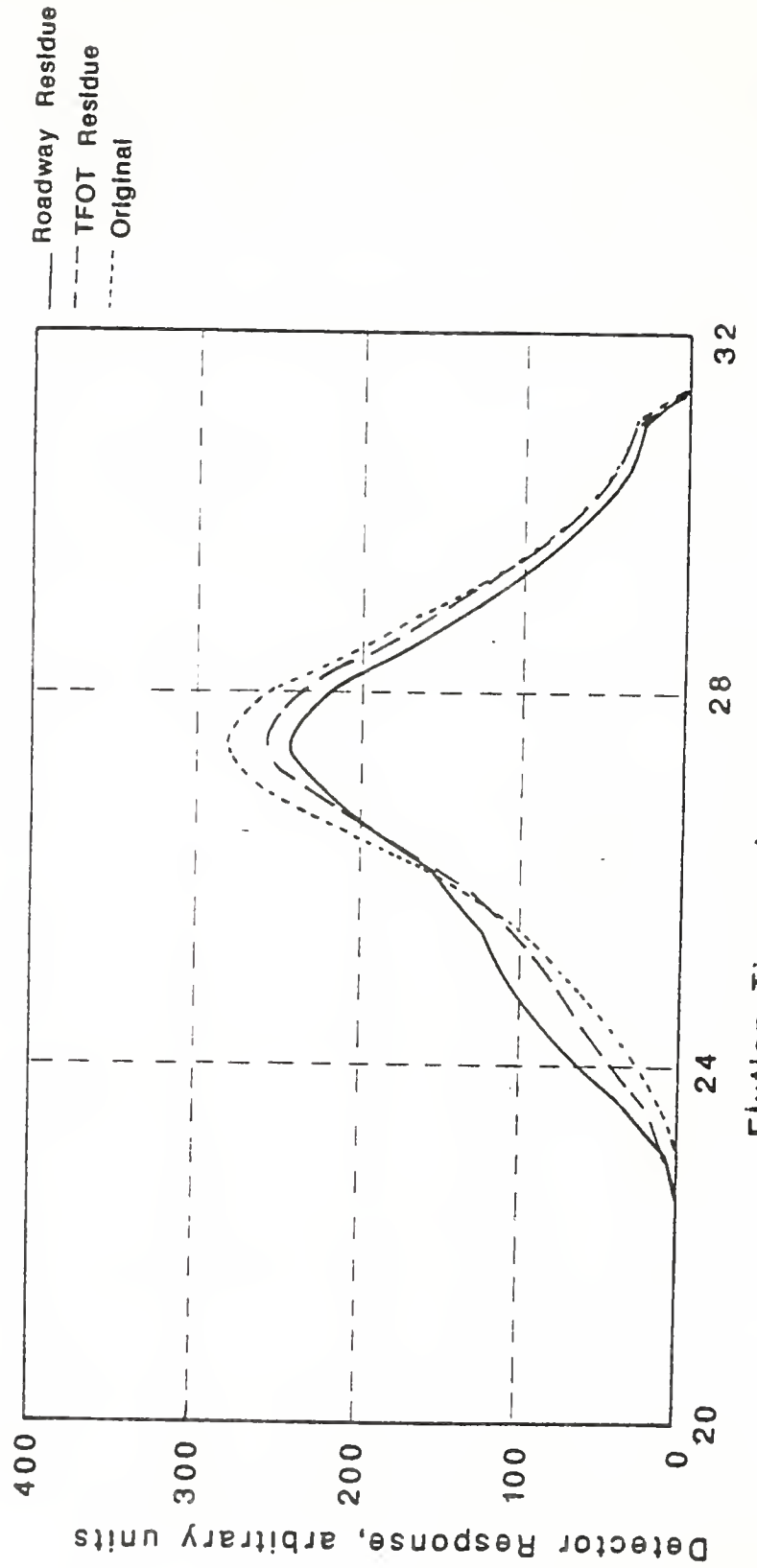

Figure 4.14 HP-GPC Profiles for Source D Original, TFOT, and Roadway Residue

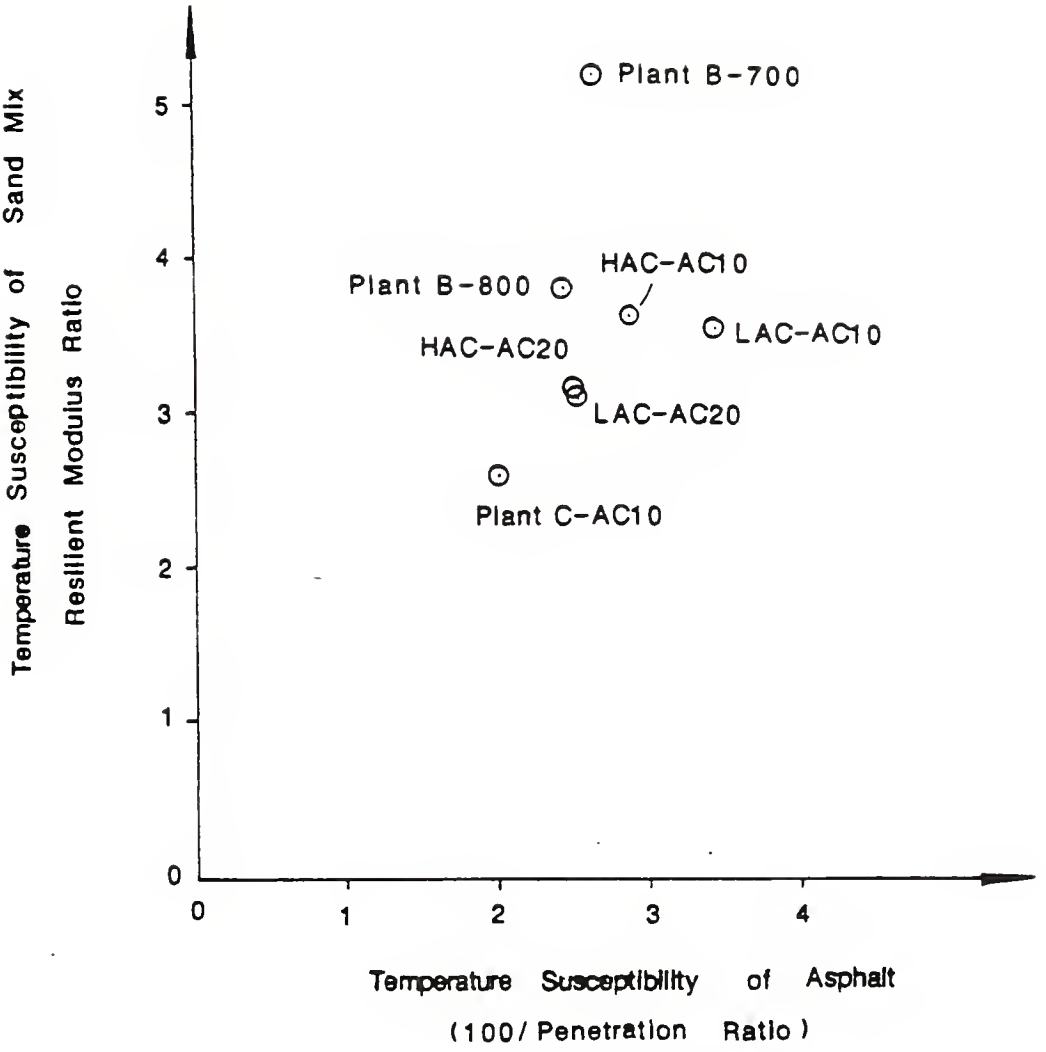

Figure 4.15 Relationship between Temperature Susceptibility of Asphalt Cement and Asphalt Concrete Sand Mixes

The heat hardening susceptibility of the asphalt concrete mixtures was also compared to that of the asphalt cements. In the case of the sand mixes, the heat hardening susceptibility of the mixes increases with that of the asphalt. However, no such trend is seen for the No. 11 mixes.

A comparison of the inverse of penetration retained at 77°F and the indirect tensile strength ratio for heat hardening of sand and No. 11 mixes showed that for sand mixes, indirect tensile strength ratio decreases with the age hardening susceptibility of the Plant A asphalts. However, this trend does not hold when the Plant C asphalt is considered. The No. 11 mixes showed a distinct trend of decreasing indirect tensile strength ratio with increasing hardening susceptibility of the asphalts.

In general, it was determined that there is little or no relationship between the physical properties of asphalts and of asphalt concrete mixes. Some researchers have suggested that too much emphasis is placed on evaluating the physical properties of the neat asphalt. They believe that more effort should be devoted to studying the behavior of the asphalt-aggregate matrix. The results shown in this section lend credence to this contention.

4.3.2 - Effects of Asphalt Composition, Grade and Source on the Properties of Concrete Mixes

The results of tests on asphalt concrete mixes indicate that there are significant differences among asphalts of different composition from the same plant and also among asphalts from different plants.

The results show that, for mixes with Plant A asphalt of a given grade, those with low asphaltene content (LAC) asphalt have a higher pulse velocity, resilient modulus and indirect tensile strength. As a result of hardening these LAC mixes show a smaller increase in resilient modulus but a greater increase in indirect tensile strength than the HAC mixes. The differences between the two types of mixes for water sensitivity and stability is not significant. Thus, the characteristics of the mixes with LAC asphalts are generally more desirable than those with HAC asphalts. This is true for both sand and No. 11 mixes.

In most cases, mixes with Plant A AC-20 asphalts have significantly higher resilient modulus and indirect tensile strength than those with AC-10. In addition, the resilient modulus ratio (temperature susceptibility) of the AC-20 mixes are lower than those of the AC-10s. However, there are little or no differences for the other properties between mixes with AC-10 or AC-20 asphalts. Differences between the two grade of asphalts are generally smaller than those among asphalts of different composition.

There are significant differences among asphalts from different sources. The resilient modulus and pulse velocity of sand mixes with AC-10 asphalts from Plant A are higher than those of mixes with AC-10 asphalts from Plant B and C. In addition, the resilient modulus ratio (temperature susceptibility) and the age hardening resilient modulus and indirect tensile strength ratios are lowest for these Plant A sand mixes. The differences for the other variables between sand mixes with asphalts from various sources are not significant.

Number 11 mixes with Plant C AC-10 asphalts have a higher resilient modulus, indirect tensile strength and water sensitivity. These Plant C mixes also have lower resilient modulus ratios (temperature susceptibility), and lower age hardening ratios. Thus it can be seen that the selection of the best asphalt depends on the aggregate gradation being used. It is not known why a given asphalt interacts so differently with aggregates of different gradation. However, this analysis would indicate that ROSE asphalts do not necessarily produce inferior mixes.

It was also determined that asphalt composition plays an important role in determining the properties of asphalt concrete mixes. This relationship between asphalt composition and asphalt mix properties is evidently affected by many factors including aggregate type and gradation, asphalt content and compaction effort. Nonetheless, these results suggest that asphalt composition is extremely important in determining the quality and durability of an asphalt pavement structure.

CHAPTER 5

SUMMARY AND CONCLUSIONS

A detailed study of the properties of asphalts blended from the products of Residuum Oil Supercritical Extraction process was conducted in this project. The three main objectives of this study were as follows: i) determine the effects of the chemical composition of the ROSE asphalts on the physical properties and of the asphalt cement and of the asphalt mixes, ii) determine if the properties of the ROSE asphalts were significantly different from that of commercially produced asphalts, and iii) develop a suitable procedure for characterizing the chemical composition of asphalts. High pressure-gel permeation chromatography was selected as a potentially suitable tool for characterizing the chemical composition of asphalt.

The majority of the tests in this project were carried out for asphalts from one ROSE source and one commercial sources. Tests were conducted on the asphalt and on asphalt mixes of two different gradation. A few tests were also performed on asphalts from a second ROSE source and three other commercial sources. All of these tests were conducted

on laboratory samples only. The major results and conclusions from this study are outlined in the following sections.

5.1 - Chemical Composition of Plant A ROSE Asphalts

It was determined in this project that it was possible to blend asphalts of different compositions which met the specifications for a given grade. Consequently, three AC-10 and three AC-20 asphalts were blended from the ROSE products from Plant A. The conclusions summarized below are based upon the effects of differences in composition on the physical properties of these asphalts.

1. The results for tests on asphalt cement show that there are only small differences in temperature susceptibility among asphalts of different composition in each grade.

2. Results from the thin film oven test indicate that at higher temperatures, the high asphaltene content (HAC) asphalt in each grade harden to a greater extent than the other two asphalts. At lower temperatures, the differences in TFOT results between asphalts of different composition are not significant.

3. It was determined that asphalt chemical composition had a significant effect on the properties of asphalt concrete mix.

5.2 - ROSE vs. Commercial Asphalts

Two sets of ROSE asphalts were evaluated in this project. The properties of these asphalt cements were compared to those of a wide cross-section of commercial asphalts produced in the United States. Data on these commercial asphalts were obtained from the literature. The properties of asphalt mixes with one set of ROSE asphalts were also compared to those of asphalt mixes with a commercial asphalt. Based on these comparisons it was concluded that there is no evidence to support the view that the blended, ROSE asphalts are significantly different from commercially produced asphalts.

5.3 - High Pressure-Gel Permeation Chromatography

The conclusions presented below resulted from the evaluation of a number of asphalts by means of high pressure-gel permeation chromatography:

1. It was determined that high pressure-gel permeation chromatography gives reproducible profiles which distinguish among asphalts of different compositions. Thus, it was concluded that HP-GPC is suitable for characterizing the chemical composition of asphalts.

2. Regression functions were developed relating HP-GPC parameters and various physical properties of asphalt

cements and of the asphalt concrete mixes. The tentative conclusion from these results is that there is a strong relationship between chemical composition of asphalts, as characterized by HP-GPC, and individual performance characteristics of asphalts of all types. These relationships are interrelated with effects of aggregate composition and gradation and asphalt content.

Part I References

1. The Asphalt Institute, "Asphalt Paving Manual", Manual Series No. 8, 1983, 138 pages.

2. ASTM Standards, "Road, Paving, Bituminous Materials; Travelled Surface Characteristics", Part 15, 1981, 1286 pages.

3. Busching, H. W., and Goetz, W. H., "Use of a Gyratory Testing Machine in Evaluating Bituminous Mixtures", Highway Research Record No. 51, 1964, pp. 1-43.

4. Casagrande, A., "The Structure of Clay and Its Importance in Foundation Engineering", Journal of the Boston Society of Civil Engineers, April, 1932.

5. Chapman, Alan J., "Heat Transfer", 4th Ed., Macmillan Publishing Company, NY, 1974.

6. Chufaror, G. L., Tatieoskaya, E. P., and Kulpina, K. I., Journal of Physical Chemistry (U.S.S.R.), 6, 152, 1935.

7. Development of the Gyratory Testing Machine and Procedures for Testing Bituminous Mixtures, U.S. Army Engineering Waterways Experiment Station, Vicksburg, Mississippi, Technical Report No. 3-595, 1962.

8. Diamond, S., "Pore Size Distribution in Clays", Clay and Clay Minerals, Vol. 18, No. 1, 1970.

9. Dickson, P. F. and Corlew, J. S., "Thermal Computations Related to the Study of Pavement Compaction Cessation Requirements", Proceedings of the Association of Asphalt Paving Technologists, Vol. 39, 1970, pp. 377-403.

10. Dillard, J. H., "Comparison of Densities of Marshall Specimens and Pavement Cores", Proceedings of the Association of Asphalt Paving Technologists, Vol. 24, 1955.

11. Endersby, V. A., "The History and Theory of Triaxial Testing and the Preparation of Realistic Test Specimens - A Report of the

Triaxial Institute", Triaxial Testing of Soils and Bituminous Mixtures, ASTM, Special Technical Publication No. 106, 1950.

12. Endersby, V. A., and Vallerga, B. A., "Laboratory Compaction Methods and their Effects on Mechanical Stability Tests for Asphaltic Pavements", Proceedings of the Association of Asphalt Paving Technologists, Vol. 21, 1952, pp. 298-348.

13. Essigman, M. F., Jr., "An Examination of the Variability Resulting from Soil Compaction", MSCE Thesis, Purdue University, West Lafayette, Indiana, 1975, 108 pages.

14. Garcia-Bengochea, I., "The Relation Between Permeability and Pore Size Distribution of Compacted Clayey Silts", MSCE Thesis, Purdue University, West Lafayette, Indiana, 1978, 179 pages.

15. Gartner, W. and Cobb, D. A., "Field Compaction Studies on Asphatic Concrete", Highway Research Record Bulletin No. 104, 1965, pp. 164-189.

16. Gaudett, N. G., Jr., "Application of the Kneading Compactor and Hveem Stabilometer to Bituminous Concrete Design in Indiana", MSCE Thesis, Purdue University, West Lafayette, Indiana, 1961, 238 pages.

17. Goetz, W. H., "Flexible Pavement Test Sections for Studying Pavement Design", Proceedings, 37th Annual Purdue Road School, 1952.

18. Griffith, J. M. and Kallas, B. F., "Influence of Fine Aggregates on Asphaltic Concrete Paving Mixtures", Proceedings of the Highway Research Board, Vol. 37, 1958.

19. Gyratory Testing Machine Product Brochure, Soil Test Inc., Evanston, Illinois, 1976.

20. Hale, T. C., "Evaluating Sand Surfaces", Construction Digest, January 5, 1987, pp. 69-72.

21. Harr, M. E., Mechanics of Particulate Media, McGraw-Hill, 1977, pp. 377-378, 462.

22. Hveem, F. N. and Davis, H. E., "Some Concepts Concerning Triaxial Compression Testing of Asphaltic Paving Mixtures and Subgrade Materials", Triaxial Testing of Soils and Bituminous Mixtures, ASTM, Special Technical Publication No. 106, 1950.

23. Hveem, F. N. and Vallerga, B. A., "Density versus Stability", Proceedings of the Association of Asphalt Paving Technologists, Vol. 21, 1952.

24. Hvorslev, Juul, "The Shearing Resistance of Remolded Cohesive Soils", Proceedings of the Soils and Foundation Conference, U.S. Engineer Department, Boston, Massachusetts, June, 1938.

25. Indiana State Highway Commission, Standard Specifications, Indianapolis, Indiana, 1978, 580 pages.

26. Indiana State Highway Commission, Standard Specifications, Indianapolis, Indiana, 1985, 601 pages.

27. Jorgensen, J. L., "Measuring the Variability of Compacted Embankments", Highway Research Record No. 290, pp. 23-34.

28. Kreith, Frank, Principles of Heat Transfer, International Textbook Company, 1961.

29. Kriech, A. J. and Rucker, A. M., "A Study of Factors which Influence Type IV Sand Mix Performance", Proceedings of the 72nd Annual Road School, Purdue University, West Lafayette, Indiana, March 11-13, 1986, pp. 97-118.

30. Luna, R., "Compaction Characterization of Thin Asphaltic Surface Courses", MSCE Thesis, Purdue University, West Lafayette, Indiana, 1985, 150 pages.

31. McBain, J. W., Journal of American Chemical Society, 57, 699, 1935.

32. Monismith, C. L. and Vallerga, B. A., "Relationship Between Density and Stability of Asphalt Paving Mixtures", Proceedings of the Association of Asphalt Paving Technologists, Vol. 25, 1956.

33. Reed, M. A., "Frost Heaving Rate of Silty Soils as a Function of Pore Size Distribution", MSCE Thesis, Purdue University, West Lafayette, Indiana, 116 pages.

34. Richard, F. E., "Foundation Vibrations", Journal of Soil Mechanics and Foundations Division, ASCE, Vol. 86, No. SM4, Part I, August 1960.

35. Rucker, A. M.,"History of (Type IV) Hot Emulsion Sand Mix in the State of Indiana", Indiana Department of Highways, Indianapolis, Indiana, 1985, 113 pages.

36. Sarakhov, A. I., "Some Comments on the Accuracy of the Method of Mercury Intrusion Porosimetry", Russian Journal of Physical Chemistry, February, 1963, pp. 242-243.

37. Sherman, et al., "A Statistical Analysis of Embankment Compaction", Highway Research Board, Highway Research Record, No. 177, 1967.

38. Smith, T. W. and Prystock, R. H., "Discussion to paper `Quality Control of Compacted Earthwork´ by Turnbull, W. J., Compton, J. R. and Ahlvin, R. G.", Journal of Soil Mechanics and Foundation Division, ASCE, Vol. 92, No. SM1, September 1966.

39. Smith, V. R., "Application of the Triaxial Test to Bituminous Mixtures California Research Corporation Method", Triaxial Testing of Soils and Bituminous Mixtures, ASTM, Special Technical Publication No. 106, 1950.

40. Tegeler, P. A., and Dempsey, B. J., "A Method of Predicting Compaction Time for Hot-Mix Bituminous Concrete", Proceedings of the Association of Asphalt Paving Technologists, Vol. 42, 1973, pp. 499-523.

41. Thiele, E. W., "Industrial and Engineering Chemistry", 31, 916, 1939.

42. Tunnicliff, D. G., "A Review of Mineral Filter", Paper presented at a meeting of the Association of Asphalt Paving Technologists, New Orleans, Louisiana, Jan. 29-31, 1962, pp. 118-150.

43. Vallerga, B. A., "Recent Laboratory Compaction Studies of Bituminous Paving Mixtures", Proceedings of the Association of Asphalt Paving Technologists, Vol. 20, 1951, pp. 117-153.

44. Volk, William, "Engineering Statistics with a Programmable Calculator", McGraw-Hill, 1982, pp. 52-60.

45. Washburn, E. W.,"Note on a Method of Determining the Distribution of Pore Sizes in a Porous Material", Proceedings of the National Academy of Sciences, Vol. 7, 1921, pp. 115-116.

46. Williamson, T. G. "Embankment Compaction Variability - Control Techniques and Statistical Implications", Highway Research Board, Highway Research Record No. 290, 1969.

47. Winslow, D. N., "Advances in Mercury Intrusion Porosimetry", Surface and Colloid Science, Vol. 13, Plenum Press, 1984, pp. 259-282.

48. White, D. M., "The Fabric of a Medium Plastic Clay Compacted in the Laboratory and in the Field", MSCE Thesis, Purdue University, West Lafayette, Indiana, 1980, 149 pages.

49. Wolfe, R. K. and Colony, D. C., "Asphalt Cooling Rates: A Computer Simulation Study", Final Report, Project No. 2844, Department of Transportation, State of Ohio, and FHWA, 1976.

50. Woods, et al., "Highway Engineering Handbook", McGraw-Hill, First Ed., pp. 1-102.

Part II References

1. -, "America's Highways - Accelarating the Search for Innovation", Transportation Research Board, Special Report 202, 1984.

2. Petersen, J.C., "Chemical Composition of Asphalt as Related to Asphalt Durability - State of the Art", presented at the 63rd Annual Meeting of the Transportation Research Board, January, 1984.

3. Halstead, W.J., "Relation of Asphalt Chemistry to Physical Properties and Specifications", Proceedings of the Association of Asphalt Paving Technologists, Vol. 54, 1985, p91.

4. Goodrich, J.L., Goodrich, J.E., and Kari, W.J., "Asphalt Composition Tests: Their Application and Relation to Field Performance", presented at the 65th Annual Meeting of the Transportation Research Board, January, 1986.

5. Rostler, F.S., White, R.M., "Influence of Chemical Composition of Asphalts on Performance, Particularly Durability", ASTM Special Technical Report No. 277, 1959, p1.

6. Rostler, F.S., White, R.M., "Composition and Changes in Composition of Highway Asphalts, 85-100 Penetration Grade", Proceedings of the Association of Asphalt Paving Technologists, Vol. 31, 1962, p35.

7. Schweyer, H.E., "Asphalt Composition and Properties", Highway Research Bulletin,No. 192, 1958, p32.

8. Griffin, R.L., Simpson, W.C., and Miles, T.K., "Influence of Composition of Paving Asphalt on Viscosity, Viscosity-Temperature Susceptibility, and Durability", Journal of Chemical and Engineering Data, Vol. 4, No. 4, October, 1959, p349.

9. Halstead, W.J., Rostler, F.S., and White, R.M., "Properties of Highway Asphalts-Part III, Influence of Chemical Composition", Proceedings of the Association of Asphalt Paving Technologists, Vol. 35, 1966, p91.

10. Jamieson, I.L., Hattingh, M.M., "The Correlation of Chemical and Physical Properties of Bitumens with Their Road Performance", Proceedings of the Australian Road Research Board, Vol. 5, Part 5, 1970, p293.

11. Simpson, W.C., Griffin, R.L., and Miles, T.K., "Relationship of Asphalt Properties to Chemical Consititution", American Chemical Society, Division of Petroleum Chemistry, September, 1960, pA-79.

12. Altgelt, K.H., Harle, O.L., "The Effect of Asphaltenes on Asphalt Viscosity", Industrial and Engineering Chemistry Product Research and Development, Vol. 14, No. 4, 1975, p240.

13. Reerink, H., "Size and Shape of Asphaltene particles in Relationship to High-Temperature Viscosity", Industrial and Engineering Product Research and Development, Vol. 12, No. 1, 1973, p82.

14. Boduszynski, M.M., McKay, J.F., and Latham, D.R., "Asphaltene Where Are You?, Proceedings of the Association of Asphalt Paving Technologists, Vol. 49, 1980, p123.

15. Akhmetova, R.S., and Glozman, E.P., "Asphalt Quality as Influenced By Nature of Asphaltene", Chemistry Technology Fuels Oils, vol. 10, no. 7-8, Jul-Aug 1974, p540.

16. Algelt, K.H., "Fractionation of Asphaltenes by Gel Permeation Chromatography", Journal of Applied Polymer Science, Vol. 9, 1965, p3389.

17. Richman, W.B., "Molecular Weight Distribution of Asphalts", Proceedings of the Association of Asphalt Paving Technologists, Vol. 36, 1967, p106.

18. Breen, J.J., Stephens, J.E., "The Interrelationship Between the Glass Transition Temperature and Molecular Characteristics of Asphalt", Proceedings of the Association of Asphalt Paving Technologists, Vol. 38, 1969, p706.

19. Jennings, P.W., "Use of High Pressure Liquid Chromatograph to Determine the Effects of Various Additives and Fillers on the Characteristica of Asphalt", Montana DOT/Federal Highway Administration, Research Project No. FHWA/MT - 82/001, June, 1982.

20. Jennings, P.W., Pribanic, J.A.S., Dawson, K.R., and Bricca, C.E., "Use of the HPLC and NMR Spectroscopy to Characterize Asphaltic Materials", Americal Chemical Society, Division of Petroleum Chemistry, August, 1981, p915.

21. Jennings, P.W., Pribanic, J.A.S., "The Expanded Montana Asphalt Quality Study Using High Pressure Liquid Chromatography", Montana DOH Research Program, Research Report No. FHWA/MT - 85/001, April, 1985.

22. Bynum, D., and Traxler, R.N., "Gel Permeation Chromatography Data on Asphalts Before and After Service in Pavements", Proceedings of the Association of Asphalt Paving Technologists, Vol, 39, 1970. p683.

23. Brule, B., "Contribution of Gel Permeation Chromatography to the Characterization of Asphalts", Liquid Chromatography of Polymers and Related Materials II, Marcel Dekker, New York, 1980.

24. Reerink, H., and Lijzenga, J., "Gel-Permeation Chromatography Calibration Curve for Asphaltenes and Bituminous Resins", Analytical Chemistry, Vol, 47, No. 13, November, 1975, p2160.

25. Albaugh, E.W., Talarico, P.C., Davis, B.E., and Wirkkala, R.A., "Fractionation of Residuals by Gel Permeation Chromatography", Seperation Science, Vol. 5(6), December, 1070, p801.

26. Jennings, P.W., Pribanic, J.A.S., "Asphalt Analytical Methodology: High Pressure Gel Permeation Chromatography", presented at the 65th Meeting of the Transportation Research Board, January, 1986.

27. Jennings, P.W., Pribanic, J.A.S., Dawson, K.R., Smith, J.A., Koontz, S., Spittler, T., and Shane, S., "Uses of High Performance Gel Permeation Chromatography for Asphalt Analysis", presented at the 64th Meeting of the Transportation Research Board Meeting, January, 1985.

28. Such, C., Brule, B., "Characterization of A Road Asphalt By Chromatographic Techniques (GPC and HPLC)", Journal of Seperation Science, Vol. 2(3), 1970, p437.

29. Algelt, K.H., and Hirsch, E., "GPC Seperation and Integrated Structural Analysis of Petroleum Heavy Ends", Seperation Science, Vol. 5(6), December, 1970, p855.

30. Dickson, F.E., Wirkkala, R.A., and Davis, B.E., "Combined Gel Permeation Chromatography-NMR Techniques in the Characterization of Petroleum Residuals", Seperation Science, Vol. 5(6), December, 1970, p811.

31. Plummer, M.A., and Zimmerman, C.C., "Asphalt Quality and Yield Predictions from Crude Oil Analyses", Proceedings of the Association of Asphalt Paving Technologists, Vol. 53, 1984, p138.

32. Hattingh, M.M., "The Fractionation of Asphalt", Proceedings of the Association of Asphalt Paving Technologists, Vol. 53, 1984, p197.

33. Anderson, D.A., Dukatz, E., "Relationship Between Asphalt Flow Properties and Asphalt Composition", Proceedings of the Association of Asphalt Paving Technologists, Vol. 53, 1984, p160.

34. Newcomer, R.M., Soltau, R.C., "Heavy Oil Extraction Ups FCC Feed at First Three-stage Grass Roots ROSE Unit in Kansas", reprint from Oil and Gas Journal, vol. 80, no. 26, July 12, 1982.

35. Gearhart, J.A., Nelson, S.R., "Upgrading Residuals and Heavy Oils with ROSE", presented at the 32nd Canadian Chemical Engineering Conference, Vancouver, British Columbia, Oct. 1982.

36. Sprague, S.B., "AC-20 Produced by Two Different Methods: A Comparison of Their Composition and Laboratory Performance", presented at the 64th Annual Transportation Research Board meeting, January 15, 1985.

37. Schmidt, R.J., "A Practical Method for Measuring the Resilient Modulus of Asphalt Treated Mixes", Highway Research Record No. 404, Highway Research Board 1972, p22.

38. Timoshenko, S., Goodier, J.N., Theory of Elasticity, 2nd Ed. M^{c}Graw-Hill, New York, 1951.

39. Frocht, M.M., Photoelasticity, Vol. 2, John Wiley and Sons, New York, 1948.

40. Little, D.N., Richey, B.L., "A Mixture Design Procedure Based on the Failure Envelope Concept", Proceedings the Association of Asphalt Paving Technologists, Vol. 52, 1983, p378.

41. Uzan, J., "An Evaluation Scheme for Conventional Requirements of Design and Construction Quality for Asphalt Concrete", Proceedings the Association of Asphalt Paving Technologists, Vol. 51, 1982, p129.

42. Santucci, L.E., Hayashida, M.T., "Design and Testing of Cold Recycled Aspalt Mixes", Proceedings of the Association of Asphalt Paving Technologists, Vol. 52, 1983, p416.

43. Anderson, K.O., Epps, J.A., "Asphalt Concrete Factors Related to Pavement Cracking in West Texas", Proceedings of the Association of Asphalt Paving Technologists, Vol. 52, 1983, p151.

44. Hicks, "Factors Influencing the Resilient Properties of Granular Materials", Ph.D. Dissertation, University of California-Berkeley, 1970.

45. Kennedy, T.W., "Characterization of Asphalt Pavement Materials Using the Indirect Tensile Test", Proceedings of the Association of Asphalt Paving Technologists, Vol. 46, 1977, p132.

46. Kandhal, P.S., "Evaluation of Sulphur Extended Asphalt Binders in Bituminous Paving Mixtures", Proceedings of the Association of Asphalt Paving Technologists, Vol. 51, 1982, p189.

47. Anderson, D.A., Dukatz, E.L., Rosenberger, J.L., "Properties of Asphalt Cement and Asphaltic Concrete", Proceedings of the Association of of Asphalt Paving Technologists, Vol. 52, 1983, p291.

48. Maupin, G.W., "The Use of Antistripping Additives in Virginia", Proceedings, Assoc. of Asphalt Paving Technologists, Vol. 51, 1982, p343.

49. Long, B.G., Kartz, H.J., Sandenau, T.A., "An Instrument and a Technic for Field Determination of the Modulus of Elasticity and Flexural Strength of Concrete (Pavements), Proceedings of the American Concrete Institue, Vol. 41, 1945, p217.

50. Goetz, W.H., "Sonic Testing of Bituminous Mixtures", Proceedings of the Assoc. of Asphalt Paving Technologists, Vol. 34, 1955, p332.

51. Manke, P.G., Gallaway, B.M., "Pulse Velocities in Flexible Pavement Construction Materials", Highway Research Record, No. 131, 1966, p128.

52. Mamlouk, M.S., "Characterization of Cold Mixed Asphalt Emulsion Treated Bases", Joint Highway Research Project, Purdue University, IN/JHRP-79-19, 1979.

53. Tia, Mang, "Characterization of Cold-recycled Asphalt Mixtures", Joint Highway Research Project, Purdue University, Project No. C-36-21D/2-8-4, 1982.

54. Ruth, E.B., "Evaluation and Prevention of Water Damage to Asphalt Pavement Materials", ASTM Special Technical Report 899, 1984, p1.

55. Tunnicliff, D.G., Root, R.E., "Antistripping Additives in Asphalt Concrete - State-of-the-Art 1981", Proceedings of the Association of Asphalt Paving Technologists, Vol. 51, 1982, p265.

56. Lottman, R.P., "Laboratory Test Method for Predicting Moisture-Induced Damage to Asphalt Concrete", Transportation Research Record No. 843, Transportation Research Record, 1982, p88.

57. Tunnicliff, D.G., Root, R.E., "Testing Asphalt Concrete for Effectiveness of Antistripping Additives", Proceedings of the Association of Asphalt Paving Technologists, Vol. 52, 1983, p535.

58. Luna, R., "Compaction Characterization of Thin Asphaltic Surface Courses", M.S. Thesis, Purdue University, 1985.

59. Garrick, N.W., Wood, L.E., "The Relationship Between HP-GPC Data and the Rheological Properties of Asphalts", presented at the 65th Annual Meeting of the Transportation Research Board, January, 1986.

60. Puzinauskas, V.P., "Properties of Asphalt Cements", Proceedings of the Association of Asphalt Paving Technologists, Vol. 48, 1979, p646.

61. Anderson, D.A., Dukatz, E.L., "Asphalt Properties and Composition: 1950-1980", Proceedings of the Association of Asphalt Paving Technologists, Vol. 49, 1980, p1.

COVER DESIGN BY ALDO GIORGINI